The University of Milano Bicocca

THE PhD PROGRAM DIMET

The PhD Program in Translational and Molecular Medicine (DIMET) is an inter-departmental project between the School of Medicine and the School of Science, organized by the University of Milano-Bicocca.

DIMET - Dr. Diego FARINELLO - A.A. 2015-16

PhD

PROGRAM IN TRANSLATIONAL AND MOLECULAR MEDICINE

DIMET

UNIVERSITY OF MILANO-BICOCCA
SCHOOL OF MEDICINE AND SCHOOL OF SCIENCE

A retinoic acid-dependent stroma-leukemia crosstalk promotes tissue remodelling and disease progression in a mouse model of chronic lymphocytic leukaemia

Coordinator: Prof. Andrea Biondi
Tutor: Prof. Silvia Brunelli
Co-Tutor: Dott. Andrea Brendolan

Dr. Diego FARINELLO

Matr. No. 056272

XXIX CYCLE
ACADEMIC YEAR
2015-2016

A retinoic acid-dependent stroma-leukaemia crosstalk promotes tissue remodelling and disease progression in a mouse model of chronic lymphocytic leukaemia

CHAPTER 1. GENERAL INTRODUCTION

1.1 THE LYMPHOID TISSUES AND THE LYMPHOID MICROENVIRONMENT

The lymphoid tissues are specialized structures responsible for both innate and adaptive immunity. Lymphoid tissues show complex structural organizations related to their function in the immune response and the microenvironments within those tissues are specific to both lymphoid tissue localization and immune functions. The lymphoid tissue microenvironment is composed by: i) leukocytes, that either patrol the tissue or are resident specialized cells; ii) endothelial cells, branching within the tissue to vehiculate factors and allowing cell migration through formed vessels, iii) mesenchymal cells, originated from CD45 negative lineages, that are important in forming microenvironment scaffold and creating a supportive niche; and iv) extracellular matrix, a tri-dimensional scaffold that plays an important role in specifying the tissue identity [1]. In particular, the subjects of this introduction are CD45 negative mesenchymally-derived stromal cells (from now onward simply called “stromal cells”) and the tumour microenvironment.

1.1.1 THE SECONDARY LYMPHOID ORGANS

Secondary lymphoid organs (SLOs) are located along the whole body and are appointed to monitor all tissues by filtering fluids and allowing immune responses to noxious agents. Examples of SLOs are the spleen, the lymph nodes and the Payer's patches. SLOs evolved together with vertebrates' evolution and maintained the same composition, with fibroblast networks that create the tissue scaffold and promote immune functions, together with the extracellular matrix scaffold, with endothelial cells connecting the lymphoid tissue to the whole circulation, nerves and leukocytes either patrolling the body and resident within the lymphoid organ and directly responding to foreign and self-antigens [2].

1.1.1.1 The Spleen

The spleen is the biggest secondary lymphoid organ in vertebrates' body derived from the lateral plate mesoderm and organized in different compartments only postnatally [3] [4] [5] [6]. The spleen is located under the diaphragm, underneath the stomach, within the omentum, and it is a highly vascularized organ responsible both for erythrocytes' iron recycling and for immune responses generated against blood-borne antigens [3]. The spleen is constituted by two different tissues, the red pulp and the white pulp, that are in turn contained by a dense fibrous tissue named splenic capsule, where mesothelial cells reside.

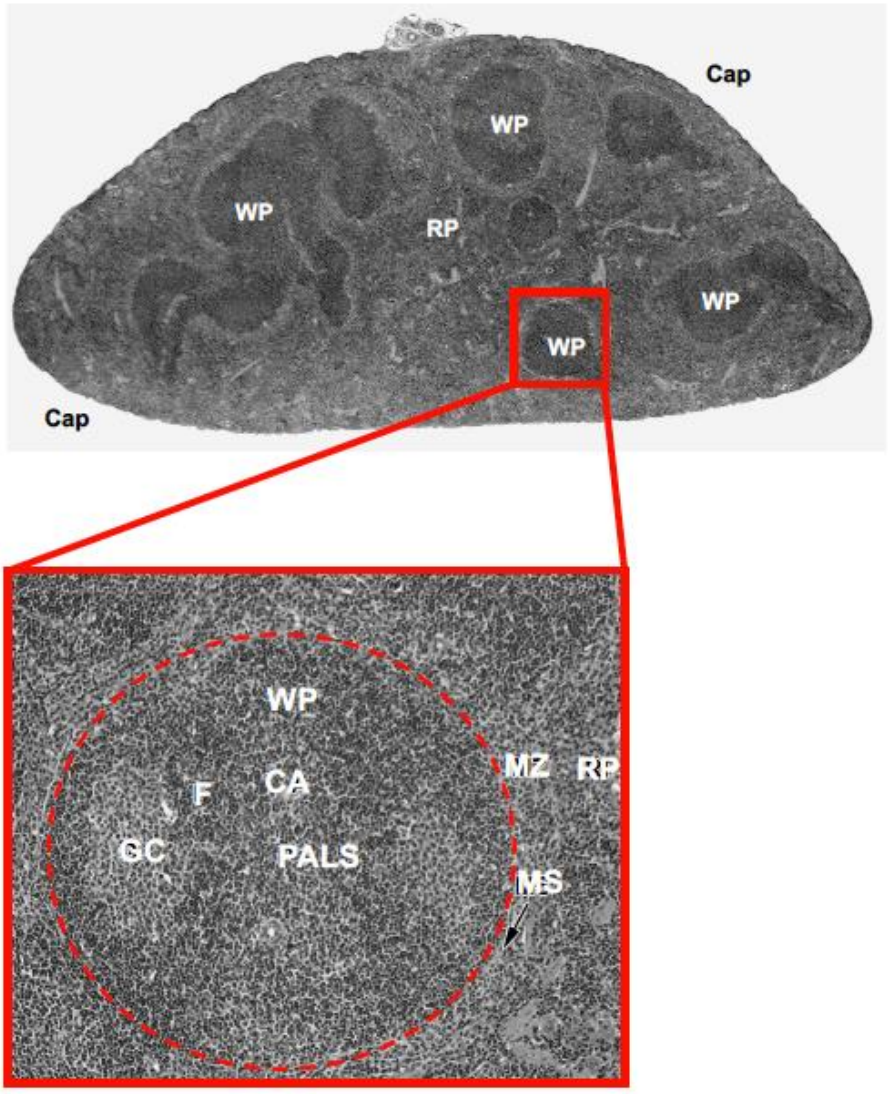

Figure i1. Spleen gross morphology.

Cross-section of an adult mouse spleen in which white pulps (WP) are distinguished from red pulp (RP) for their darker colour. The inset shows the composition of a white pulp, in which the marginal zone, that includes the marginal sinus (MS), contours the WP and represents a region where there is an opened arterial blood stream between RP and WP; the central arteriole (CA) is located in the middle of the WP and is

surrounded by periarteriolar lymphoid sheats (PALS), largely populated by T-cells. In the WP are also present follicles (F), populated by B-cells that massively proliferate in the germinal centers (GC). Adapted from Cesta M.F. et al., 2006 [3].

The red pulp is a unique tissue specialized in filtering blood for old erythrocytes and removing bacteria from blood circulation. The red pulp is characterized by the presence of an open blood system that conveys filtered blood into venous sinuses toward the efferent circulation. The splenic red pulp microenvironment is constituted by different resident cell type. First, the endothelial cells spread along the macro and micro-vasculature of the spleen, apart from open blood system areas which are devoid of endothelium.

The red pulp fibroblasts are spread along the whole splenic tissue; they share some properties with myofibroblasts (e.g. expression of αSMA and desmin) and possibly play a role in spleen contractions [7]; moreover, they are responsible for the secretion of extracellular matrix protein important for the tissue architecture, such as collagens, and the secretion of the so-called basal lamina ECM proteins, like laminins, collagen IV and nidogens. In red pulp, another very important cell type is the red pulp macrophage. This particular macrophage subset, positive for F4/80 and CD11b markers, is critical for blood maintenance and surveillance by phagocytosing old or malfunctioning erythrocytes, and so they are important for iron recycle, and blood-borne particulates [8]; they are also reported to play a role in parasitic infections.

The white pulp is the second compartment present in the spleen. It is a very important structure that exerts functions of classical secondary lymphoid organs and it has similar composition to lymph nodes, although there are some relevant differences [9] [10]. Both in human and in mice, white pulps are spheroidal masses distributed within the splenic red pulp and are organized into compartments.

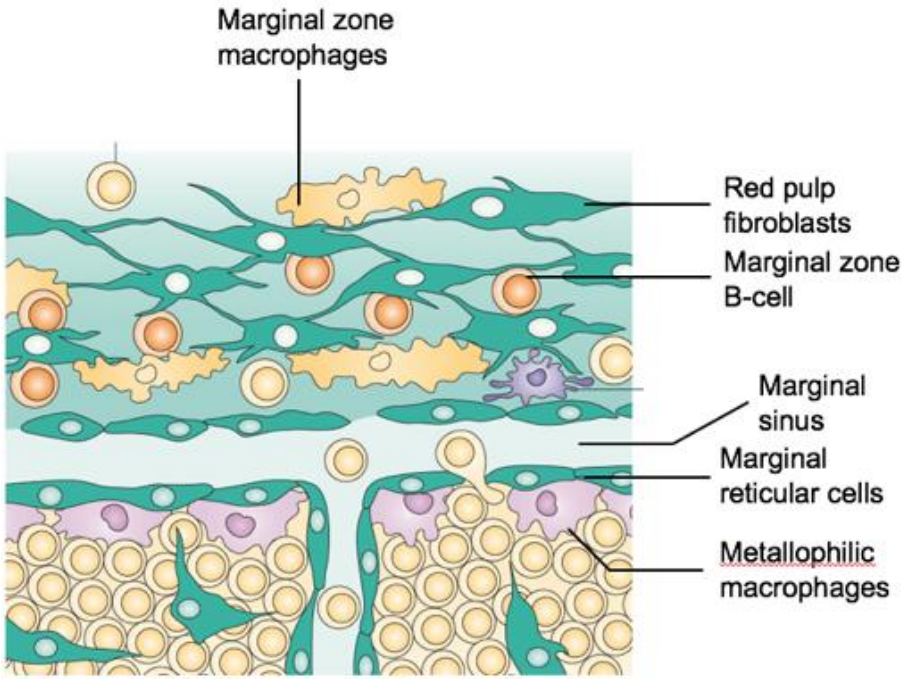

Figure i2. Marginal zone microenvironment.

Marginal zone (MZ) is the region between the red pulp and the white pulp. The MZ is composed by unique cell types, like marginal zone macrophages ($MARCO^+$), metallophilic macrophages ($MOMA\text{-}1^+$), MZ B-cells and the MRCs. These cell types localize near the marginal sinus (MS), that is an open blood system receiving fluids from the red pulp. Adapted from Mebius R.E. and Kraal G., 2005 [9].

The external white pulp portion that lies beneath the red pulp is called marginal zone (MZ) and forms a discontinuous ring along the white pulp. Other than being a transit area, the marginal zone is characterized by the presence of several specific cell subsets specific for this region; there are marginal zone macrophages (expressing MARCO and SIGNR1) and reticular fibroblasts in the proximity of the red pulp, forming a ring around the white pulp, in close contact with the blood stream [11], where the latter are involved in the secretion of the lamininα5, fundamental for the MZ B-cell fate and survival. There are the invariant natural killer T-cells (iNKTs) and the MZ B-cells, crucial in the immune responses against blood-borne pathogens [12] and lastly, there are marginal zone metallophilic macrophages (SIGLEC-1^{+}/MOMA-1^{+}) that are in close contact with the white pulp and particularly with the outer part of the follicle, in close proximity to the mesenchymally-derived marginal reticular cells (MRCs).

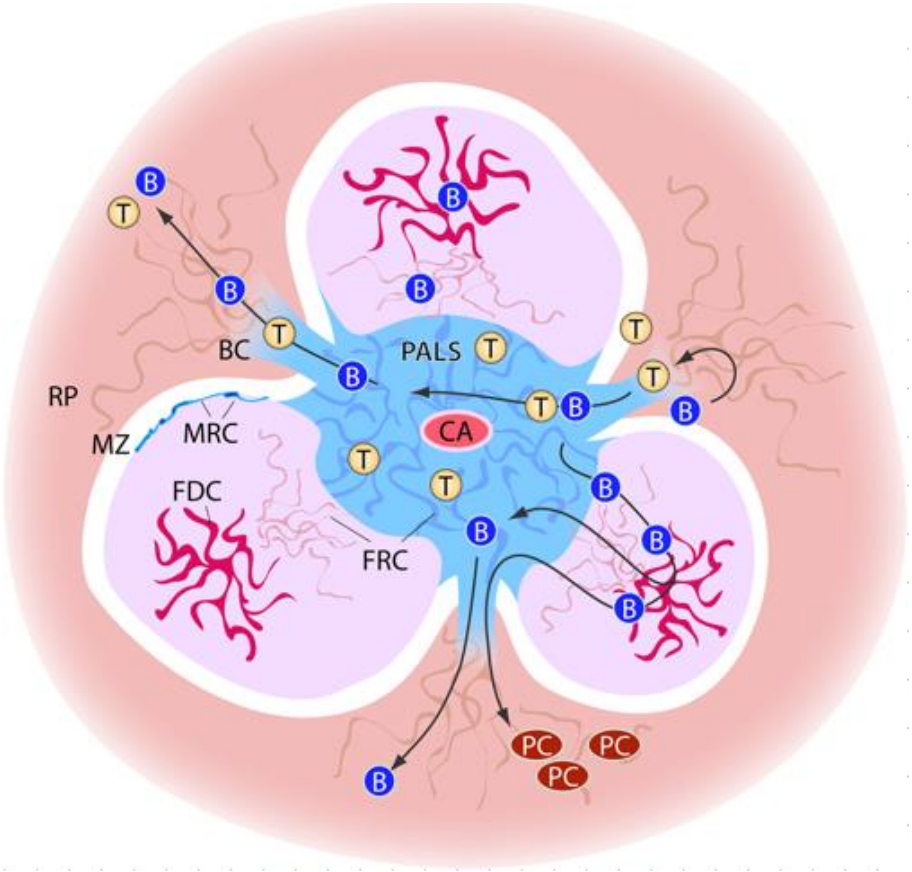

Figure i3. White pulp composition.

Splenic white pulp (WP) is a lymphoid tissue located within the red pulp (RP) of the spleen and surrounded by the marginal zone. It is constituted by different lymphoid and myeloid cell types and three main stromal cell subsets: the MRC, in the outer part of the follicle, the FDC that plays a crucial role in B-cell function and homeostasis, and the FRC, localized in the T-cell area [10].

Within the proper white pulp, lymphocytes are compartmentalized into B- and T-cell compartments. On one hand, T-lymphocytes are mostly

localized in proximity to the central arteriole, a blood vessel that comes from the red pulp and crosses the white pulp, within a region called periarteriolar lymphoid sheath (PALS). On the other hand, B-lymphocytes are present in the follicle, underneath the MZ.

The follicle has great relevance in B-mediated immunity, since local APCs (both $CD45^+$ lineage-derived and mesenchymally-derived) present antigens to B-cells. These regions are characterized by different non-hematopoietic mesenchymally-derived stromal cell subsets [13] that play a crucial role both in leukocytes homing, homeostasis and compartmentalization, and in lymphoid tissue architecture and the formation of resident stromal compartment is LT-pathway dependent [14] [15].

White pulp stromal cells are divided into three main subpopulations. First, the fibroblastic reticular cells (FRCs) are stromal cells resident in PALS and they are also present in the MZ discontinuity to form marginal zone bridging channels (MZBC) [16] [17]; they are important in forming the collagen-based conduit system that crosses the white pulp to deliver antigens to this tissue [18] and to create migration routes for lymphocytes [19]. Moreover, FRCs are the only cells in lymphoid organs capable of maintaining the survival of T-cells through secretion of IL-7 [20]. This stromal cell subset is also known to express and secrete CCL21 and CCL19, it is positive for the glycoprotein gp38 (podoplanin), for myofibroblast markers as aSMA and desmin and it is also capable to produce the matrix proteins such as collagens, laminins, nidogens and the undefined protein named ER-TR7 [21].

The major stromal population belonging to the follicle is the follicular dendritic cell (FDC). FDCs are one of the most studied secondary

lymphoid organ (SLO) stromal cell subset, due to their importance in B-cell mediated immunity. FDCs are non-hematopoietic stromal cell normally present in lymphoid organs [22], but they are also reported to be present in other lymphoid tissues such as mucosa associated lymphoid tissues (MALTs), nasal associated lymphoid tissues (NALTs) and bronchus associated lymphoid tissues (BALTs).

The importance of FDCs arise from the knowledge of their role in the presentation of antigens to B-lymphocytes [23] in the form of immune-complexes [24], and to allow the formation and maintenance of germinal centres (GCs); GCs are transient formations within follicles where B-cells that encountered antigens undergo somatic hypermutation (SHM) and massively proliferate [25]. This massive proliferation determines the formation of two areas in this "secondary follicle": the light zone with $CXCL13^+$ $CD23^+$ FDCs, where there is B-cell selection, and the dark zone with $CXCL12^+$, characterized by proliferating lymphocytes [26] [27]. One of the peculiarity of the FDC area is that it is quite devoid of ECM proteins. Typical markers for FDCs are CD21 (CR2) and CD35 (CR1), that are complement receptors allowing the antigen presentation, and CXCL13, one of the most important B-chemoattractant; moreover, during GC reaction, FDCs can differentiate into light zone FDC (LZFDC) becoming CD23 positive, and dark zone FDC (DZFDC) positive for CXCL12, where the centroblasts start massively proliferating and can occur class switching [26] [28].

Lastly, the third stromal subpopulation called marginal reticular cell (MRC) localizes in the external part of the follicle, directly beneath the marginal sinus and the marginal zone. Very little is known about this

stromal cell subtype. In the steady state condition, both lymphocytes and antigens will enter the white pulp by entering the marginal zone and crossing the MRC ring [17], thank to the conduit system that in turn can be possibly formed with the MRC help. These marginal fibroblastic-shaped cells share both FRCs and FDCs markers, indeed they are reported to be gp38, ER-TR7 and VCAM-1 positive and are probably responsible to produce collagens and laminins of the outer region of the follicle, and they also positive for MAdCAM-1 and BP-3 and they are capable to secrete CXCL13 upon LTβR engagement [29]. Of note, in 2014 Jarjour and colleagues demonstrated that MRCs have some precursor cell capacity at least in lymph node, since MRCs are possibly the solely cell type contributing to the FDC expansion in follicles during immune responses, so that neither FRC or circulating progenitors are significantly contributing to this [30].

1.1.1.2 The Lymph Node

The lymph nodes (LN) are SLOs disseminated along the body in specific position to allow quick responses to foreign antigen drained from the circulation [31]. As the splenic white pulp, lymph nodes are divided into substructures in which B and T cells separate into different areas. Lymph nodes are very plastic SLOs, since that, after infections and inflammatory state, they enlarge to host an increased number of lymphocytes, due to massive recruitment and to in situ proliferation (e.g. germinal centre reaction) and increased number of other hematopoietic and non-hematopoietic cell recruitment and proliferation [32]. This process is further exacerbated by the fact that few days after

the infection, the lymphocyte egress is transiently blocked by the expression of interferon type-1 (IFNI) and the upregulation of homing [27].

The LN swelling and the consequent enhancement of immune response lasts about three weeks, then there is the return of the organ to the steady state condition. LNs are encapsulated organs filtering whole body fluids thanks to a diffused lymphatic system that collects fluids from tissues and from vascular circulation [27]. Lymph nodal lobules are subunits that divide the organ, arranged side-by-side and connected by fibrous radial trabeculae [33] and lobular architecture may vary based on anatomical location, age, diet and antigen exposure. Each lobule is connected with an afferent lymphatic vessel that transports the lymph towards the LN and in particular in the subcapsular sinus (SNS), where antigens, microbes, leukocytes are released. The lymphatic system usually runs along the blood vessel system, both for a functional reason and for a developmental reason, since lymphatic vasculature during embryogenesis arises from a mature, functional cardiovascular system [34].

Afferent lymphatic vessels collect lymphs throughout the body to release it in LNs, efferent lymphatic vessel drains lymphs from lymph nodes medulla towards the thoracic duct; both type of vessels are composed by lymphatic endothelial cells (LECs), surrounded by myofibroblasts expressing αSMA, that help fluids flow through contraction, and these vessels have valves $VECad^{+}$, but not $PECAM\text{-}1^{+}$, that allow a correct circulation without any back-flow [35] [36]. Apart from lobules, lymph node capsule and lymphatic vessels, there are clear similarities between lymph node structure and composition,

and the splenic white pulp. Within the SCS, where lymphatics empty their load, there is a macrophage line resembling the splenic marginal zone macrophage line [27], while lymphocytes mainly enter through high endothelial venules (HEVs) and then segregate into specific B/T cell areas populated by specific stromal cell subsets.

The three stromal cell subsets previously described are present also in LNs, so that T-cell zone is populated by FRCs, that provide a structural support for conveying antigens through the conduit system and for the anchored dendritic cells (DCs), other than providing a supportive microenvironment by secreting homing chemokine and homeostatic cytokines; the B-cell zone is also called the follicle, where FDCs support both homing, homeostasis and antigen-presented B-cell maturation and so GC reaction. Moreover, similarly to spleen, in the outer region of the follicle, next to the SCS, there is the third SLO stromal population, the MRCs, characterized by retaining some precursor features, other than sharing some FDCs markers.

Recently, it has been described by Bajénoff laboratory the presence in LNs of a fourth kind of stromal population, that lays between FRCs and FDCs and that are probably a FRC subpopulation, which is called versatile stromal cell (VSC) [37]. These VSCs share FRC origin and markers, although, during LN swelling that follows infections, these stromal cells greatly expand and acquire some FDCs markers, for example the expression of CXCL13 upon LTβR engagement, although they continue secreting ECM proteins, such as collagens. These stromal cells reflect the LN plasticity upon and after infection resolution, when after lymphocytes withdrawal they indeed regress to the previous limited area and they lose CXCL13 expression. In all of these

processes, the ECM plays a crucial role since the LN scaffold need to have elasticity to host that huge number of cells required for lymph nodal immune response, but need also to be solid and not loose. The ECM is indeed degraded and synthesized mostly by mesenchymal and endothelial cells in order to facilitate LN enlargement and return to steady state (where also vasculature is modified).

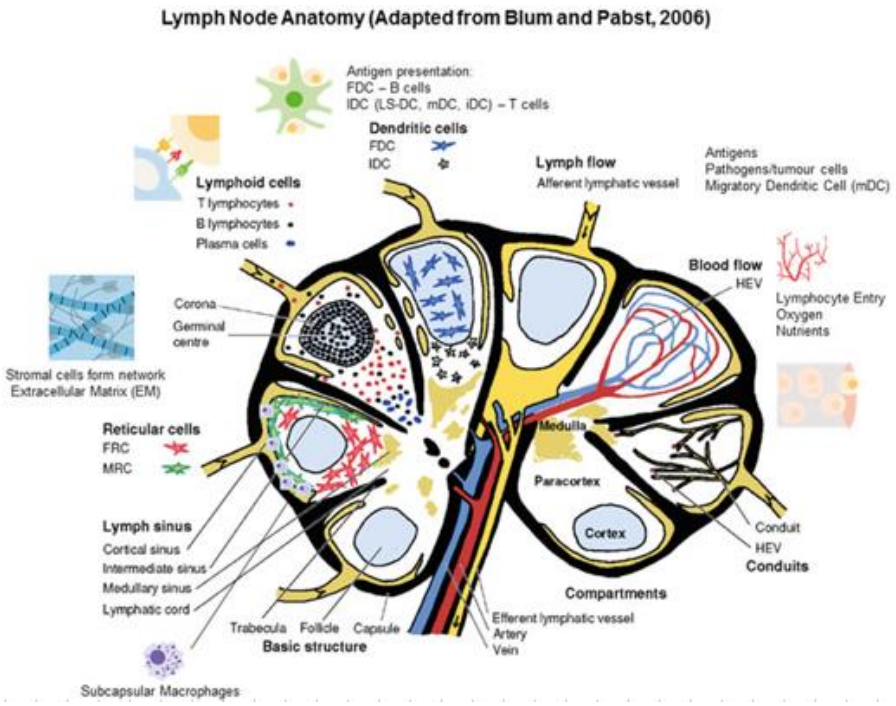

Figure i4. Lymph node structure and composition.

The LN is divided in lobules, each of them is constituted by the same structures and cell types. Afferent lymphatic vessels release their content within the LN subcapsular sinus (SNS), while efferent lymphatic vessel drains lymph from medullary region. Lymphocytes and APC can exploit this system to enter in B/T-cell areas, where immune responses take place [38].

1.1.2 THE PERITONEUM-ASSOCIATED LYMPHOID TISSUES

The peritoneum is a lining of the abdominal cavity and it is constituted by mesothelial cells and connective tissue. The peritoneum includes different lymphoid tissues, as the mesentery, the omentum and in

general the peritoneum-associated lymphoid tissues (PALTs) that play role in both mechanical stresses and in cavity safeguard.The peritoneum is protected by both innate and adaptive immunity, as other organs are, although most of the immune clearance is based on innate cells such as macrophages and neutrophils [39], and adaptive immune system plays a secondary amplification role in the case of persistent infections.

1.1.2.1 The Omentum

The omentum is tissue mainly composed by adipocytes and pre-adipocytes localized from stomach to colon, including spleen and pancreas. Omentum has been reported from surgeons to have both wound-healing and angiogenic capacities [40], other than playing a role in both innate and adaptive immunity. Its wound-healing properties has been extensively exploited in decades in breast cancer; after radical surgery of the mass, the local omental transposition proved to be a valid method to restore epithelial cover of the injured area [41]. The omentum is characterized by the presence of cell aggregates called milky spots (MS, now called omental FALC) [42], which are enriched in leukocytes and mesenchymal stromal cells, surrounded by endothelial cells [39]. These clusters can grow in number and dimension depending first on the age of the subject, secondly it depends on the inflammation status.
During both human and murine embryogenesis, $CD5^+$ B-cells, which is one of the markers of B1-lymphocytes, are the most present B-subset and their precursors arise from the fetal omentum and liver [43]. Afterwards, B1 cells are maintained and their progenitors self-renew in the peritoneal cavity, including the omentum, making it a niche for this

particular cell type. It is still debated whether this organ is a SLO or not. It is considered a sort of SLOs for the immulogical responses that induces, but on the other hand it is not included in this category since it doesn't share the same microenvironmental components.

The omentum shows an enriched population of macrophages, of B1 cells and neutrophils, but there are less B2 lymphocytes as compared to SLOs, there are stromal cell, but there is no presence at all of FDCs, normally present in SLOs, the only described population is indeed a $CXCL13^{+}$ mesenchymal cell type and moreover there is no capsule separating the MS tissue from the outside. The ECM matrix present in the omentum shares some SLOs components, such as collagens, mostly collagen IV, and laminins, but it is also present ER-TR7, a matrical protein usually associated to FRCs in SLOs and to red pulp fibroblasts [44]. More interestingly, the ablation of lymphotoxin pathway (LT) in lymphoid tissues usually results in loss of the tissue or in a complete disorganization of the organ such as spleen disorganization or absence of inguinal lymph nodes, while the LT pathway ablation does not result in any particular phenotype in omental lymphoid tissues, that of *Cxcl13* causes the loss of MS. This suggests also the independency of omental MS formation on $CD45^{+}$ lymphoid tissue inducer (LTi) cell stimulation on CD45- lymphoid tissue organizer (LTo), but still it should be considered a lymphoid tissue since it is embryonically defined.

As previously said, omentum plays a crucial role in immunity because it represents a B2 cell route of circulation from SLOs that are nearby the peritoneal cavity, making them to upregulate integrins when entering the peritoneal cavity, for example VLA-4 and down-modulating those integrins in peritoneum egress [45]. Although the

importance of the omentum in controlling infections and in experiencing both innate and adaptive immunity in the peritoneal cavity, omentum also shows a dark side in cancers and this depends primarily on resident fibroblasts. It has been recently demonstrated that ovarian cancer, that usually metastasizes in the peritoneal cavity, preferentially seeds and then creates metastasis in the omentum [46]; only after this event, ovarian cancer starts spreading along the peritoneal cavity and in other organs.

1.1.2.2 The Fat-Associated Lymphoid Cluster

The fat-associated lymphoid cluster (FALC) is a very recently described tissue that localizes in the peritoneal cavity, along with the mesentery [47] and in close contact to visceral fat. FALCs are considered atypical secondary lymphoid tissues, since they do not have all SLOs features [42]. They do not have any capsule surrounding cell clusters and still it is unclear whether they are embryonically present and if they are genetically pre-determined. The parallelism between FALCs (also called mesenteric FALCs, mesFALCs) and omental MS is suggested in different papers, given that they share localization, general composition and immune responses sustained. FALCs microenvironment is constituted, in steady state, by macrophages, iNKT cells, B-1 cells, vascular endothelial cells and lymphatic endothelial cells, and stromal cells. Resident stromal cells are defined as CXCL13+ non-proper FDC, because of the lack of CD35 (CR1) and FDC-M1 markers on their surface, albeit, they are described to contribute to B-cell homing and retention, and B-lymphocytes

proliferation and germinal centre-like reactions [48]. FALCs formation is LT pathway independent, like the omentum, but their formation is inflammation-dependent and the number and the dimension of these tissues are also related to age of the subject [49].

Among all different inflammatory stimuli, TNF pathway activation is the most important route for triggering the inflammation-dependent generation of FALCs [48]. Myeloid cells and adipose tissue are the candidate for that TNF pathway triggering. Myeloid cells, such as macrophages and monocytes, induce the formation *ex novo* of mesenteric lymphoid clusters, the ablation of TNF signalling blocks the newly formation of FALCs indeed, but not the migration of myeloid cells [42]; moreover, also iNKT-derived inflammatory stimulation through CD1d-glycolipids binding is able to induce FALCs, it has been demonstrated indeed by Caamano's group that CD1d knockout mice do not develop any mesFALC [48]. Adipose tissue can also participate in FALCs formation. The reason why also this tissue is such a candidate is that adipose tissue resident stromal cells secrete a discrete amount of TNFα [50] (it has been described indeed a direct correlation between obesity and sera TNFα) and given that FALCs arise from mesenteric fat tissue, also the latter can play a role in the formation of these lymphoid clusters.

1.2. THE CANCER MICROENVIRONMENT

In general, tumours are composed of cells that bypass classical cell cycle checkpoints and proliferate, but still retain some features of the original tissue from which they arose. Tumours result from continuous cell insults that transform more and more this tissue unit to give rise to

cancer initiating cell. There are two mayor kinds of insults that can occur: DNA damage or chronic inflammation. These two tumourigenic mechanisms can occur concomitantly or sequentially during cancer onset and progression. Tumours are usually defined as heterogeneous populations of cancer cells that modify the microenvironment to increase their survival and chemoresistance [51].

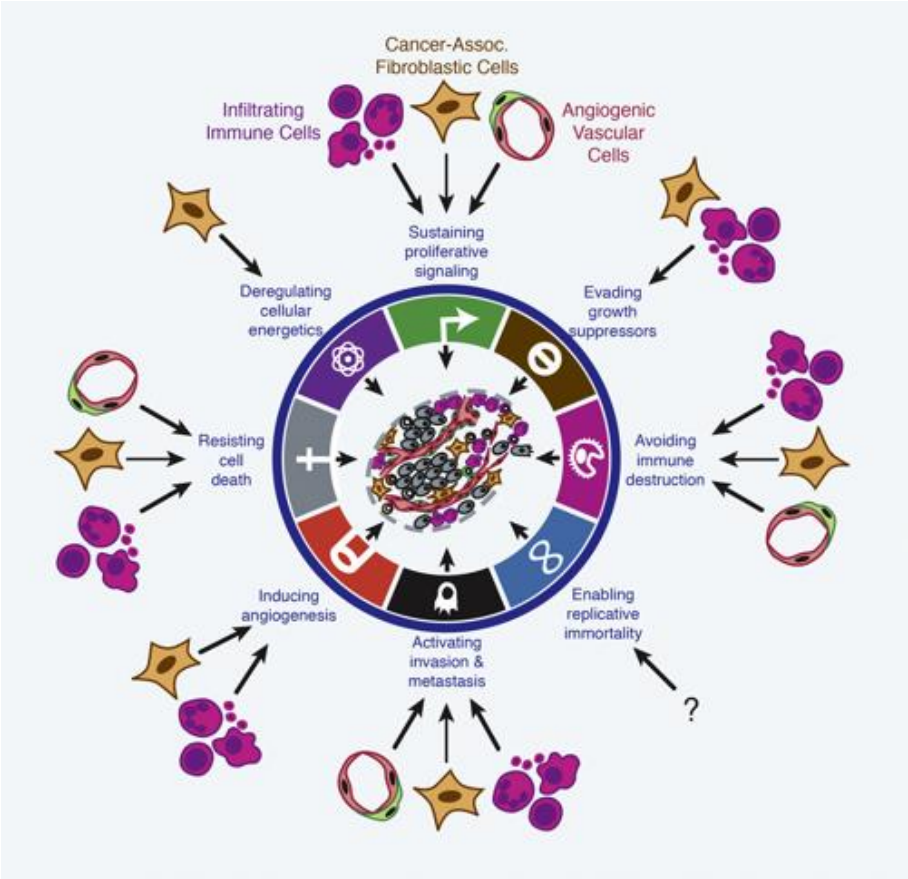

Figure i6. The cancer hallmarks.

Cancers deregulate several pathways to survive and expand; moreover, tumours interact with microenvironment components and

cause changes in the milieu that increase their survival. Myeloid cells, endothelial cells and stromal cells, educated by cancer cells, activate pathway that contribute to the expansion of malignancies and the metastasis [52].

Along with the multistep development of a tumour, cancers acquire skills that improve their survival. In order to remain alive, a tumour should proliferate, despite adverse conditions, or at least resist to cell death, other than activating invasive mechanisms in later stages [53]. Although the mechanisms described in the previous picture seem to be sufficient, cancer needs the microenvironment to improve survival, chemoresistance and to satisfy its metabolic demand.
Recently, attention has focused on the tumour microenvironment, so that the mutual dependency between tumour and its surrounding milieu actually becomes crucial in cancer research. There are indeed several reports claiming that targeting the microenvironment improves routine therapies. The tumour microenvironment is generally composed by $CD45^+$ cells such as i) lymphoid and myeloid cells, ii) secreted factors including exosomes, chemokines and cytokines, iii) ECM proteins, iv) blood endothelial cells, and v) $CD45^-$ stromal cells.

1.2.1 THE SOLID TUMOUR MICROENVIRONMENT

Solid tumours develop in tissues with diverse microenvironment depending on the tissue itself. Along with disease progression, tissue microenvironment undergoes remodelling, and this is based on the

cancer specific requirements, given that every cancer depends on a proper microenvironment for sustaining its survival, its growth and finally its invasion and metastasis. From this perspective, tumours can be seen as organs with eventually high level of complexity. The increasing interest in the tumour microenvironment arising in last decade is due to the continuous observations that the disease phenotype is not only the result of cancer cells, but it is also the result of the corrupted microenvironment.

The long work of microenvironment "instruction" operated by malignant cells creates a collaborative situation in which both resident and BM-derived stroma support the formation of a neoplastic tissue [52]. Altogether, tumour microenvironment (TME) is becoming a new broad field of investigation, given that it is genetically stable and the targeting of TME with chemotherapeutic drugs appears to be an attractive method to co-adjuvate the proper anti-cancer therapies [54].

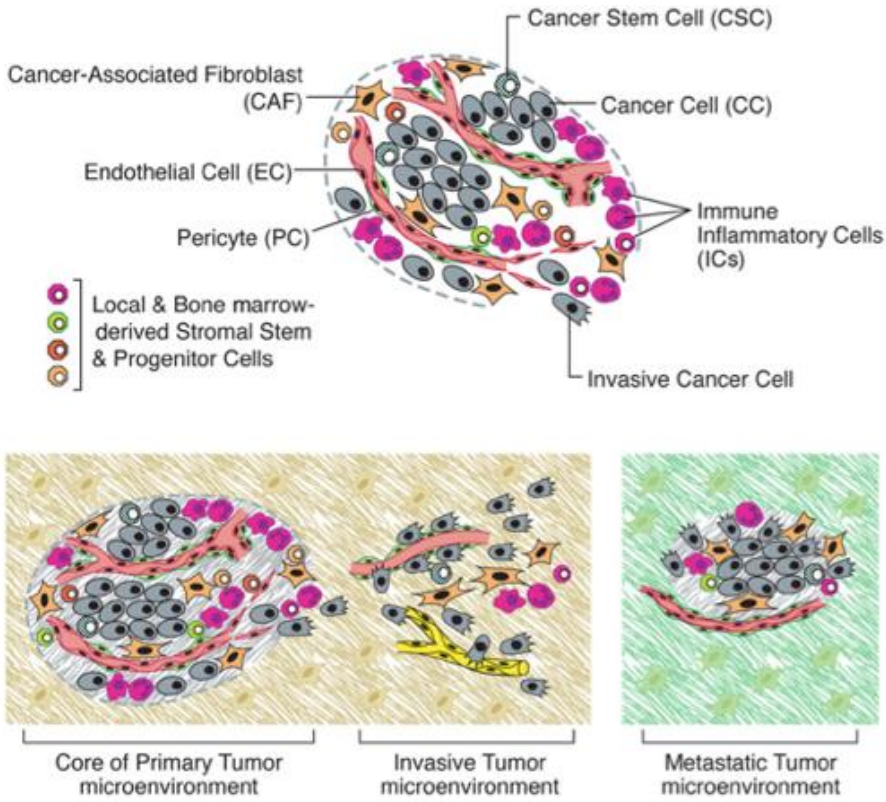

Figure i7. The cancer microenvironment.

The cancer microenvironment is constituted by different kind of cells that exert different functions. T-reg lymphocytes and M2 tumour associated macrophages (TAMs) that determine the formation of an immunosuppressive microenvironment; stromal cells participate in cancer chemoresistance and in tumour support. Moreover, these cell types are able to recruit endothelial cells to the tumour burden and remodel the native ECM to further support tumour growth and metastasis [53].

The solid tumour microenvironment is usually constituted by a consistent population of M2-like macrophages, which are considered by the most the tumour associated macrophages (TAMs), that contribute to neo-vasculogenesis and immune-suppression [55] [56], T-reg cells, that abolish T-cell mediated anti-cancer immunity, endothelial cells, allowing tumour nourishing and spreading in other tissues, and stromal cells, usually called cancer-associated fibroblasts (CAFs). Fibroblasts associate to cancer from its onset to the terminal metastatic phase [57].

CAFs are always found associated to tumour burden and can also localize within the tumour mass; while on one hand, pre-CAFs show an anti-tumoural activity, mature CAFs sustain tumour foci in different ways. CAF refers to a category that includes mainly two kinds of stromal cells: the myofibroblasts, the activated fibroblasts, and the activated adipocytes [58] [59]. Each of these two stromal population are associated to a more aggressive disease, since they proved to be involved in several functions important for malignant cells: CAFs exhibit pro-angiogenic functions through the secretion of VEGFs and the MMP-driven ECM proteolysis of fragments with angiogenic functions through MMP-9 and MMP-2 action (also for the release of VEGFA bound to ECM) [60]. Moreover, activated stroma can recruit immune cells to tumour site that in turn are modulated by the immune-suppressive environment to a cancer-permissive phenotype.

One other important function of the stroma is the secretion of ECM proteins; if the functional parenchyma insult is chronic, CAFs can secrete ECM-related proteins as normal stromal cells do, although they either secrete abundant ECM with the forming tumoural tissue, creating

the so called desmoplastic stroma, or remodel the normal organ architecture to create a more favourable niche to cancer cells. Only activated fibroblasts participate in the creation of a tumour microenvironment (TME).

The *primum movens* for the recruitment, proliferation and activation of resident parenchymal and BM recruited stroma is the secretion of TGFβ, PDGFα/β and FGF2 in solid cancers, as exhaustively explained by Elenbaas and Weinberg in 2001 [61]. These factors are both released by fibroblasts themselves, so that these factors act in paracrine and autocrine fashion, and by epithelial cells (e.g. in breast cancer). Other key molecules for fibroblast activation in malignancies are IL-1β, that induces NF-kB and promotes its pro-inflammatory function, and LIF, that in turn has been associated with myofibroblast functions with an invasive profile [62]. Concerning the mature CAFs phenotype, in general they are referred to as αSMA^+ and $Vimentin^+$ fibroblasts that express VCAM-1 on their surface and secrete chemokines related to the tissue of origin and factors like TGFβ; moreover, they usually secrete ECM-related proteins such as collagen I, III and IV, fibronectin and tenascin C [57].

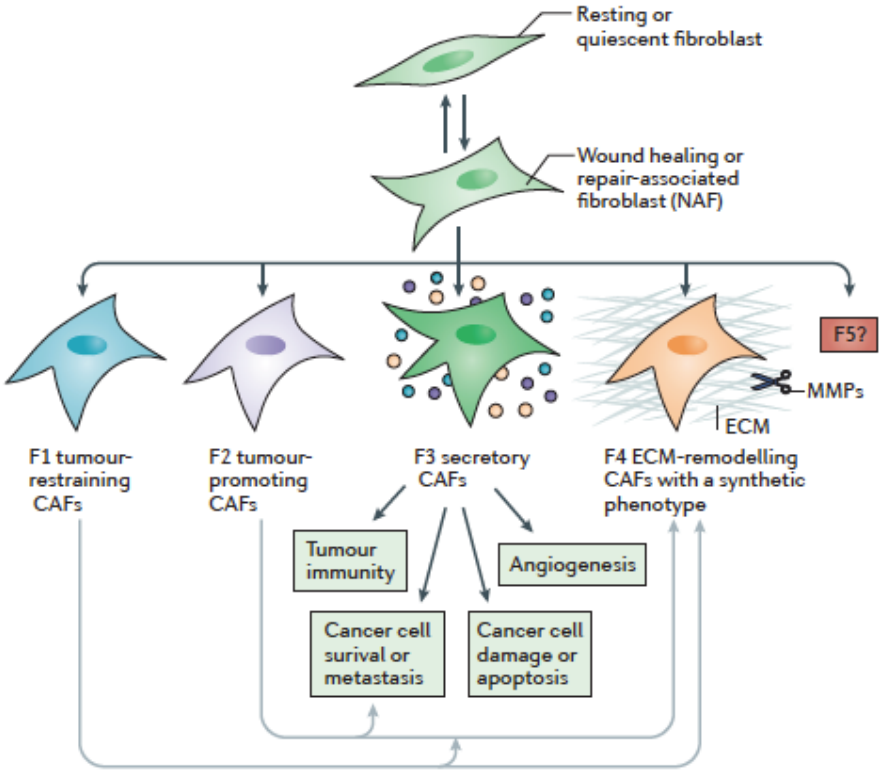

Figure i8. The fibroblast differentiation to cancer-associated fibroblast.

Cancers-associated fibroblasts (CAFs) arise from resident fibroblasts that, depending on stimuli received, transform into a tumour-prone stromal cell. CAFs sustain cancer progression through ECM remodelling, endothelium recruitment and cancer cell sustenance [57].

CAFs, as reported in an overwhelming number of papers, are able to produce large amount of ECM and to remodel native ECM scaffolds. The role of the stromal-secreted ECM and ECM-related proteins in

cancer progression have been demonstrated. Indeed ECM determines the formation of a pro-survival and chemo-resistant cancer niche.

A remodelled ECM can directly affect cell transformation and metastasis [63]; moreover, an aberrant ECM also affects stromal cells by promoting a fibroblast conversion to CAF-like phenotype. During cancer progression, several ECM proteins are deregulated, as a result of a microenvironment reprogramming. This sort of "soil priming" is a hallmark of quite all solid tumour lesions [64], but before becoming a fully formed solid tumour microenvironment, cancer cells need to prime tumour foci. Primary malignant mass and pre-metastatic niches are initially characterized by the secretion of collagen I and IV, by the expression of fibronectin, and by the upregulation of LOX enzymes. These lysyl oxidase enzymes have been demonstrated to play a crucial role in the formation of pre-metastatic foci, where hypoxic malignant cells (and perhaps activated fibroblasts). LOXes cross-link collagen IV fibers in basal lamina [65], thus increasing matrix stiffness, that in turn allows leukocytes adhesion. Then, leukocytes secrete MMPs (in particular MMP-2) that cleave collagen to release portions that recruit cells to the forming focus, exacerbating the microenvironment modification. Of note, serum collagen I cleaved fraction has proved to be a prognostic factor, so that the presence of soluble form of this protein in solid tumour patients in sera correlates with bad prognosis in recurrent breast cancer (amino-terminal pro-peptide of type I procollagen, PINP) [66].

There are other ECM related proteins frequently found overexpressed in cancer that can be proteoglycan, such as nidogen I, receptor like heparan sulfate - that binds VEGF to sequestrate it from circulation -

and glycoproteins such as CD44 that play a role in cell-cell interactions [63]. New therapies recently developed focus on modulating the pro-inflammatory microenvironment and on resolving the ECM remodelling to better deliver drugs, avoiding in this way the microenvironment-derived chemoresistance, and to prevent relapses due to a cancer-conditioned tissue [57]. Some examples are the addition of anti-TGFβ therapy to the usual chemotherapy for modulating the immunosuppressive malignant environment, or the use of CP4H (collagen prolyl-4-hydroxylases, an enzyme responsible for the correct biosynthesis of collagens) inhibitors that decrease or even abrogate the formation of breast and lung cancer metastasis [67].

1.2.2 THE BLOOD CANCER MICROENVIRONMENT

Blood malignancies are tumours involving circulating cells of hematopoietic origin, both myeloid and erythroid lineages, and lymphoid origin. As such, blood malignancies are proper tissues, although they usually rely on organ-specific microenvironment for maintenance and expansion. Blood cancers, defined as leukaemia, arise from different stage of myeloid and lymphoid maturation and every blood cellular constituents can develop in cancer.

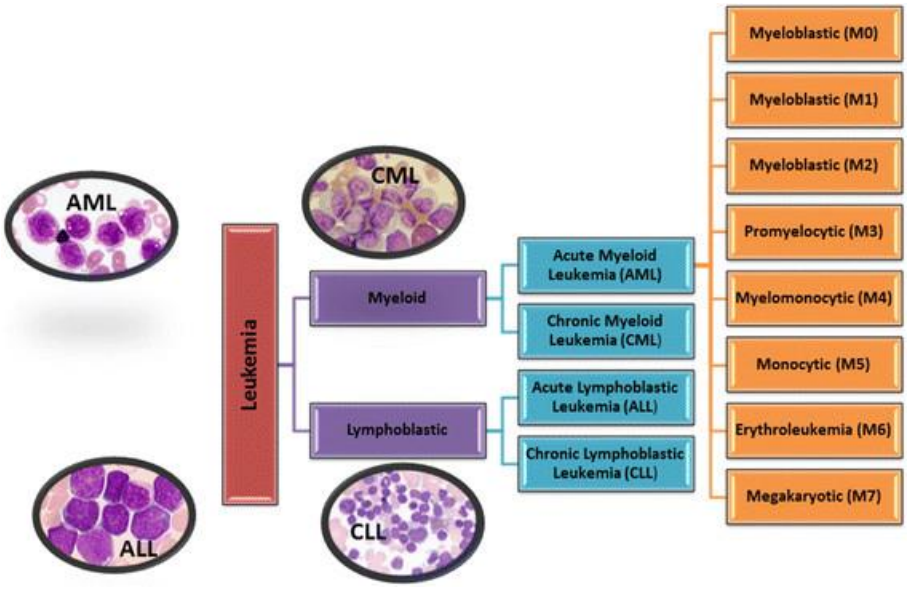

Figure i9. The leukaemia classification.

Leukaemia can affect every blood cell type. The two main classification of leukaemia are based on developmental evidences: a blood cancer can be either acute or chronic, and it can derive from a lymphoid lineage (lymphoblastic/lymphocytic) or from myeloid [68].

Leukaemia in USA accounts for about 3% of all cancer, with a clear prevalence of onset on white male as compared to white female and Afro-American population [69]; moreover, the most of leukaemia are diagnosed in adulthood, after 40 years. The classification of blood malignancies is based on the onset and trend of progression (acute or chronic) and the cell lineage affected (lymphoid or myeloid). The most common blood cancers are: acute myeloid leukaemia (AML), acute lymphoblastic leukaemia (ALL), chronic myeloid leukaemia (CML) and chronic lymphocytic leukaemia (CLL) [68].

The leukaemia microenvironment is constituted by quite the same kind of cells that form the solid tumour microenvironment, although the development of this blood malignancy occurs in lymphoid organ niches that usually host hematopoietic precursors or mature cells. The link between lymphoid organs and leukaemia is strong, bone marrow infiltration is indeed one of the diagnostic parameter used in patients. The microenvironment is fundamental in these blood cancers, and it is found differentially modulated in all blood malignancies; as example for explaining this phenomenon, I will briefly talk about hairy cells leukaemia (HCL) and multiple myeloma (MM), two pathologies highly related to their microenvironment.

Hairy cell leukaemia (HCL) belongs to the CLL group, in which a still debated mature B-cell subtype (thought to arise from splenic marginal zone B-cells, SMZB) evolves towards a malignant phenotype characterized by the presence of an irregular cell surface with hair-like protrusions [70].

HCL is characterized by the BM and spleen infiltration, but not lymph node. The HCL spreading is only the reflex of the pattern of adhesion molecules found on the surface of these malignant cells; they consistently express VLA-4 ($\alpha_4\beta_1$) and $\alpha_v\beta_3$ [71] [72]. The integrins $\alpha_4\beta_1$ and $\alpha_v\beta_3$ are the ligands for VCAM-1 and Vitronectin, where the first is a classical marker for fibroblasts and the second is a typical fibroblast-secreted ECM protein, in particular splenic red pulp fibroblasts and BM sinusoid fibroblasts, and that partially addresses the question of HCL preferential localization within organs. To further confirm this data, HCL shows also strong binding to fibronectin, that is another important fibroblast-secreted glycoprotein. HCL cells migrate

to sinusoidal part of lymphoid organ towards a CXCL12 gradient, expressed in part by endothelial cells, where they adhere to vascular cell membrane for extravasating and reaching the most favourable niche [73]. In this process, HCLs modify the microenvironment for creating a more leukaemia-prone local milieu; HCL is indeed characterized by profound remodelling of sinusoidal vasculature, where hairy cells attach to laminins of the basal lamina and where they displace endothelial cells, thus forming the so-called "pseudosinuses" [74]. The most important microenvironment modification occurring in HCL is the BM fibrosis. The HCL-induced BM fibrosis is a mechanism caused by release of FGF-2 and TGFb1 by HCLs that act on HCL itself (the first) and on resident fibroblasts (the second) by determining an increased production of fibronectin and "reticulin fibers", that are mainly composed by collagen III fibres [75] [76] [77]. This reticulum differs from the one of myelofibrosis because of the excessive presence of collagen III instead of collagen I and for no evident signs of fibroblasts proliferation.

Multiple myeloma (MM) is characterized by accumulation of leukemic B-cell, at the stage of plasma cells, in the BM. MM can develop *ex novo* or it arises from benign monoclonal gammopathy of undetermined significance (MGUS), that indeed has a milder phenotype as compared to MM, so that it has a mild marrow plasmacytosis but there is absence of bone lesions and other leukaemia features. MM is a pathology that, along with the disease progression, is associated with high levels of monoclonal antibody proteins [78], anaemia and osteolytic lesions. In addition to this, MM can further progress in acute myelogenous leukaemia [79]. Given that, normal plasma cells usually localize within

bone marrow and that also MM cells house in the marrow, BM microenvironment appear to be fundamental for the malignancy sustainment. BM stromal cells are relevant sources of IL-6, SDF-1α, FGF and VEGF, that are in turn up-regulated in the presence of MM cells. The engagement of myeloma integrins with VCAM-1 and ICAM-1 on stromal cells triggers the NF-kB pathway on the latter [80], and furthermore MM cells secrete relatively high amount of TGFβ and TNFα that induces stromal cells to produce and remodel the surrounding ECM; moreover, bone marrow mesenchymal cells express SDF-1α and VEGF that are important in MM homing to BM and their level are also regulated by *in situ* MM cells [81]. The interactions between stroma and cancer cells activate proliferation and anti-apoptotic signalling, thus creating a supportive MM niche, although the release of IL6, IL1, VEGF, SDF1α by BM stromal cells stimulates osteoclastogenesis [82].

1.2.3 THE RETINOIC ACID PATHWAY IN LYMPHOID HOMEOSTASIS AND IN THE CANCER MICROENVIRONMENT

The retinoic acid is a vitamin A and β-carotene metabolite whose intake comes primarily from the diet. The retinoic acid (RA) is metabolized by specific retinaldehyde dehydrogenases (Raldhs) that catalyse its reaction from retinaldehyde, that in turn is synthesized by the conversion of retinol into its aldehydic form, thank to retinol dehydrogenases (Rdhs) [83].

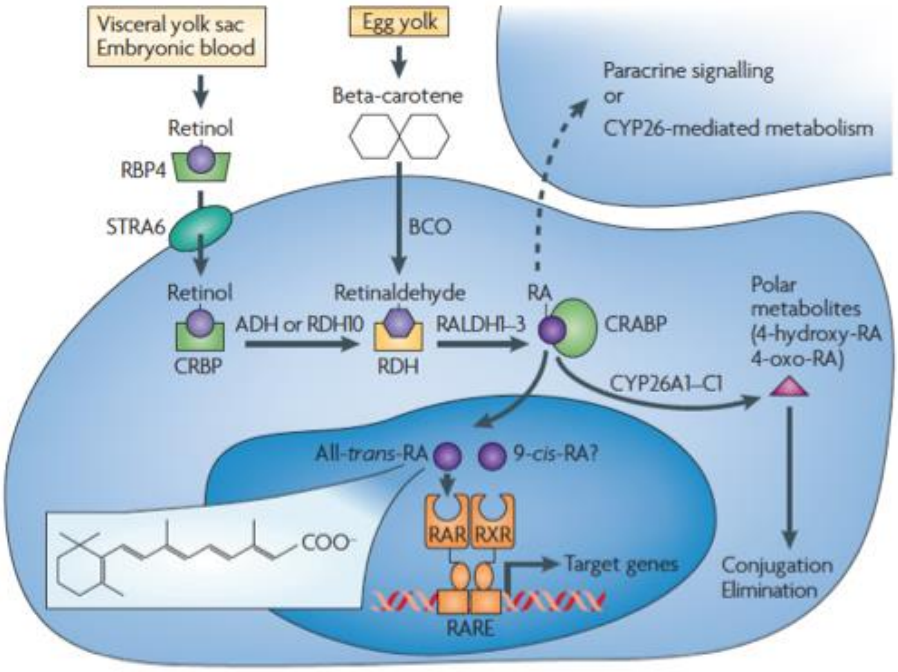

Figure i5. The retinoic acid pathway.

The RA pathway is constituted by different kind of proteins like serum transporters (RBPs), transmembrane receptors (STRA6), synthesizing and degrading enzymes (RALDHs and CYP26s) and nuclear receptors (RARs and RXRs) that bind retinoic acid responsive elements (RARE). The binding of RA with its receptors causes the release of the inhibitory complex bound to RARs proteins, and this triggers the transcription [83].

During embryonic development, RA is important in the development of a plethora of organs; to do that, RA is distributed along embryonic axis in gradients finely regulated [84] [85]. Moreover, RA pathway is still important in adulthood, since it regulates fertility, maintains the

ocular steady state and it is important for immunity. The central role of RA in immunity is well known and well established. It is involved both in proliferation and in cell fate specification; for example, RA determines the innate lymphoid cell (ILC) specification towards the ILC3 phenotype through the RORγt receptor engagement [86].

The ablation of vitamin A signalling in adult immunity impairs several mechanisms [87], such as the normal regeneration of mucosa after infections, it decreases the effects of neutrophils, macrophages and NK cells, and it also impairs the normal B and T-cell differentiation and proliferation [88] [89]. RA acid signalling is also described to be important for α4β7 integrin expression; this integrin plays a crucial role for gut-homing BM-derived progenitors (mostly phagocytes with a immuno-suppressive potential, albeit lymphocytes also express α4β7), that in turn regulate the gut inflammation, so that lack of α4β7 for RA pathway inhibition can result in increase in intestinal inflammation, for example colitis [90]. Of note, it has been shown that RA causes B1 cells, localized in the peritoneal cavity, to undergo Ig isotype switching from IgM to IgA in the presence of RA and TGF-β [91], and that RA can alter T-mediated immunity both via inducing generation of T-reg cells and by favouring the evolution of type 2 T-helper cells instead of Th1, which play a crucial role in immunity against parasitic worms [92]. This further underlines the importance of RA in also triggering different kind of immune responses.

The retinoic acid pathway shows its importance also in regulating the development and the maintenance of secondary lymphoid organs. RA is involved in the formation of lymphatic and blood endothelial cells layers; the increase in RA signalling indeed induces the formation of

large waving vessels with less sproutings, as compared to normal RA signalling condition, and in addition, this increase determines the up-regulation of αSMA in mural cells outside the vessel beds [93].

The lymphatic system transports body fluids towards lymphoid tissues; LECs arise from blood vasculature, RA on BECs induces an increased proliferation and a decreased differentiation [94], but on the other hand, another paper showed how the retinoic acid signalling determined the differentiation from precursors to mature LECs; the block of RA signalling indeed produced an expansion of lymphatic cell precursors at the expenses of mature lymphatic vasculature [95].

A finely tuned retinoids concentration and gradient is fundamental in SLOs formation. For lymph nodes development, retinoic acid acts on the two cell types involved in the generation of the lymph node anlage: the hematopoietic lymphoid tissue inducer (LTi) and the mesenchymal lymphoid tissue organizer (LTo). LTi cells are described to belong to type 3 innate lymphoid cell (ILC3) lineage and RA induces the maturation in LTi of ILC precursors through RORγt engagement [86]. Secondly, LTo cells, the mesenchymal precursors of adult stromal cells, express CXCL13 and CCL19/21 to recruit LTi cells (albeit CXCL13 has a preeminent role in SLOs bud formation); CXCL13 has been proved to be under the control of LT pathway, but also RA. *In vitro* RA challenge proved to consistently improve *CXCL13* as compared to control situation. *In vivo* assays showed that Raldh2 is highly enriched in the neuronal structures near the LN anlage and that, nerves stimulation caused the increase in *Cxcl13* expression in mesenchymal cell, probably caused by the local release of RA by neurons [96]. Of note, vitamin A deficit in maternal dietary regimen causes the reduction

in SLOs size and moreover some LNs do not form [86]. On the other hand, the spleen forms in a quite different way, but it is also dependent on RA.

The development of the spleen from E10.5 onward (in mouse) is a matter of sequential transcription factors activation that affects mesenchymal cell migration, cell fate specification and proliferation [13] [6] [97]. Very recently, we have demonstrated the role of RA in spleen formation and that RA signalling must be precisely tuned, since the absence or the over-activation of this pathway show exactly the same phenotype, the absence of the organ [5]. Taken together, all these data obtained so far by many different groups shed light on the crucial role of RA in both immunity and the evolution of secondary lymphoid organs and this can suggest that RA should play a role in malignancies affecting cell immunity or affecting SLO microenvironment.

The retinoic acid pathway is involved in a plethora of cellular and tissue maturation and maintenance steps that also occur in cancer. Cancer cells, as well as normal cells, need to finely tune RA signalling in order to maintain their state, and it is commonly thought that malignancies suffer high RA levels. Together with cancer cells, the tumour microenvironment has to regulate in a very precise way the RA content in the milieu. RA importance in malignancies has been deeply investigated on different kind of pathologies for its properties in inducing maturation in incompletely differentiated tumour cells, thus inducing a proliferation stop and indirectly causing apoptosis [98].

Retinoids and rexinoids are actually used both solely or in synergistic combination with other chemotherapeutic drugs to directly affect cancer growth and survival. It has been demonstrated that retinoids

actively inhibit breast cancer proliferation promoting a senescent cell phenotype in a p53/p21-indipendent manner [99]. The intriguing fact is that RA exploits its anti-tumoural activity independently from breast cancer back-ground; it blocks indeed carcinogenesis and affects the formation of a second cancer focus in the contra-lateral breast after surgery of the primary tumour both on estrogen receptor positive (ER^+) and in ER^- breast cancers. Of note, there is a report underlining the opposite functions of two RARβ isoforms in breast cancer, where $RAR\beta_2$ is down-modulated and on the other hand $RAR\beta_4$ isoform is up-regulated, so that this data, together with the $RAR\beta_4$ conformation, suggests a potential role for this latter isoform as a negative regulator of the RA pathway [100].

Many other solid malignancies show sensitivity to retinoid-mediated chemotherapy [101], while it has also been found that many cancers show the loss of RARs for gaining proliferative advantage; for example, pancreatic adenocarcinoma shows a consistent loss of the isoform $RAR\beta_2$ that is important in controlling proliferation and senescence in normal pancreatic cells, thus underlining the role of RA signalling in controlling the expression of genes related to several processes [102]. Moreover, the control of RA pathway by tumour cells is also a blood cancer milestone, where RA treatment is approved for therapy; for example, acute lymphoblastic leukaemia (ALL) and acute promyelocytic leukaemia (APL) patients show in several cases complete remission from cancer upon atRA treatment, throught the differentiation of blasts [103] [104]. The RA pathway has been deeply explored with its functions on cancer cells, albeit very few papers

talking about the relationship between the retinoic acid signalling and the TME.

The retinoic acid pathway is implicated in the development and the functions of immune system [88], so given its importance in inflammatory response, an inflammatory TME should have increased levels of RA to enhance cell-mediated tumour rejection, at least in the early phases. It has indeed found that there is a great increase in the content of RA in the TME in a melanoma mouse model [105]. In this case, the RA signalling in the TME (but not the tumour itself, where no signalling was found) has the function of tumour rejection, since this vitamin A active metabolite drives CD8+ T-cells clonal expansion, that in turn exert the proper anti-tumoural activity.

There are also TME in which there is the suppression of the RA signalling, because in some cases tumours suffer of differentiation stimuli induced by RA. That is the case of MM BM microenvironment, in which human BM stromal cells express high levels of *CYP26A1* mRNA, that is part of the cytochrome p450 family and it metabolizes the RA in non-active compounds [106]. MM-like Bortezomib resistant cells are responsible for *CYP26A1* induction in stroma through a bi-directional crosstalk, so that the stromal cells of the TME protect leukaemia niche maintaining a MM undifferentiated phenotype. The RA signalling in the TME has not only an anti-cancer activity, it is also reported for Erb2 mammary gland carcinoma that the presence of a functional RARβ in stromal cells of the breast TME characterize a stromal subset capable to support tumour growth [107]. The ablation of the RARβ-mediated signalling in stromal cells determines indeed the suppression of mammary gland carcinoma. These data support the

notion that RA is important in the tumour microenvironment, although different type of malignancies are characterized by different sensitivity and different use of the RA pathway.

1.3. B-CELL CHRONIC LYMPHOCYTIC LEUKAEMIA

B-cell chronic lymphocytic leukaemia is the western world most common leukaemia, taking account, for example, of almost 1% of all malignancies in UK (referred to 2014, Chronic lymphocytic leukaemia (CLL) statistics, Cancer Research UK). It develops as an indolent malignancy prevalently affecting the elderly, with major incidence for male subjects, that along the blood cancer progression becomes more invasive and more lethal [108]. CLL is usually preceded by a previous asymptomatic phase called monoclonal B-cell lymphocytosis (MBL), in which the only observable phenotype is the presence in the peripheral blood of monoclonal CLL-like cells [109].

The B-CLL progression is characterized by the expansion of a monoclonal malignant B-cell with feature of anergic, mature, self-reactive lymphocyte. The precise origin of the CLL cell is still debated since it is still unclear whether this blood cancer originates from marginal zone B-lymphocytes or from B1 cells or from lymphoid precursors [110]. The expression profile of leukemic cells resembles the one of the mature antigen-experienced memory B-cells [111] since the $CD19^{+}/CD5^{+}$ CLL population consistently expresses CD23 as compared to the normal $CD19^{+}/CD5^{+}$ counterpart of age-matched donor; on the other hand, monoclonal CLL cells express lower levels of CD20, CD40L, CD79b and IgD as compared to the normal donor. The diagnosis of this kind of leukaemia involves first of all a high count of monoclonal B-lymphocytes (higher that $5x10^{9}/L$) in peripheral blood, the cell morphology and the immunophenotype, prevalently

defined as $CD19^{+}$ $CD5^{+}$ $CD23^{+}$ $CD20^{low}$ $SmIg^{low}$ [112] [113]. Once established the presence of this blood cancer, prognostic markers are assessed, to determine the tumour load on involved subjects. Usually, molecular assays are useful prognosis tests. The interphase FISH is generally exploited to predict CLL outcome; 11q and 17p genetic aberrations are usually associated with a bad prognosis [114], while on the other hand 13q deletion correlates with a better outcome. Other prognostic factors usually evaluated are the mutational status of IgV_H gene, in which the mutation correlates with a good prognosis, and the expression of ZAP-70 and CD38, that in turn are found to correlate with IgV_H mutations: the more expression of ZAP-70 and CD38 are found in unmutated patients (bad prognosis), hence are also markers for the determination of the general outcome, as TCL1 is [115]. These are the most frequent parameters analysed to determine the prognosis for B-CLL patients:

IgV_H mutational status

The somatic mutation that involves Ig V-D-J loci is a characteristic of mature B-cells that occurs in GC microenvironment [116]. The finding of IgV_H mutations was quite in contrast in the late ’90 with the conventional association between B-CLL to naïve B-cell making reconsider CLL as a mature B-cell blood cancer. IgV_H mutational status is considered as one of the elective markers for determining the prognosis of this kind of leukaemia, together with CD38 expression. The unmutated IgV_H gene is indeed considered a bad prognosis factor, as CD38 expression is.

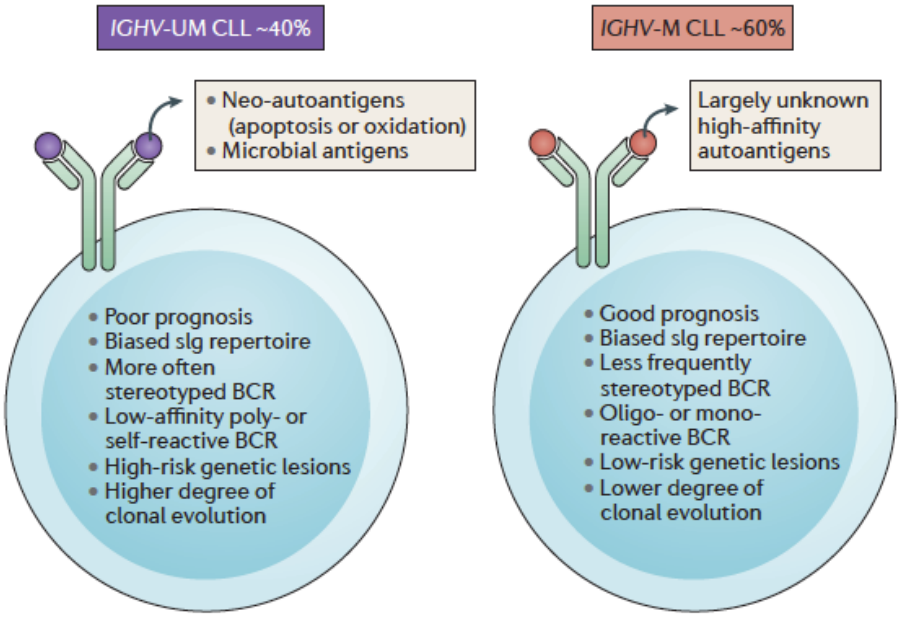

Figure i10. The *IGV$_H$* mutational status and its molecular consequences.

The *IGV$_H$* mutational status is one of the elective prediction markers for human B-CLL. The *IGV$_H$* unmutated locus is associated with bad prognosis and it accounts for roughly 40% of CLL patients [117].

CD38 expression

CD38 is a marker for the determination of the prognosis of CLL patients. During normal development, CD38 is expressed in B-cell precursors present in the bone marrow, but it is also expressed in GC B-cells and in plasma cells [118]; moreover, it has been found expressed also in a plethora of other cell types such as thymocytes, monocytes, platelets, erythrocytes and surprisingly also some kind of solid tumours [119]. CD38 is one of the markers associated with bad

prognosis and it does not correlate with mutational status of IgV_H gene [118], although the presence of both CD38 expression and unmutated IgV_H causes a clear reduction in the overall survival (OS) of CLL patients. In addition to this, CD38 expression may vary during disease progression. CD38 is expressed in actively proliferating lymphocytes where it blocks apoptosis in GC B-cells. In this way, leukemic B-cells may acquire, together with CD38 expression, proliferation and anti-apoptotic stimuli that can be either given from outside (e.g. binding with CD31) or by inside, since it has been reported that CD38 can be found both on the external portion of the cytoplasmic membrane, and in cellular organelles (e.g. nucleus) [120].

ZAP-70 expression

ZAP-70 is a signalling molecule normally associated with T-cells involved in the TCR signalling pathway. This 70kDa ζ-chain CD3 receptor–associated protein tyrosine kinase (PTK) is the homologous of Syk, which is involved in the B-cell maturation through BCR stimulation. Both flow cytometry analyses and gene expression profiling showed how a CLL subgroup also expresses ZAP-70 [121]. More interestingly, *ZAP-70*$^+$ patients show an adverse prognosis and this marker also has a weak correlation with mutation of IgV_H, therefore strengthening its association with a more aggressive form of B-CLL. Functional observations revealed that ZAP-70 associates with BCR complex in CLL probably to positively modulating the BCR signalling. It was also discovered that, in aggressive CLL cases expressing *ZAP-70*, ZAP-70 phosphorilates Syk, which in turn activates Bruton's tyrosine kinase (BTK) to regulate proliferation, survival and apoptosis

through NFAT and NF-kB [122]. This data further underlines the importance of BCR signalling in B-CLL.

13q deletion

The 13q deletion is the most frequent genetic aberration found in CLL patients, and it accounts for about 50% of B-CLL cases [123]. This patient subgroup is associated with good prognosis and longer overall survival rate as compared to the other patients carrying chromosomal aberration such as 17p and 11q. The 13q is frequently mutate in solid and blood malignancies, thus implying the presence in this region of oncosuppressors. Along with this, additional studies shed light on deleted the locus and the minimal deleted region (MDR) for 13q14 correspond to the sequence encoding for the cluster with the presence of two particular micro-RNA: the miR-15a and the miR-16-1 (the cluster is *DLEU2/miR-15a/16-1*) [124]. These two miRNA are frequently found either deleted or down-modulated in CLL. Since miR15a/16-1 are cell cycle regulators, affecting in a negative way proliferation, and they also are able to promote apoptosis, their deletion causes the dysregulation of cell cycle control. Moreover, miR15a/16-1 are found to control the cell cycle also by inhibiting the expression of genes such as *BCL2* that is indeed found overexpressed in 13q del CLL patients. Its inhibition results in harbouring high-risk genetic aberrations [125]. Albeit *DLEU2* is the host gene for the two miRNAs, Ulf Klein and colleagues described [126] how DLEU2 can be spliced into other RNA forms that may have other regulatory functions. This is important to underline that the deletion of the locus of the cluster affects B-cell normal development to give rise to an indolent CLL.

11q deletion

The 11q deletion is the second most frequent chromosome abnormality found in CLL patients [127] and it appears mostly as an acquired modification. The subset of 11q deleted CLL patients are characterized by extensive SLOs involvement and an adverse prognosis with an accelerated disease progression as compared to the other CLL subsets. Interestingly, 11q deletions are more frequent than expected, since other blood malignancies, for example T-cell prolymphocytic leukaemia (T-PLL) and mantle zone lymphoma (MCL), harbour the same kind of aberration in the 11q23 region, thus suggesting the presence of a hot spot cluster [128]. Further analyses of the region showed that in this breakpoint is located the ataxia telangiectasia mutated (*ATM*) gene that is an oncosuppressor that normally acts during the cell cycle and DNA repair [88]. Since the deletion involving the 11q chromosomal arm is quite wide (from 2 to 20 Mb), it has been investigated the presence of other potential genes involved in the CLL pathogenesis and exacerbation. These studies highlighted the deletion of *BIRC3* locus, which encodes for a protein that acts on Nf-kB modulating its activity by down-modulating the non-canonical pathway. This data, together with the knowledge of the maintained membrane receptors implicated in immune signalling, strengthen the idea of a leukaemia with high dependency on the microenvironment for getting survival and proliferation stimuli.

12 trisomy

Although he trisomy of chromosome 12 has been previously associated to a high-risk leukaemia, it is actually included in the low-intermediate risk CLL. The 12 trisomy is one of the least studied genetic aberrations in CLL. One possible mechanism underlying the effect of this modification to B-CLL is the genic over-dosage of *MDM2*. MDM2 acts through indirectly degrading TP53 and this can lead to cell cycle deregulation [129]. It has been found that the 12 trisomy and an upregulation of *GLI1* lead to the over-activation of the hedgehog pathway, so that this leukemic subgroup is more sensitive to HH pathway blockers [130].

17p deletion

The 17p deletion occurs in quite a third of refractory CLL (Puiggros A., 2014) [123], while on the other hand it marks only a minority of newly diagnosed CLL patients. It is associated with the highest risk for very low overall survival of patients. 17p deletion, as like the 11q23, is found in several blood malignancies, since it impairs TP53 function and its crucial role in cell cycle and DNA repair. In addition to this, the bad prognosis for patients bearing this mutation is worsened by the inefficacy of conventional CLL treatments in this subgroup [131]. The adverse prognosis for this subgroup is indeed confirmed by the expression profile of these patients showing high level of CD38 and ZAP-70, other than that most of 17p have an unmutated IGHV gene.

1.3.1 MOUSE MODELS FOR B-CLL

Since the interest in CLL grew, laboratories have started generating mouse models mimicking the human disease. The search for the B-CLL mouse model included transgenic mice with genetic lesion found in humans: the 13q14 deletion, the overexpression of TCL1, APRIL, BCL2 and ROR1 and the ectopic expression of oncogenes [132]. Actually, the preferred leukemic model is the *Eμ-TCL1* transgenic mouse, since it recapitulates features of progressive CLL rather than indolent. The expansion sites for leukaemia cells in this mouse model are the same as patients and the histology resemble the patient biopsies [133], although in human patients the major sites for expansion are thought to be LN and BM. The first group represents mutation in the human 13q14, whose locus in mouse is situated in 14qC3.

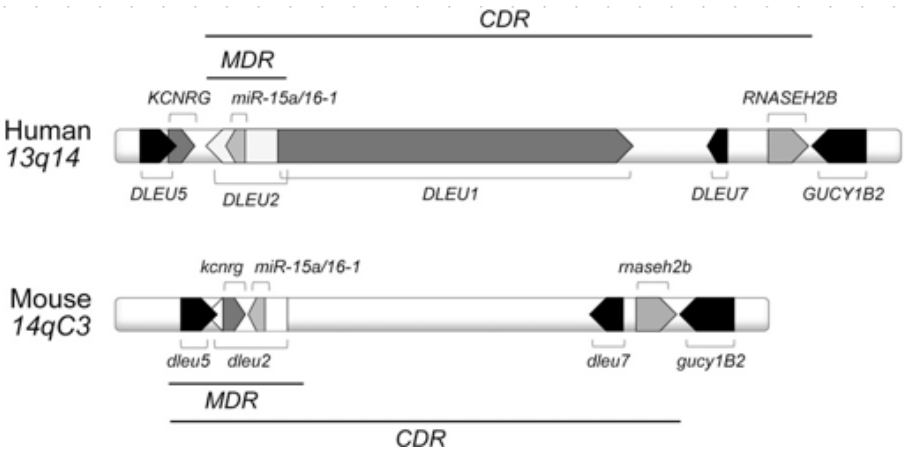

Figure i11. The 13q deletion region and it homologue in mouse.
The deletion of 13q14 in human patients involves the deletion of DLEUs loci, among which *DLEU2* and *DLEU5*. The mouse homologue for those loci is on 14C3, although in this region some DLEUs homologues are missing as compared to human model [132].

Five different mice have been engineered to recapitulate the CLL phenotype which are the *mir-15a/16-1*$^{-/-}$ and *mir-15a/16-1*^{floxed} CD19-Cre [126] that display normal features until 12 months of age when they start developing MBL and then B-CLL, the *14qC3-MDR*$^{-/-}$ and *MDR*^{floxed}CD19-Cre, developed also those two by Dalla-Favera's group in the same paper and displaying the same phenotype, and the *14qC3-CDR*^{floxed}CD19-Cre that is developed 2 years later by the same group; the latter is characterized by having a greater chromosomal deletion as compared to previous mouse models, in addition to the minimal deleted region (MDR) of 110kb it has the deletion of the common deleted region (CDR) of 690kb. This further deletion causes the worsening in CLL phenotype, thus suggesting that the longer deletion is present in the chromosome, the worse CLL phenotype is present.

The *Eμ-TCL1* transgenic mouse was created by cloning the human *TCL1* gene into plasmid containing promoters of mouse immunoglobulin, and then the construct TCL1 plus promoter region and terminal region without vector sequences was injected into fertilized oocytes [133]. This mouse model represents the aggressive form of CLL and it is the one with higher degree of similarities to this human blood cancer.

The *APRIL* transgenic mouse has been created with the rational that CLL patients show increased level of APRIL in the sera; since APRIL belongs to the TNF family and causes enhanced T-cell survival and B-cell proliferation, other than reported proliferative stimuli in solid tumours cells, this transgenic mouse was first generated to determine

the role of APRIL in immunity, and then to autoimmunity [134]. Of note, this mouse displays, from 9 months onwards, a B1 derived neoplasia resembling CLL [135], albeit these cells maintain the expression of B220 on the membrane, that on the contrary it is absent in patients.

The *BCL2* X *traf2dn* transgenic mouse is a double positive mouse strain for the transgene for the expression of human *BCL2* that mimics the translocation of BCL2 in the IgH locus, and the mouse expressing a dominant negative form of Traf2 which lack the RING domain and that mutation causes Traf2 to resemble Traf1; the mouse develops a CLL-like malignancy that is age dependent and recapitulates some important CLL characteristics [136].

The *ROR1* transgenic mouse was developed in 2013 based on the evidence that CLL cells express this embryonic-restricted marker; this mouse has a transgene constituted by the human *ROR1* under the control of promoter and enhancer region of murine IgH. This model is characterized by the insurgence of a CLL-like disease after 15 months; of note, crossing *Eμ-TCL1* with *ROR1* results in accelerated pathology as compared to both single transgenic mouse models [137].

The *Eμ-mir-29* transgenic mouse model, which expresses mir-29 under the control of IgH-Eμ promoter, was generated since *miR-29* is overexpressed in CLL, but in particular in indolent non-aggressive forms, so that the overexpression of this miRNA produces a mouse model slowly developing leukaemia [138].

The *Vh11* X *irf4*$^{-/-}$ model was created by crossing a knock-in mouse for immunoglobulin heavy chain *Vh11*, that give rise to great expansion of B1 cells with the *irf4* knock-out, a gene that has recently been identified

to be down-regulated in CLL. The mouse model is characterized by an early B-CLL onset, mostly within the spleen. Interestingly, the restoration of *irf4* expression determines an increased apoptosis, shedding light on the possible role for IRF4 in CLL [139].

The *IgH.TEμ* model displays a very aggressive form of leukaemia with a great expansion of $CD5^+$ B-cell clones, although in a big portion of mice it has V(D)J rearrangements in Ig heavy chains as a critical difference with aggressive forms of CLL. In this model, the SV40 T antigen, a very powerful oncogene, is inserted in the IgH locus and unmutated IgV_H showed preferential Vh11 family members [140].

Mouse model	Disease penetrance	Appearance circulating leukaemia	Age of death	Ig gene rearrangements
mir-15a/16-1$^{-/-}$ and *mir-15a/16-1*^{floxed} *CD19-Cre*	~20% CLL ~8% MBL ~2%CD5^{-} NHL	12-18 mo.	15-18 mo.	Unmut. and stereotypic IGHV genes
14qC3-MDR$^{-/-}$ and *MDR*^{floxed}*CD19-Cre*	~22% CLL ~12% MBL ~6%CD5^{-} NHL	6-18 mo.	12-18 mo.	Unmut. and stereotypic IGHV genes
14qC3-CDR^{floxed}*CD19-Cre*	~50% CLL ~3% MBL	6-18 mo.	12-18 mo.	Unmut. and stereotypic IGHV genes
Eμ-TCL1 tg	100% CLL	6 mo.	12-18 mo.	Unmut. IGHV and stereotypic IGHV and IGHV genes
APRIL tg	40% CLL	Not analysed	12-15 mo.	Not analysed
BCL2 X *traf2dn* tg	80% CLL	9-15 mo.	>80% dead at 14 mo.	Clonal IGHV rearrangements
ROR1 tg	5% CLL	>15 mo.	>15 mo.	Clonal IGHV rearrangements
Eμ-mir-29 tg	20% CLL	12-24 mo.	24-26 mo.	Clonal IGHV rearrangements
Vh11 X *irf4*$^{-/-}$	100% CLL (preceded by MBL in >40% cases)	5-10 mo.	>9 mo.	Clonal IGHV rearrangements (determined by flow cytometry)
IgH.TEμ	100% CLL	<5 mo.	Killed at 2-10 mo.	Unmut. IGHV genes (preferentially Vh11) and some highly mutated

Figure i11. The developed mouse models for human CLL.

Mouse models for human CLL developed are based on human mutations and deregulation, although some of these models do not develop only CLL [132].

1.3.1.1 The *Eμ-TCL1* Transgenic Mouse Model

The *Eμ-TCL1* transgenic mouse is the most used mouse model in CLL. It was first developed in Croce's lab in 2002 [133] by integrating the *TCL1* human gene together with the 3'end and the untranslated human b-globin gene under the control of the promoter of the murine IGHV and the Eμ enhancer. Indeed, TCL1 gene has been found up-regulated in the vast majority of hCLL. The overexpression of the human *TCL1* gene into mouse strain gave rise to a CLL form highly resembling the aggressive form of the human pathology, thus highlighting the importance of TCL1 in B-CLL. It has been proved indeed that only a minority of hCLL are negative for *TCL1* and that *TCL1* expression is correlated with the leukaemia proliferative status [115].

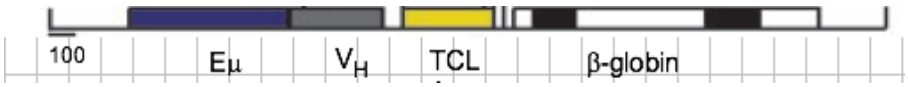

Figure i12. The *Eμ-TCL1* transgene.

The *Eμ-TCL1* transgene allows the overexpression of human TCL1, found overexpressed in the vast majority of human CLL patients, in mice that will develop an aggressive form of human CLL [133].

The *Eμ-TCL1* homozygous transgenic mice are characterized by the accumulation of monoclonal or at least oligoclonal $CD19^+CD5^+IgM^+$ leukaemia in the peritoneal cavity, spleen, lymph nodes and bone marrow, comparable to hCLL. In peripheral blood, CLL cells starts to

be detectable at around 5-6 months, while from 12 months onwards B-CLL infiltrates other organs, such as liver and lymph nodes [133] [141]. CLL patients frequently develop secondary cancers not CLL associated (both solid and blood malignancies), and that is the same for the *Eμ-TCL1* model. This mouse strain is prone to develop in particular skin cancer and other kind of tumours like histiocytic sarcoma and this is related to the overexpression of *TCL1* [142]. Moreover, this useful model demonstrated further similarities to hCLL, since fludarabine treatment showed efficacy in TCL1 in reducing whole-blood lymphocyte count (as in patients) and spleen size, but it also showed another important hCLL feature, the *in vivo* emergence of chemoresistance [141]. The *Eμ-TCL1* model has another important characteristic; its B-CLL is transplantable, so that it can be expanded and transplanted mice can be used for treatment schedule trials.

1.3.2 THE B-CLL MICROENVIRONMENT

In CLL, leukemic B cells survive and expand primarily in lymphoid tissue, such as LNs, spleen and BM, where they establish a leukaemia-supportive niche by interacting with different population of cells, like T-cells, monocytes (that are described to become NLC upon CLL engagement), macrophages, neutrophils, endothelial cells and stromal cells, that all together constitute the lymphoid microenvironment. The dependency of CLL on lymphoid niches was confirmed by Messmer and colleagues [143], as they found that human leukemic cells in peripheral blood circulation are in a resting state, while, in their own niches, show a proliferation rate of approximated 1% per day.

The lymphoid microenvironment of B-CLL, plays a crucial role creating these niches in which leukemic B-cell were progressively recruited, and where different stimuli promote B-CLL proliferation and survival. Among these stimuli, that influence normal and leukemic B cell, were chemokines, such as CXCL12 and CXCL13, and the Toll Like Receptors (TLRs) [144] [145]. In support to the idea that B-CLL is a blood cancer heavily dependent on the microenvironment, comes from the evidence that CLL cells in vitro without either stromal cells or monocyte-derived nurse-like cells (NLCs) do not proliferate and undergo apoptosis within few days [108].

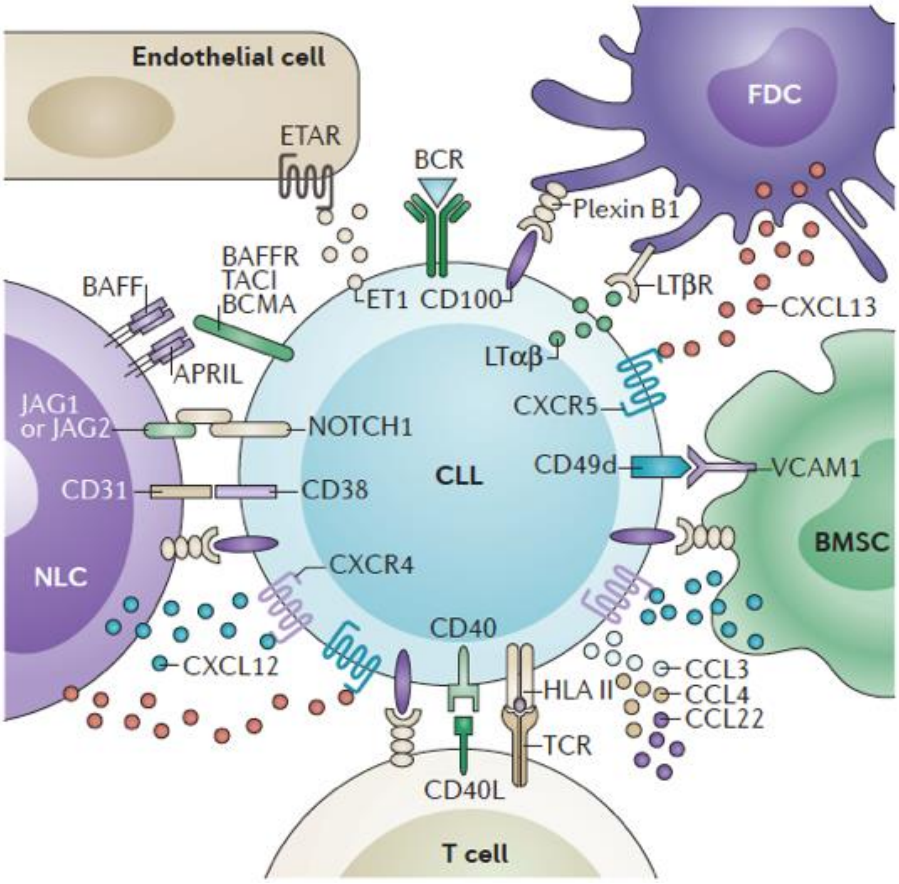

Figure i14. The B-CLL microenvironment components.

The B-CLL cell in its microenvironment interacts with different cell type. In these interactions, different CLL receptors are exploited, based on the interacting cell type. In the CLL milieu, leukemic B-cell cross-talks with stromal cells, T-cells, macrophages (NLCs) and endothelial cells. Moreover, CLL cells exploits also ECM. These cross-talk determine transcription regulation on each cell type and induces a survival advantage for leukaemia in direct or indirect way
[117].

In B-CLL, the most studied SLO milieu components are T-cells and NLCs, and recently the stromal cells. In BM and LNs patients' biopsies, a great predominance of $CD4^+$ T-cells with a T-helper phenotype has been observed, as in other kind of autoimmune diseases like rheumatoid arthritis and Sjögren's syndrome [146] [147]; it has been strongly suggested that CD4+ T-cells can also be forced to differentiate into T-reg cells by CLL, since in leukemic mice B-CLL induces the formation of $CD4^+CD25^+Foxp3^+/CTLA4^+$ thymocytes [148]. Regarding NLCs, these cells are found both in lymphoid niches and in peripheral blood (PB) and in CLL-infiltrated tissues, NLCs shown a macrophage-like shape and are positive for CD45 and CD68, thus indicating their myeloid origin [149]. NLCs are also positive for markers such as vimentin, CXCL13 and CXCL12 (SDF-1), markers also found in stromal cells [150]. Of note, this last chemokine (CXCL12) was secreted by NLCs in vitro, and in vivo it has a relevant role for the attraction of B-cells and for protection of CLL cells from undergoing apoptosis.

Finally, the last cell type crucially involved in CLL survival and proliferation is the non-hematopoietic mesenchymal-derived stromal cell type. In healthy condition, stromal cells play a fundamental role providing a supportive microenvironment for lymphoid cells, and creating a scaffold for resident cells by secreting the extracellular matrix factors and proteins. In leukemic lymphoid tissues, CLL B-cells actively cross-talk with stromal cells, shaping the microenvironment and creating a favourable supportive malignant niche through the secretion of chemokines and cytokines. These stimuli were in part secreted by the different stromal cell populations. The FDCs through

the secretion of CXCL12 and CXCL13 recruit B-CLL cells that in turn express high level of CXCR4 and CXCR5, the receptors for those chemokines [149]; the FRCs secrete CCL19 and CCL21 that determine CLL homing towards chemokine gradients. Moreover, stromal cells express on their surface adhesion molecules such as VCAM-1 and ICAM-1, and in turn leukemic cells express their own integrin ligands (e.g. VLA-4). Lastly, stromal cells have an active role in creation and modification of ECM networks that can be exploited by malignant B-cells for migration.

Although the knowledge about the stromal cell role in CLL is currently limited, it has been described a bi-directional cross talk between stroma and leukaemia that affects the microenvironment to develop a CLL-permissive niche. In human BM biopsies was described that CLL cells are in close contact with stromal cells, instead in spleen or LNs human biopsies it is still unknown.

However, *in vitro* experiments on human samples showed that stroma is crucial for CLL homing, maintenance and proliferation. hCLL cells cultured solely remain in the supernatant fraction and slowly die for apoptosis; while on the other hand, hCLL cells cultured with BM-derived stromal cells show increased survival and spontaneous migration, as well as adhesion to stromal cells through the so called "pseoudoemperipolesis" [151]. This phenomenon is clearly visible using a contrast phase microscopy and highlights the need of the CLL to remain in close contact with stromal cells.

In human LNs biopsies, and in fewer cases in patients' splenectomies, CLL is associated with the creation of proliferation centres (also known as pseudofollicle) that resemble ectopic GC. This finding further

suggests that CLL impacts on microenvironment and then also favours the formation of niche ex novo [152]. The tumour cells are able to activate stromal cell proliferation and modulate stromal secretome to sustain cancer progression. More evidences of stromal cell activation in CLL context are shown through *in vitro* experiments culturing either BM MSC lines or primary cells from patients' BM biopsies in presence of conditioned medium from CLL cultured alone., In this conditions, for example, stromal cells upregulate PDGFRs, that in turn activate stroma proliferation [153]; this experiment demonstrates that CLL can activate the microenvironment through small molecules/factors (PDGF, VEGF), secreted in the conditioned medium, in a paracrine fashion. Although the CLL secreted proteins and exosomes appear to be important for shaping the microenvironment, right now stroma-CLL bidirectional cross-talk was explored as cell-to-cell contact mechanisms. In literature is reported that direct contact of leukaemia cells with stromal cells causes the protection from spontaneous apoptosis, other than chemotherapy-driven apoptosis [154], and mouse fibroblasts induce the upregulation of anti-apoptotic molecules upon CLL engagement. The cell-to-cell contact in this malignancy is important for example in re-constructing the lymphoid niche through the protective role of the VLA-4 engagement. In detail, B-CLL is found to express high levels of $\alpha_4\beta_1$ [155] that can bind ECM fibronectin, which confers drug resistance to CLL, or can bind VCAM-1. The VCAM-1/VLA-4 binding determines on B-CLL the expression of MMP-9 that helps in microenvironment remodelling through ECM digestion [156]; this digestion allows the deposition of ECM molecules *ex novo* and the release of factors normally bound to the ECM, for

example VEGFs and FGFs. Also, stromal cells are important in metabolic sustenance of CLL cells. Usually, cancer cells reprogram their metabolism with a glycolytic metabolism shift to support a different growth rate and to acquire chemoresistance, and this is known as the Warburg effect. In literature was reported that BM resident stromal cells are able to decrease CLL drug sensitivity in situ and as the stroma-CLL cross-talk causes a Notch-dependent metabolic shift that increase the aerobic glycolysis in stromal cells [157].

Among the stromal cells, seems that one of the most important player in CLL-microenvironment cross-talk is the FDC. In human, very little is known about the role of FDCs in CLL onset and progression. FDCs are lymphoid tissue accessory cell that sustain B-cell homeostasis, through adhesion molecule signals and chemokines secretion (e.g. CXCL13, a potent B-chemoattractant), and antigen presentation-mediated B-cell responses within follicles. FDC networks in CLL are often found reduced in size and in numbers, and remodelled [158] [159]. The only mechanism-related study on FDC is based on HK cells, which are a FDC-like cell line derived from human tonsils; the authors demonstrated that FDCs, through cell-cell contact, protect the CLL cells against chemotherapy, as BM MSCs [160]. In leukemic mouse models, such as in *Eμ-TCL1*, different studies suggested SLO FDCs as major stromal players in B-CLL, given that these cells play a crucial role in the B-cell maturation and in the antigen presentation. In mouse, it has been demonstrated that FDCs are exploited by B-CLL cells for survival and proliferation [110]. Indeed, FDCs are the main producer within the follicle of CXCL13, one of the most important B-chemoattractant; moreover, they capability as antigen presenting cell

(APC) can trigger the BCR signalling through heterologous stimulation, so that CLL proliferates.

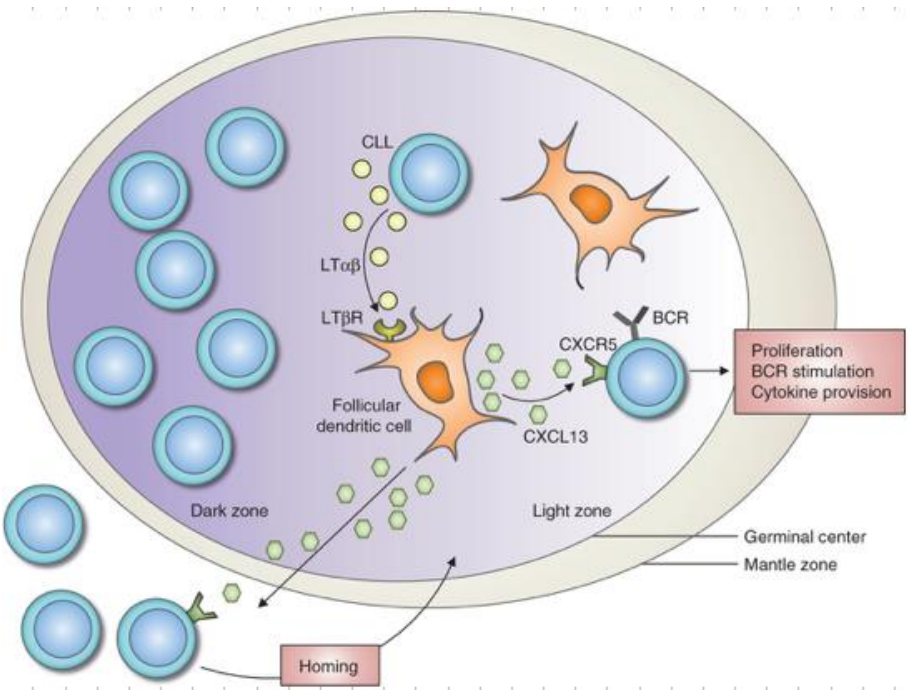

Figure i15. The LTβR-based stroma-leukaemia cross-talk model. The LTbR-based stroma-leukaemia cross-talk that affect the follicle and more precisely the FDC and the CLL. CLL cells migrate to FDC networks towards CXCL13 gradients, where they interact with FDCs and in turn they activate a positive feedback loop based on LTβR-LTαβ engagement. This engagement determines an increase in proliferation and an increase in chemokines secretion [161].

Heinig and collaborators described that at first B-CLL cells goes towards the follicle to take contact with FDCs, and then leukemic cells

get survival stimuli. This fast migration mechanism is CXCR5 mediated, thus confirming the importance of CXCL13, its ligand. One other important issue of this paper is that the FDC-CLL cross-talk is LT-mediated. The block of LT pathway with a specific antibody in immunodeficient mice indeed caused a delay in CLL onset and progression, together with a strong decrease of stromal markers such as CXCL13 and CD35 (FDC markers). Although these results are convincing, several questions remain unclear: since immunodeficient mouse models are characterized by immature stromal cells, what happens to stroma if you treat normal leukemic mice with the LT antibody? What happens to the leukaemia in normal mice with LTβR–Ig treatment? And the last but most important question, what happens in later CLL stages to stromal compartment?

There is another player in CLL microenvironment that can play a role in leukaemogenesis and in its progression and it is the ECM. The actual knowledge about the role of ECM in CLL is currently limited. Actually, the ECM role in CLL is still controversial, since different reports that investigated ECM pattern and composition showed opposite results. On one hand, there is the report on reticulin fibres (that are composed in large majority by type III collagen structures) and BM in which they screened more than 170 patient biopsies and they found that the degree of reticulin fibrosis inversely correlates with the OS and directly correlates with both mortality and the presence of bad prognostic markers, so that the more fibrotic the marrow is, the bad prognosis the patient has [162]. On the other hand, Colombo's group shed light on the role of SPARC in LNs of CLL biopsies [163], as SPARC is thought to have a role in the collagen fibers assembly. Indeed, SPARC KO shows

a disorganized ECM that also causes a disorganization in lymphoid and myeloid compartmentalization; and moreover, this mouse model is more prone to develop lymphoproliferative autoimmune disease. On the same line, CLL-affected mice have a decrease in SPARC content and hCLL biopsies show less ECM as compared to reactive LNs and other kind of non-Hodgkin lymphoma (NHL) malignancies. Taken together, the role of ECM remodelling in CLL is still controversial and there is the need to clarify its role since ECM in steady state condition and in malignancies plays a crucial role in the homeostasis and in progression.

1.3.3 B-CLL THERAPEUTIC TREATMENTS

The CLL is mostly an indolent pathology affecting elderly. Since the CLL usually appears in a non-aggressive form, treatments are assessed based on diagnosis and prognostic factors. As treated before, CLL develops from the more indolent MBL, that of note is found in about 5% of 40-70 years old adults; this initial phase in the leukaemia onset is not included into treatments and clinical trials [109]. Treatment of early indolent CLL proved to be ineffective against leukaemia progression, although it palliates secondary symptoms [164]. Treatment of CLL includes four kind of agents that act at different levels: the cytostatic agents, the monoclonal antibodies, the BCR-signalling inhibitors and the immunomodulating drugs [165].

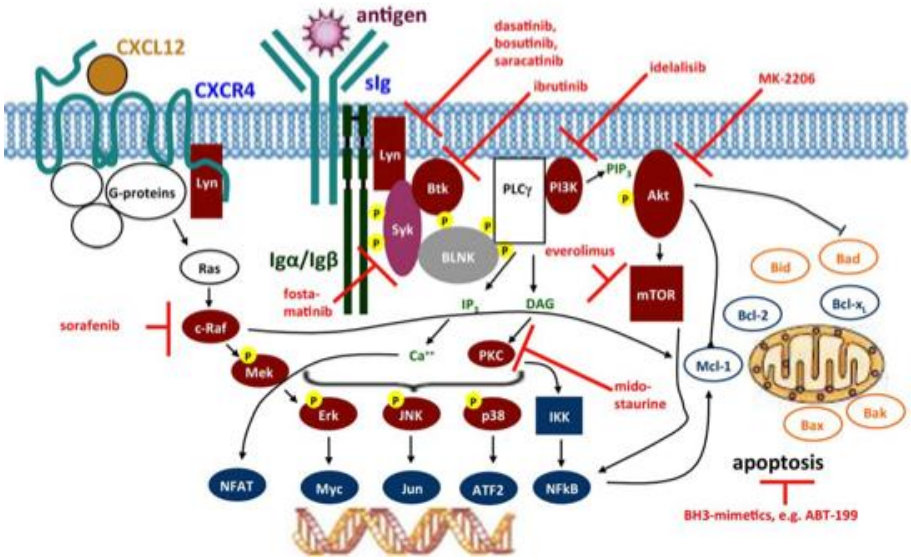

Figure i13. BCR receptor pathway and targeting molecules.

The BCR signalling has actually been targeted by different chemotherapeutic drugs, since in CLL BCR appears to be active and to induce proliferation. The BCR signalling have been targeted in each of its components with the same final effect, thus highlighting the importance of BCR signalling in CLL survival [165].

The cytostatic agents are compounds that block the cell proliferation and so they stabilize the pathology, but the most of them do not eradicate it. Since the most of cytostatic agents do not show complete remission in treating patients with those drugs, they are usually prescribed in combination with other chemotherapeutic compounds. Examples of alkylating cytostatic agents are chlorambucil, one of the first cytostatic drug used in CLL, and fludarabine, whose monotherapy is able to induce more remission than other conventional

chemotherapies [166], so that in the last decade it has become the CLL treatment gold standard.

The monoclonal antibody used in CLL are mainly antibody against CD20, with the exception of Alemtuzumab, an anti-CD52, that proves to be effective against bad prognosis CLL patients that also are resistant to classical chemotherapy [167]; anti-CD20 therapy, for example rituximab therapy, shows higher efficacy when combined to other therapies (e.g. fludarabine), thus demonstrating a synergistic combinatorial effect.

The BCR signalling inhibitors arise from the knowledge that BCR signalling in CLL is still active, the continuous BCR stimulation induces leukaemia survival and proliferation [168]; the most famous in drug in this group is ibrutinib, a BTK inhibitor [169]. BTK is a kinase whose downstream targets are NF-kB and MAPK and the block of this signalling determines partial remission in every CLL patient category, also in relapse and in refractory CLL.

The immunomodulatory drugs, for example lenalidomide, are able to modulate immune responses other than having an effect on microenvironment through the exertion of anti-angiogenic functions. Although there are plenty of chemotherapeutic drugs targeting CLL, actually there is still the need of compound modulating the leukemic microenvironment, that can cause chemoresistance through the metabolism of drugs and the creation of protective niches. Indeed, growing evidences suggest a strong role for microenvironment in tumour progression, and the impairment of the niche milieu appears to be an attractive target, in combination with classical therapies.

1.3.3.1 The Role Of The Microenvironment In B-CLL Chemotherapy

The microenvironment in tumours and most of all in blood malignancies are often reported to damper the immune response against cancer cells and it is also the main player in determining the chemoresistance [170], through either the metabolism of drugs or making the cancer niche less accessible to therapeutic compounds. Recently, new therapies targeting the tumour-microenvironment cross-talk have been developed. Since CLL is a blood cancer heavily dependent of the milieu, the interest in the disruption of the cross-talk affecting CLL-microenvironment is growing. CLL cells exploit their niches through receptors and ligands, where the most characterized are the receptors, because they directly act on the leukemic cell itself to allow proliferation and migration. The BCR signalling pathway has been targeted in many of its constituents: Lyn, a TK belonging to the Src family important in BCR signal transduction, is blocked by compound like dasatinib; it has recently been discovered that Lyn is important for CLL pathogenesis mostly for its action in leukemic lymphoid niches macrophages and possibly stromal cells. The absence of Lyn signalling in B-CLL reduces the BCR activity, but this does not impair the leukaemia proliferation [171]; conversely, its block in the microenvironment determines the delay of the malignancy, which expansion relied on cell-to-cell contact. Btk, on the same line, is a TK phosphorylated by Lyn, important in CLL onset and progression and it is blocked by drugs like ibrutinib. Like Lyn, Btk is actually known to exert its function also in the microenvironment, since $Btk^{-/-}$ recipients

show a reduction in CLL progression and in spleen involvement as compared to WT cohorts. CXCR4 is the lymphoid receptor for myeloid and stromal CXCL12 and it is the perfect example of how targeting the CLL-microenvironment cross-talk is an effective strategy, albeit still it is a matter of targeting malignant cell that *per se* can change in a more plastic way as compared to the microenvironment. CXCR4 directly orchestrates chemotaxis and the phosphorylation of MAPK and STAT3, and indirectly exerts anti-apoptotic functions [172]. CXCR4 inhibitors were first created for chemotherapy against HIV-1 infections, since it was found a strain exploiting this receptor in a T-cell lineage, thus blocking the virus entry in these thymocytes [173]. AMD3100 is one of the CXCR4 inhibitors. The inhibition of CXCL12 principal receptor interferes with the stroma-leukaemia cross-talk, blocking the CLL migration towards niches and causing the release of these cells from stromal milieu, as a readout of initial lymphocytosis. The efficacy of anti-CXCR4 drugs can only be evaluated in combination with other chemotherapeutic drugs, since the CLL release from lymphoid tissues itself does not cause either remission or partial remission, but determines an increase in therapy sensitivity for leukemic cells. This is the meaning of targeting the microenvironment, it allows to the dramatic increase in the efficacy of classical chemotherapies, since there is no more the protective role of the microenvironment. There are other compound targeting different pathways, either in clinical trials or in translational research phase, that affects the microenvironment and inducing effects on CLL directly or indirectly: the PI3Kδ inhibitor, CAL-101, that inhibits CLL chemotaxis towards CXCL12 and CXCL13 gradients and also impairs the stromal secretion of these

chemoattractants [174]; HIF-1α inhibitor, EZN2208, that inhibits CLL migration to lymphoid niches and determines the release of leukemic cells from lymphoid organs to the peripheral blood, since this compound indirectly blocks the CXCR4-CXCL12 axis and induces the down-modulation of integrins such as *Itgβ1* and *Itgα4* [175]. Taken together, several groups are exploiting the possibility to target the microenvironment instead of targeting the CLL cell solely, since the microenvironment is more genetically stable as compared to the leukaemia, and because the block of the CLL-microenvironment cross-talk will damper all the chemoresistance mechanisms exploited by the milieu; the microenvironment targeting will also allow the release of B-CLL cells from niches to enhance their sensitivity to common chemotherapy and further increase the CLL remission rate.

1.3.4 IS THERE A ROLE FOR THE RETINOIC ACID PATHWAY IN B-CLL?

The retinoic acid pathway is involved in several physiologic mechanisms and it is also involved in cancer, either in anti-tumoural activity or in pro-tumourigenic activity; regarding the B-CLL, is there any role for the RA pathway in either B-CLL oncogenesis and progression or against B-CLL? Actually, there is no answer to this question. There are some data in CLL mouse models and in human experiments that suggest that RA can participate somehow in CLL tumourigenesis. In mouse models, CLL is thought to arise from the B1a sub-population, given that B1a and B-CLL share site of expansion and surface markers. B1a subpopulation has the RA signalling up-

modulated as compared to other B-cell population, for instance the RA receptor RARγ2 [47], so that retinoids may exert some functions also in B-CLL. Leukemic B-cells are also positive for CD11b, an integrin normally present in the myeloid compartment; this integrin is under the control of RARE elements, so that in the presence of RA *CD11b* is expressed [176] and this suggests that murine B-CLL cells up-regulates CD11b in response to a RA-enriched milieu. In human PB samples, it has been assessed that hCLL B-cells have ALDHs activity. To do that, the Carson D.A. group exploited the Aldefluor assay on progressive (ZAP-70^+ or unmutated IgV_H) and stable (ZAP-70^- or mutated IgV_H) patients' PB [177]. Aldefluor assay is commonly used to identify stem cells, and usually solid tumour cells result positive for this assay, at least a part of their cell population. Moreover, Aldefluor positivity is associated with activity of RALDH enzymes, so that an increase in Aldefluor positivity should correspond to increased vitamin A/β-carotene metabolism to obtain RA. The finding that aggressive forms of hCLL show an increase in RA pathway as compared to non-aggressive forms suggests that RA signalling is involved in the progression of leukaemia. It has been also demonstrated that the addition of RA together with IL-21 determines an increase in CpG-mediated proliferation of hCLL cultures *in vitro*, further strengthening the importance of RA signalling in CLL B-cells. What about human stromal compartment? It has been described by Burger J.A. group in human CLL LN biopsies the presence of NLCs $CXCL13^+$ [149]. Since it is known by developmental literature that *CXCL13* expression is driven by different pathways among which the RA pathway, where indeed RARE elements were found in its promoter region, and given

that lymphoid organ stromal cells are the main producer of CXCL13, it is plausible that in CLL there is the activation of RA signalling that leads to an increase of the stromal CXCL13 secretion. Altogether, these findings suggest that CLL cells, by exploiting the lymphoid niches, activate a RA-based stroma-leukaemia cross-talk that affects both the microenvironment and the leukaemia itself to create a favourable CLL niche that in turn helps CLL to survive and progress.

CHAPTER 2. SCOPE OF THE THESIS

B-CLL is a blood cancer that strongly depends on the supportive microenvironment of lymphoid organs for survival, chemoresistance and disease progression. Non-hematopoietic stromal cells of lymphoid tissues have been implicated in CLL pathogenesis, however their role in disease onset and progression is still largely unknown. Understanding how the stromal compartment changes during disease evolution, which stromal cell subsets cross-talk to leukaemia cells at different disease stages, and what signalling pathways are involved is crucial to elucidate the contribution of the stromal compartment in CLL pathogenesis, and to design therapeutic strategies aiming to target the microenvironment.

To this end, the aim of my work is:

1) to define the changes occurring in the lymphoid microenvironment during B-CLL onset and progression in *Eμ-TCL1* transgenic mice, a model that recapitulates the progressive CLL;
2) to unravel the molecular pathways induced in stromal cells upon CLL interactions that are involved in disease progression, through *in vitro* and *ex vivo* approaches;
3) to validate candidate pathways in mouse models and determine whether they are conserved between mouse and human CLL.

CHAPTER 3. INTRODUCTION

BIBLIOGRAPHY

1. Xu, R., A. Boudreau, and M.J. Bissell, *Tissue architecture and function: dynamic reciprocity via extra- and intra-cellular matrices.* Cancer Metastasis Rev, 2009. **28**(1-2): p. 167-76.
2. Barone, F., et al., *Stromal Fibroblasts in Tertiary Lymphoid Structures: A Novel Target in Chronic Inflammation.* Front Immunol, 2016. **7**: p. 477.
3. Cesta, M.F., *Normal structure, function, and histology of the spleen.* Toxicol Pathol, 2006. **34**(5): p. 455-65.
4. Tischendorf, F., *On the evolution of the spleen.* Experientia, 1985. **41**(2): p. 145-52.
5. Lenti, E., et al., *Transcription factor TLX1 controls retinoic acid signalling to ensure spleen development.* J Clin Invest, 2016. **126**(7): p. 2452-64.
6. Brendolan, A., et al., *Development and function of the mammalian spleen.* Bioessays, 2007. **29**(2): p. 166-77.
7. Saito, H., et al., *Reticular meshwork of the spleen in rats studied by electron microscopy.* Am J Anat, 1988. **181**(3): p. 235-52.
8. Kurotaki, D., T. Uede, and T. Tamura, *Functions and development of red pulp macrophages.* Microbiol Immunol, 2015. **59**(2): p. 55-62.
9. Mebius, R.E. and G. Kraal, *Structure and function of the spleen.* Nat Rev Immunol, 2005. **5**(8): p. 606-16.
10. den Haan, J.M., R.E. Mebius, and G. Kraal, *Stromal cells of the mouse spleen.* Front Immunol, 2012. **3**: p. 201.
11. Geijtenbeek, T.B., et al., *Marginal zone macrophages express a murine homologue of DC-SIGN that captures blood-borne antigens in vivo.* Blood, 2002. **100**(8): p. 2908-16.
12. Pillai, S. and A. Cariappa, *The follicular versus marginal zone B lymphocyte cell fate decision.* Nat Rev Immunol, 2009. **9**(11): p. 767-77.

13. Castagnaro, L., et al., *Nkx2-5(+)islet1(+) mesenchymal precursors generate distinct spleen stromal cell subsets and participate in restoring stromal network integrity.* Immunity, 2013. **38**(4): p. 782-91.
14. Banks, T.A., et al., *Lymphotoxin-alpha-deficient mice. Effects on secondary lymphoid organ development and humoral immune responsiveness.* J Immunol, 1995. **155**(4): p. 1685-93.
15. Oldstone, M.B., et al., *Lymphotoxin-alpha- and lymphotoxin-beta-deficient mice differ in susceptibility to scrapie: evidence against dendritic cell involvement in neuroinvasion.* J Virol, 2002. **76**(9): p. 4357-63.
16. Mitchell, J., *Lymphocyte circulation in the spleen. Marginal zone bridging channels and their possible role in cell traffic.* Immunology, 1973. **24**(1): p. 93-107.
17. Bajenoff, M., N. Glaichenhaus, and R.N. Germain, *Fibroblastic reticular cells guide T lymphocyte entry into and migration within the splenic T cell zone.* J Immunol, 2008. **181**(6): p. 3947-54.
18. Nolte, M.A., et al., *A conduit system distributes chemokines and small blood-borne molecules through the splenic white pulp.* J Exp Med, 2003. **198**(3): p. 505-12.
19. Bajenoff, M., et al., *Stromal cell networks regulate lymphocyte entry, migration, and territoriality in lymph nodes.* Immunity, 2006. **25**(6): p. 989-1001.
20. Link, A., et al., *Fibroblastic reticular cells in lymph nodes regulate the homeostasis of naive T cells.* Nat Immunol, 2007. **8**(11): p. 1255-65.
21. Malhotra, D., et al., *Transcriptional profiling of stroma from inflamed and resting lymph nodes defines immunological hallmarks.* Nat Immunol, 2012. **13**(5): p. 499-510.
22. Liu, Y.J., et al., *Follicular dendritic cells and germinal centers.* Int Rev Cytol, 1996. **166**: p. 139-79.
23. Munoz-Fernandez, R., et al., *Follicular dendritic cells are related to bone marrow stromal cell progenitors and to myofibroblasts.* J Immunol, 2006. **177**(1): p. 280-9.
24. Allen, C.D. and J.G. Cyster, *Follicular dendritic cell networks of primary follicles and germinal centers: phenotype and function.* Semin Immunol, 2008. **20**(1): p. 14-25.
25. De Silva, N.S. and U. Klein, *Dynamics of B cells in germinal centres.* Nat Rev Immunol, 2015. **15**(3): p. 137-48.

26. Allen, C.D., T. Okada, and J.G. Cyster, *Germinal-center organization and cellular dynamics.* Immunity, 2007. **27**(2): p. 190-202.
27. Mueller, S.N. and R.N. Germain, *Stromal cell contributions to the homeostasis and functionality of the immune system.* Nat Rev Immunol, 2009. **9**(9): p. 618-29.
28. Zhang, J., et al., *Is rapid proliferation in B centroblasts linked to somatic mutation in memory B cell clones?* Immunol Lett, 1988. **18**(4): p. 297-9.
29. Katakai, T., et al., *Organizer-like reticular stromal cell layer common to adult secondary lymphoid organs.* J Immunol, 2008. **181**(9): p. 6189-200.
30. Jarjour, M., et al., *Fate mapping reveals origin and dynamics of lymph node follicular dendritic cells.* J Exp Med, 2014. **211**(6): p. 1109-22.
31. Blum, K.S. and R. Pabst, *Keystones in lymph node development.* J Anat, 2006. **209**(5): p. 585-95.
32. Hall, J.G. and B. Morris, *The immediate effect of antigens on the cell output of a lymph node.* Br J Exp Pathol, 1965. **46**(4): p. 450-4.
33. Willard-Mack, C.L., *Normal structure, function, and histology of lymph nodes.* Toxicol Pathol, 2006. **34**(5): p. 409-24.
34. Tammela, T. and K. Alitalo, *Lymphangiogenesis: Molecular mechanisms and future promise.* Cell, 2010. **140**(4): p. 460-76.
35. Baluk, P., et al., *Functionally specialized junctions between endothelial cells of lymphatic vessels.* J Exp Med, 2007. **204**(10): p. 2349-62.
36. Betterman, K.L. and N.L. Harvey, *The lymphatic vasculature: development and role in shaping immunity.* Immunol Rev, 2016. **271**(1): p. 276-92.
37. Mionnet, C., et al., *Identification of a new stromal cell type involved in the regulation of inflamed B cell follicles.* PLoS Biol, 2013. **11**(10): p. e1001672.
38. Butler, J., et al., *Imaging Immunity in Lymph Nodes: Past, Present and Future.* Adv Exp Med Biol, 2016. **915**: p. 329-46.
39. Heel, K.A. and J.C. Hall, *Peritoneal defences and peritoneum-associated lymphoid tissue.* Br J Surg, 1996. **83**(8): p. 1031-6.
40. Williams, R. and H. White, *The greater omentum: its applicability to cancer surgery and cancer therapy.* Curr Probl Surg, 1986. **23**(11): p. 789-865.

41. Williams, R.J., et al., *Omental transposition in the treatment of locally advanced and recurrent breast cancer.* Br J Surg, 1989. **76**(6): p. 559-63.
42. Cruz-Migoni, S. and J. Caamano, *Fat-Associated Lymphoid Clusters in Inflammation and Immunity.* Front Immunol, 2016. **7**: p. 612.
43. Solvason, N., et al., *The fetal omentum in mice and humans. A site enriched for precursors of CD5 B cells early in development.* Ann N Y Acad Sci, 1992. **651**: p. 10-20.
44. Rangel-Moreno, J., et al., *Omental milky spots develop in the absence of lymphoid tissue-inducer cells and support B and T cell responses to peritoneal antigens.* Immunity, 2009. **30**(5): p. 731-43.
45. Berberich, S., et al., *Differential molecular and anatomical basis for B cell migration into the peritoneal cavity and omental milky spots.* J Immunol, 2008. **180**(4): p. 2196-203.
46. Pradeep, S., et al., *Hematogenous metastasis of ovarian cancer: rethinking mode of spread.* Cancer Cell, 2014. **26**(1): p. 77-91.
47. Moro, K., et al., *Innate production of T(H)2 cytokines by adipose tissue-associated c-Kit(+)Sca-1(+) lymphoid cells.* Nature, 2010. **463**(7280): p. 540-4.
48. Benezech, C., et al., *Inflammation-induced formation of fat-associated lymphoid clusters.* Nat Immunol, 2015. **16**(8): p. 819-28.
49. Elewa, Y.H., et al., *Characterization of mouse mediastinal fat-associated lymphoid clusters.* Cell Tissue Res, 2014. **357**(3): p. 731-41.
50. Kershaw, E.E. and J.S. Flier, *Adipose tissue as an endocrine organ.* J Clin Endocrinol Metab, 2004. **89**(6): p. 2548-56.
51. Yu, H., J.K. Mouw, and V.M. Weaver, *Forcing form and function: biomechanical regulation of tumour evolution.* Trends Cell Biol, 2011. **21**(1): p. 47-56.
52. Hanahan, D. and L.M. Coussens, *Accessories to the crime: functions of cells recruited to the tumour microenvironment.* Cancer Cell, 2012. **21**(3): p. 309-22.
53. Hanahan, D. and R.A. Weinberg, *Hallmarks of cancer: the next generation.* Cell, 2011. **144**(5): p. 646-74.
54. Quail, D.F. and J.A. Joyce, *Microenvironmental regulation of tumour progression and metastasis.* Nat Med, 2013. **19**(11): p. 1423-37.

55. Yuan, A., et al., *Opposite Effects of M1 and M2 Macrophage Subtypes on Lung Cancer Progression.* Sci Rep, 2015. **5**: p. 14273.
56. Mantovani, A., et al., *Cancer-related inflammation.* Nature, 2008. **454**(7203): p. 436-44.
57. Kalluri, R., *The biology and function of fibroblasts in cancer.* Nat Rev Cancer, 2016. **16**(9): p. 582-98.
58. Dirat, B., et al., *Cancer-associated adipocytes exhibit an activated phenotype and contribute to breast cancer invasion.* Cancer Res, 2011. **71**(7): p. 2455-65.
59. Erez, N., et al., *Cancer-Associated Fibroblasts Are Activated in Incipient Neoplasia to Orchestrate Tumour-Promoting Inflammation in an NF-kappaB-Dependent Manner.* Cancer Cell, 2010. **17**(2): p. 135-47.
60. Vempati, P., A.S. Popel, and F. Mac Gabhann, *Formation of VEGF isoform-specific spatial distributions governing angiogenesis: computational analysis.* BMC Syst Biol, 2011. **5**: p. 59.
61. Elenbaas, B. and R.A. Weinberg, *Heterotypic signalling between epithelial tumour cells and fibroblasts in carcinoma formation.* Exp Cell Res, 2001. **264**(1): p. 169-84.
62. Albrengues, J., et al., *LIF mediates proinvasive activation of stromal fibroblasts in cancer.* Cell Rep, 2014. **7**(5): p. 1664-78.
63. Lu, P., V.M. Weaver, and Z. Werb, *The extracellular matrix: a dynamic niche in cancer progression.* J Cell Biol, 2012. **196**(4): p. 395-406.
64. Barkan, D., J.E. Green, and A.F. Chambers, *Extracellular matrix: a gatekeeper in the transition from dormancy to metastatic growth.* Eur J Cancer, 2010. **46**(7): p. 1181-8.
65. Erler, J.T., et al., *Hypoxia-induced lysyl oxidase is a critical mediator of bone marrow cell recruitment to form the premetastatic niche.* Cancer Cell, 2009. **15**(1): p. 35-44.
66. Jensen, B.V., et al., *Extracellular matrix building marked by the N-terminal propeptide of procollagen type I reflect aggressiveness of recurrent breast cancer.* Int J Cancer, 2002. **98**(4): p. 582-9.
67. Gilkes, D.M., et al., *Collagen prolyl hydroxylases are essential for breast cancer metastasis.* Cancer Res, 2013. **73**(11): p. 3285-96.

68. Udensi, U.K. and P.B. Tchounwou, *Dual effect of oxidative stress on leukaemia cancer induction and treatment.* J Exp Clin Cancer Res, 2014. **33**: p. 106.
69. Siegel, R., D. Naishadham, and A. Jemal, *Cancer statistics, 2013.* CA Cancer J Clin, 2013. **63**(1): p. 11-30.
70. Schrek, R. and W.J. Donnelly, *"Hairy" cells in blood in lymphoreticular neoplastic disease and "flagellated" cells of normal lymph nodes.* Blood, 1966. **27**(2): p. 199-211.
71. Angelopoulou, M.K., F.N. Kontopidou, and G.A. Pangalis, *Adhesion molecules in B-chronic lymphoproliferative disorders.* Semin Hematol, 1999. **36**(2): p. 178-97.
72. Burthem, J., et al., *Hairy cell interactions with extracellular matrix: expression of specific integrin receptors and their role in the cell's response to specific adhesive proteins.* Blood, 1994. **84**(3): p. 873-82.
73. Sivina, M. and J.A. Burger, *The importance of the tissue microenvironment in hairy cell leukaemia.* Best Pract Res Clin Haematol, 2015. **28**(4): p. 208-16.
74. Nanba, K., et al., *Splenic pseudosinuses and hepatic angiomatous lesions. Distinctive features of hairy cell leukaemia.* Am J Clin Pathol, 1977. **67**(5): p. 415-26.
75. Burthem, J. and J.C. Cawley, *The bone marrow fibrosis of hairy-cell leukaemia is caused by the synthesis and assembly of a fibronectin matrix by the hairy cells.* Blood, 1994. **83**(2): p. 497-504.
76. Aziz, K.A., et al., *The role of autocrine FGF-2 in the distinctive bone marrow fibrosis of hairy-cell leukaemia (HCL).* Blood, 2003. **102**(3): p. 1051-6.
77. Shehata, M., et al., *TGF-beta1 induces bone marrow reticulin fibrosis in hairy cell leukaemia.* J Clin Invest, 2004. **113**(5): p. 676-85.
78. Hideshima, T., et al., *Understanding multiple myeloma pathogenesis in the bone marrow to identify new therapeutic targets.* Nat Rev Cancer, 2007. **7**(8): p. 585-98.
79. Barlogie, B. and R.P. Gale, *Multiple myeloma and chronic lymphocytic leukaemia: parallels and contrasts.* Am J Med, 1992. **93**(4): p. 443-50.
80. Hideshima, T. and K.C. Anderson, *Molecular mechanisms of novel therapeutic approaches for multiple myeloma.* Nat Rev Cancer, 2002. **2**(12): p. 927-37.

81. Gupta, D., et al., *Adherence of multiple myeloma cells to bone marrow stromal cells upregulates vascular endothelial growth factor secretion: therapeutic applications.* Leukaemia, 2001. **15**(12): p. 1950-61.
82. Yaccoby, S., et al., *Myeloma interacts with the bone marrow microenvironment to induce osteoclastogenesis and is dependent on osteoclast activity.* Br J Haematol, 2002. **116**(2): p. 278-90.
83. Niederreither, K. and P. Dolle, *Retinoic acid in development: towards an integrated view.* Nat Rev Genet, 2008. **9**(7): p. 541-53.
84. Sirbu, I.O. and G. Duester, *Retinoic-acid signalling in node ectoderm and posterior neural plate directs left-right patterning of somitic mesoderm.* Nat Cell Biol, 2006. **8**(3): p. 271-7.
85. Niederreither, K., et al., *Embryonic retinoic acid synthesis is required for forelimb growth and anteroposterior patterning in the mouse.* Development, 2002. **129**(15): p. 3563-74.
86. van de Pavert, S.A., et al., *Maternal retinoids control type 3 innate lymphoid cells and set the offspring immunity.* Nature, 2014. **508**(7494): p. 123-7.
87. Stephensen, C.B., *Vitamin A, infection, and immune function.* Annu Rev Nutr, 2001. **21**: p. 167-92.
88. Pino-Lagos, K., et al., *A retinoic acid-dependent checkpoint in the development of CD4+ T cell-mediated immunity.* J Exp Med, 2011. **208**(9): p. 1767-75.
89. Ertesvag, A., S. Naderi, and H.K. Blomhoff, *Regulation of B cell proliferation and differentiation by retinoic acid.* Semin Immunol, 2009. **21**(1): p. 36-41.
90. Villablanca, E.J., et al., *beta7 integrins are required to give rise to intestinal mononuclear phagocytes with tolerogenic potential.* Gut, 2014. **63**(9): p. 1431-40.
91. Roy, B., et al., *An intrinsic propensity of murine peritoneal B1b cells to switch to IgA in presence of TGF-beta and retinoic acid.* PLoS One, 2013. **8**(12): p. e82121.
92. Mucida, D., et al., *Retinoic acid can directly promote TGF-beta-mediated Foxp3(+) Treg cell conversion of naive T cells.* Immunity, 2009. **30**(4): p. 471-2; author reply 472-3.
93. Suzuki, Y., et al., *Retinoic acid controls blood vessel formation by modulating endothelial and mural cell interaction via suppression of Tie2 signalling in vascular progenitor cells.* Blood, 2004. **104**(1): p. 166-9.

94. Lai, L., et al., *Retinoic acid regulates endothelial cell proliferation during vasculogenesis.* Development, 2003. **130**(26): p. 6465-74.
95. Burger, N.B., et al., *Involvement of neurons and retinoic acid in lymphatic development: new insights in increased nuchal translucency.* Prenat Diagn, 2014. **34**(13): p. 1312-9.
96. van de Pavert, S.A., et al., *Chemokine CXCL13 is essential for lymph node initiation and is induced by retinoic acid and neuronal stimulation.* Nat Immunol, 2009. **10**(11): p. 1193-9.
97. Burn, S.F., et al., *The dynamics of spleen morphogenesis.* Dev Biol, 2008. **318**(2): p. 303-11.
98. El-Metwally, T.H., et al., *High concentrations of retinoids induce differentiation and late apoptosis in pancreatic cancer cells in vitro.* Cancer Biol Ther, 2005. **4**(5): p. 602-11.
99. Shilkaitis, A., A. Green, and K. Christov, *Retinoids induce cellular senescence in breast cancer cells by RAR-beta dependent and independent pathways: Potential clinical implications (Review).* Int J Oncol, 2015. **47**(1): p. 35-42.
100. Sommer, K.M., et al., *Elevated retinoic acid receptor beta(4) protein in human breast tumour cells with nuclear and cytoplasmic localization.* Proc Natl Acad Sci U S A, 1999. **96**(15): p. 8651-6.
101. Tang, X.H. and L.J. Gudas, *Retinoids, retinoic acid receptors, and cancer.* Annu Rev Pathol, 2011. **6**: p. 345-64.
102. Xu, X.C., *Tumour-suppressive activity of retinoic acid receptor-beta in cancer.* Cancer Lett, 2007. **253**(1): p. 14-24.
103. Degos, L. and Z.Y. Wang, *All trans retinoic acid in acute promyelocytic leukaemia.* Oncogene, 2001. **20**(49): p. 7140-5.
104. Churchman, M.L., et al., *Efficacy of Retinoids in IKZF1-Mutated BCR-ABL1 Acute Lymphoblastic Leukaemia.* Cancer Cell, 2015. **28**(3): p. 343-56.
105. Guo, Y., et al., *A retinoic acid--rich tumour microenvironment provides clonal survival cues for tumour-specific CD8(+) T cells.* Cancer Res, 2012. **72**(20): p. 5230-9.
106. Alonso, S., et al., *Hedgehog and retinoid signalling alters multiple myeloma microenvironment and generates bortezomib resistance.* J Clin Invest, 2016. **126**(12): p. 4460-4468.
107. Liu, X., et al., *Stromal retinoic acid receptor beta promotes mammary gland tumourigenesis.* Proc Natl Acad Sci U S A, 2011. **108**(2): p. 774-9.

108. Caligaris-Cappio, F. and T.J. Hamblin, *B-cell chronic lymphocytic leukaemia: a bird of a different feather.* J Clin Oncol, 1999. **17**(1): p. 399-408.
109. Strati, P. and T.D. Shanafelt, *Monoclonal B-cell lymphocytosis and early-stage chronic lymphocytic leukaemia: diagnosis, natural history, and risk stratification.* Blood, 2015. **126**(4): p. 454-62.
110. Heinig, K., et al., *Access to follicular dendritic cells is a pivotal step in murine chronic lymphocytic leukaemia B-cell activation and proliferation.* Cancer Discov, 2014. **4**(12): p. 1448-65.
111. Damle, R.N., et al., *B-cell chronic lymphocytic leukaemia cells express a surface membrane phenotype of activated, antigen-experienced B lymphocytes.* Blood, 2002. **99**(11): p. 4087-93.
112. Ginaldi, L., et al., *Levels of expression of CD19 and CD20 in chronic B cell leukaemias.* J Clin Pathol, 1998. **51**(5): p. 364-9.
113. Hallek, M., et al., *Guidelines for the diagnosis and treatment of chronic lymphocytic leukaemia: a report from the International Workshop on Chronic Lymphocytic Leukaemia updating the National Cancer Institute-Working Group 1996 guidelines.* Blood, 2008. **111**(12): p. 5446-56.
114. Dohner, H., et al., *Genomic aberrations and survival in chronic lymphocytic leukaemia.* N Engl J Med, 2000. **343**(26): p. 1910-6.
115. Herling, M., et al., *TCL1 shows a regulated expression pattern in chronic lymphocytic leukaemia that correlates with molecular subtypes and proliferative state.* Leukaemia, 2006. **20**(2): p. 280-5.
116. Berek, C. and C. Milstein, *Mutation drift and repertoire shift in the maturation of the immune response.* Immunol Rev, 1987. **96**: p. 23-41.
117. Fabbri, G. and R. Dalla-Favera, *The molecular pathogenesis of chronic lymphocytic leukaemia.* Nat Rev Cancer, 2016. **16**(3): p. 145-62.
118. Hamblin, T.J., et al., *CD38 expression and immunoglobulin variable region mutations are independent prognostic variables in chronic lymphocytic leukaemia, but CD38 expression may vary during the course of the disease.* Blood, 2002. **99**(3): p. 1023-9.
119. Deaglio, S., et al., *CD38/CD31, a receptor/ligand system ruling adhesion and signalling in human leukocytes.* Chem Immunol, 2000. **75**: p. 99-120.

120. Lee, H.C., *Structure and enzymatic functions of human CD38.* Mol Med, 2006. **12**(11-12): p. 317-23.
121. Wiestner, A., et al., *ZAP-70 expression identifies a chronic lymphocytic leukaemia subtype with unmutated immunoglobulin genes, inferior clinical outcome, and distinct gene expression profile.* Blood, 2003. **101**(12): p. 4944-51.
122. Feng, G. and X. Wang, *Role of spleen tyrosine kinase in the pathogenesis of chronic lymphocytic leukaemia.* Leuk Lymphoma, 2014. **55**(12): p. 2699-705.
123. Puiggros, A., G. Blanco, and B. Espinet, *Genetic abnormalities in chronic lymphocytic leukaemia: where we are and where we go.* Biomed Res Int, 2014. **2014**: p. 435983.
124. Calin, G.A., et al., *Frequent deletions and down-regulation of micro- RNA genes miR15 and miR16 at 13q14 in chronic lymphocytic leukaemia.* Proc Natl Acad Sci U S A, 2002. **99**(24): p. 15524-9.
125. Roberts, A.W., et al., *Targeting BCL2 with Venetoclax in Relapsed Chronic Lymphocytic Leukaemia.* N Engl J Med, 2016. **374**(4): p. 311-22.
126. Klein, U., et al., *The DLEU2/miR-15a/16-1 cluster controls B cell proliferation and its deletion leads to chronic lymphocytic leukaemia.* Cancer Cell, 2010. **17**(1): p. 28-40.
127. Dohner, H., et al., *11q deletions identify a new subset of B-cell chronic lymphocytic leukaemia characterized by extensive nodal involvement and inferior prognosis.* Blood, 1997. **89**(7): p. 2516-22.
128. Monni, O. and S. Knuutila, *11q deletions in hematological malignancies.* Leuk Lymphoma, 2001. **40**(3-4): p. 259-66.
129. Brown, J.R., *Insulin receptor activation in deletion 11q chronic lymphocytic leukaemia.* Clin Cancer Res, 2011. **17**(9): p. 2605-7.
130. Konikova, E. and J. Kusenda, *Altered expression of p53 and MDM2 proteins in hematological malignancies.* Neoplasma, 2003. **50**(1): p. 31-40.
131. Decker, S., et al., *Trisomy 12 and elevated GLI1 and PTCH1 transcript levels are biomarkers for Hedgehog-inhibitor responsiveness in CLL.* Blood, 2012. **119**(4): p. 997-1007.
132. el Rouby, S., et al., *p53 gene mutation in B-cell chronic lymphocytic leukaemia is associated with drug resistance and is independent of MDR1/MDR3 gene expression.* Blood, 1993. **82**(11): p. 3452-9.

133. Simonetti, G., et al., *Mouse models in the study of chronic lymphocytic leukaemia pathogenesis and therapy.* Blood, 2014. **124**(7): p. 1010-9.
134. Bichi, R., et al., *Human chronic lymphocytic leukaemia modeled in mouse by targeted TCL1 expression.* Proc Natl Acad Sci U S A, 2002. **99**(10): p. 6955-60.
135. Stein, J.V., et al., *APRIL modulates B and T cell immunity.* J Clin Invest, 2002. **109**(12): p. 1587-98.
136. Planelles, L., et al., *APRIL promotes B-1 cell-associated neoplasm.* Cancer Cell, 2004. **6**(4): p. 399-408.
137. Zapata, J.M., et al., *TNF receptor-associated factor (TRAF) domain and Bcl-2 cooperate to induce small B cell lymphoma/chronic lymphocytic leukaemia in transgenic mice.* Proc Natl Acad Sci U S A, 2004. **101**(47): p. 16600-5.
138. Widhopf, G.F., 2nd, et al., *ROR1 can interact with TCL1 and enhance leukemogenesis in Emu-TCL1 transgenic mice.* Proc Natl Acad Sci U S A, 2014. **111**(2): p. 793-8.
139. Santanam, U., et al., *Chronic lymphocytic leukaemia modeled in mouse by targeted miR-29 expression.* Proc Natl Acad Sci U S A, 2010. **107**(27): p. 12210-5.
140. Shukla, V., et al., *A role for IRF4 in the development of CLL.* Blood, 2013. **122**(16): p. 2848-55.
141. ter Brugge, P.J., et al., *A mouse model for chronic lymphocytic leukaemia based on expression of the SV40 large T antigen.* Blood, 2009. **114**(1): p. 119-27.
142. Johnson, A.J., et al., *Characterization of the TCL-1 transgenic mouse as a preclinical drug development tool for human chronic lymphocytic leukaemia.* Blood, 2006. **108**(4): p. 1334-8.
143. Zanesi, N., et al., *Effect of rapamycin on mouse chronic lymphocytic leukaemia and the development of nonhematopoietic malignancies in Emu-TCL1 transgenic mice.* Cancer Res, 2006. **66**(2): p. 915-20.
144. Messmer, B.T., et al., *In vivo measurements document the dynamic cellular kinetics of chronic lymphocytic leukaemia B cells.* J Clin Invest, 2005. **115**(3): p. 755-64.
145. Burger, J.A. and N. Chiorazzi, *B cell receptor signalling in chronic lymphocytic leukaemia.* Trends Immunol, 2013. **34**(12): p. 592-601.
146. Muzio, M., et al., *The role of toll-like receptors in chronic B-cell malignancies.* Leuk Lymphoma, 2009. **50**(10): p. 1573-80.

147. Pizzolo, G., et al., *Immunohistologic study of bone marrow involvement in B-chronic lymphocytic leukaemia.* Blood, 1983. **62**(6): p. 1289-96.
148. Nikolov, N.P. and G.G. Illei, *Pathogenesis of Sjogren's syndrome.* Curr Opin Rheumatol, 2009. **21**(5): p. 465-70.
149. Gorgun, G., et al., *E(mu)-TCL1 mice represent a model for immunotherapeutic reversal of chronic lymphocytic leukaemia-induced T-cell dysfunction.* Proc Natl Acad Sci U S A, 2009. **106**(15): p. 6250-5.
150. Burkle, A., et al., *Overexpression of the CXCR5 chemokine receptor, and its ligand, CXCL13 in B-cell chronic lymphocytic leukaemia.* Blood, 2007. **110**(9): p. 3316-25.
151. Burger, J.A., et al., *Blood-derived nurse-like cells protect chronic lymphocytic leukaemia B cells from spontaneous apoptosis through stromal cell-derived factor-1.* Blood, 2000. **96**(8): p. 2655-63.
152. Burger, J.A., M. Burger, and T.J. Kipps, *Chronic lymphocytic leukaemia B cells express functional CXCR4 chemokine receptors that mediate spontaneous migration beneath bone marrow stromal cells.* Blood, 1999. **94**(11): p. 3658-67.
153. Schmid, C. and P.G. Isaacson, *Proliferation centres in B-cell malignant lymphoma, lymphocytic (B-CLL): an immunophenotypic study.* Histopathology, 1994. **24**(5): p. 445-51.
154. Ding, W., et al., *Platelet-derived growth factor (PDGF)-PDGF receptor interaction activates bone marrow-derived mesenchymal stromal cells derived from chronic lymphocytic leukaemia: implications for an angiogenic switch.* Blood, 2010. **116**(16): p. 2984-93.
155. Panayiotidis, P., et al., *Human bone marrow stromal cells prevent apoptosis and support the survival of chronic lymphocytic leukaemia cells in vitro.* Br J Haematol, 1996. **92**(1): p. 97-103.
156. Redondo-Munoz, J., et al., *MMP-9 in B-cell chronic lymphocytic leukaemia is up-regulated by alpha4beta1 integrin or CXCR4 engagement via distinct signalling pathways, localizes to podosomes, and is involved in cell invasion and migration.* Blood, 2006. **108**(9): p. 3143-51.
157. Redondo-Munoz, J., et al., *Matrix metalloproteinase-9 is up-regulated by CCL21/CCR7 interaction via extracellular signal-regulated kinase-1/2 signalling and is involved in CCL21-*

driven B-cell chronic lymphocytic leukaemia cell invasion and migration. Blood, 2008. **111**(1): p. 383-6.
158. Jitschin, R., et al., *Stromal cell-mediated glycolytic switch in CLL cells involves Notch-c-Myc signalling.* Blood, 2015. **125**(22): p. 3432-6.
159. Bagdi, E., et al., *Follicular dendritic cells in reactive and neoplastic lymphoid tissues: a reevaluation of staining patterns of CD21, CD23, and CD35 antibodies in paraffin sections after wet heat-induced epitope retrieval.* Appl Immunohistochem Mol Morphol, 2001. **9**(2): p. 117-24.
160. Fakan, F., L. Boudova, and A. Skalova, *[Immunohistochemical detection of follicular dendritic cells in the diagnosis of small B-cell lymphomas]*. Cesk Patol, 2003. **39**(3): p. 96-101.
161. Pedersen, I.M., et al., *Protection of CLL B cells by a follicular dendritic cell line is dependent on induction of Mcl-1.* Blood, 2002. **100**(5): p. 1795-801.
162. Lopez-Guerra, M., S. Xargay-Torrent, and D. Colomer, *CXCR5-mediated shaping of the lymphoid follicle in chronic lymphocytic leukaemia.* Cancer Discov, 2014. **4**(12): p. 1374-6.
163. Tadmor, T., et al., *Significance of bone marrow reticulin fibrosis in chronic lymphocytic leukaemia at diagnosis: a study of 176 patients with prognostic implications.* Cancer, 2013. **119**(10): p. 1853-9.
164. Sangaletti, S., et al., *Defective stromal remodelling and neutrophil extracellular traps in lymphoid tissues favour the transition from autoimmunity to lymphoma.* Cancer Discov, 2014. **4**(1): p. 110-29.
165. Dighiero, G., et al., *Chlorambucil in indolent chronic lymphocytic leukaemia. French Cooperative Group on Chronic Lymphocytic Leukaemia*. N Engl J Med, 1998. **338**(21): p. 1506-14.
166. Hallek, M., *Chronic lymphocytic leukaemia: 2015 Update on diagnosis, risk stratification, and treatment.* Am J Hematol, 2015. **90**(5): p. 446-60.
167. Rai, K.R., et al., *Fludarabine compared with chlorambucil as primary therapy for chronic lymphocytic leukaemia*. N Engl J Med, 2000. **343**(24): p. 1750-7.
168. Lozanski, G., et al., *Alemtuzumab is an effective therapy for chronic lymphocytic leukaemia with p53 mutations and deletions.* Blood, 2004. **103**(9): p. 3278-81.

169. Stevenson, F.K., et al., *B-cell receptor signalling in chronic lymphocytic leukaemia.* Blood, 2011. **118**(16): p. 4313-20.
170. Herman, S.E., et al., *Bruton tyrosine kinase represents a promising therapeutic target for treatment of chronic lymphocytic leukaemia and is effectively targeted by PCI-32765.* Blood, 2011. **117**(23): p. 6287-96.
171. ten Hacken, E. and J.A. Burger, *Molecular pathways: targeting the microenvironment in chronic lymphocytic leukaemia--focus on the B-cell receptor.* Clin Cancer Res, 2014. **20**(3): p. 548-56.
172. Nguyen, P.H., et al., *LYN Kinase in the Tumour Microenvironment Is Essential for the Progression of Chronic Lymphocytic Leukaemia.* Cancer Cell, 2016. **30**(4): p. 610-622.
173. Burger, M., et al., *Small peptide inhibitors of the CXCR4 chemokine receptor (CD184) antagonize the activation, migration, and antiapoptotic responses of CXCL12 in chronic lymphocytic leukaemia B cells.* Blood, 2005. **106**(5): p. 1824-30.
174. Burger, J.A. and A. Peled, *CXCR4 antagonists: targeting the microenvironment in leukaemia and other cancers.* Leukaemia, 2009. **23**(1): p. 43-52.
175. Hoellenriegel, J., et al., *The phosphoinositide 3'-kinase delta inhibitor, CAL-101, inhibits B-cell receptor signalling and chemokine networks in chronic lymphocytic leukaemia.* Blood, 2011. **118**(13): p. 3603-12.
176. Valsecchi, R., et al., *HIF-1alpha regulates the interaction of chronic lymphocytic leukaemia cells with the tumour microenvironment.* Blood, 2016. **127**(16): p. 1987-97.
177. Hickstein, D.D., et al., *Identification of the promoter of the myelomonocytic leukocyte integrin CD11b.* Proc Natl Acad Sci U S A, 1992. **89**(6): p. 2105-9.

CHAPTER 4. Transcription factor TLX1 controls retinoic acid signalling to ensure spleen development

RESEARCH ARTICLE The Journal of Clinical Investigation

Transcription factor TLX1 controls retinoic acid signaling to ensure spleen development

Elisa Lenti,[1] Diego Farinello,[1] Kazunari K. Yokoyama,[2] Dmitry Penkov,[3,4] Laura Castagnaro,[1] Giovanni Lavorgna,[5] Kenly Wuputra,[2] Lisa L. Sandell,[6] Naomi E. Butler Tjaden,[7,8] Francesca Bernassola,[9] Nicoletta Caridi,[10] Anna De Antoni,[4] Michael Wagner,[11] Katja Kozinc,[12] Karen Niederreither,[13] Francesco Blasi,[4] Diego Pasini,[14] Gregor Majdic,[12] Giovanni Tonon,[10] Paul A. Trainor,[7,8] and Andrea Brendolan[1]

[1]Laboratory of Lymphoid Organ Development, Istituto di Ricovero e Cura a Carattere Scientifico (IRCCS), San Raffaele Scientific Institute, Milan, Italy. [2]Graduate School of Medicine, Kaohsiung Medical University, Kaohsiung, Taiwan. [3]Department of Basic Medicine, Moscow State University, Moscow, Russia. [4]Fondazione Italiana per la Ricerca sul Cancro (FIRC) Institute of Molecular Oncology, Milan, Italy. [5]Center for Translational Genomics and Bioinformatics, IRCCS, San Raffaele Scientific Institute, Milan, Italy. [6]University of Louisville School of Dentistry, Louisville, Kentucky, USA. [7]Stowers Institute for Medical Research, Kansas City, Missouri, USA. [8]Department of Anatomy and Cell Biology, University of Kansas Medical Center, Kansas City, Kansas, USA. [9]Department of Experimental Medicine and Surgery, University of Rome "Tor Vergata," Rome, Italy. [10]Laboratory of Functional Genomics of Cancer, IRCCS, San Raffaele Scientific Institute, Milan, Italy. [11]Department of Anatomy and Cell Biology, State University of New York Health Science Center, New York, New York, USA. [12]Centre for Animal Genomics, Veterinary Faculty, University of Ljubljana, Ljubljana, Slovenia. [13]Institut de Génétique et de Biologie Moléculaire et Cellulaire, CNRS UMR 7104, Inserm U964, Université de Strasbourg, Illkirch-Strasbourg, France. [14]European Institute of Oncology, Milan, Italy.

The molecular mechanisms that underlie spleen development and congenital asplenia, a condition linked to increased risk of overwhelming infections, remain largely unknown. The transcription factor TLX1 controls cell fate specification and organ expansion during spleen development, and *Tlx1* deletion causes asplenia in mice. Deregulation of *TLX1* expression has recently been proposed in the pathogenesis of congenital asplenia in patients carrying mutations of the gene-encoding transcription factor SF-1. Herein, we have shown that TLX1-dependent regulation of retinoic acid (RA) metabolism is critical for spleen organogenesis. In a murine model, loss of *Tlx1* during formation of the splenic anlage increased RA signaling by regulating several genes involved in RA metabolism. Uncontrolled RA activity resulted in premature differentiation of mesenchymal cells and reduced vasculogenesis of the splenic primordium. Pharmacological inhibition of RA signaling in *Tlx1*-deficient animals partially rescued the spleen defect. Finally, spleen growth was impaired in mice lacking either cytochrome P450 26B1 (*Cyp26b1*), which results in excess RA, or retinol dehydrogenase 10 (*Rdh10*), which results in RA deficiency. Together, these findings establish TLX1 as a critical regulator of RA metabolism and provide mechanistic insights into the molecular determinants of human congenital asplenia.

Introduction

The mammalian spleen is a secondary lymphoid organ that plays a central role in host defense. As a result, asplenia or hyposplenia and postsplenectomy patients often have an increased risk of overwhelming infections, particularly by encapsulated bacteria (1–5). Spleen development involves coordination of cell fate specification, migration, and proliferation to form a vascularized splenic primordium (6–9). In mice, these processes are coordinated by a limited set of transcription factors (10). Among these, T cell leukemia homeobox 1 (TLX1, also known as HOX11) (6, 11) acts downstream of the genetic cascade governing spleen development by promoting cell fate specification and organ expansion. At present, however, the precise downstream transcriptional networks and signaling pathways controlled by TLX1 remain unknown.

Tlx1-deficient mice are asplenic without any other abnormalities (6, 11), a phenotype resembling human isolated congenital asplenia (OMIM 271400), a condition in which the lack of the spleen exists as a sole organ defect (9, 12). Currently, only the ribosomal protein SA (*RPSA*) gene has been found mutated in isolated congenital asplenia patients (13); however, the precise role of RPSA during spleen development remains unknown. Congenital asplenia can be also associated with other abnormalities, such as laterality defects as observed in patients with Ivemark syndrome (OMIM 208530), patients with cardiac defects and transposition of great arteries (14), or patients with disorders of sexual development (OMIM 612965) carrying mutations in the gene encoding for steroidogenic factor 1 (SF-1/NR5a1) (15). Interestingly, a mutant form of SF-1 was recently shown to be defective in activating *TLX1* transcription in patients with disorders of sexual development and asplenia, thus providing the first evidence that perturbation of *TLX1* expression may be implicated in human congenital asplenia (16).

TLX1 regulates cellular proliferation and differentiation in different cellular systems (6, 8, 17–22). During spleen development, loss of *Tlx1* causes reduced proliferation of the splenic mesenchyme (SPM) and growth arrest (8, 23). Conversely, ectopic expression of *Tlx1* in thymocytes blocks differentiation and promotes

Conflict of interest: The authors have declared that no conflict of interest exists.
Submitted: June 22, 2015; **Accepted:** April 5, 2016.
Reference information: *J Clin Invest*. 2016;126(7):2452–2464. doi:10.1172/JCI82956.

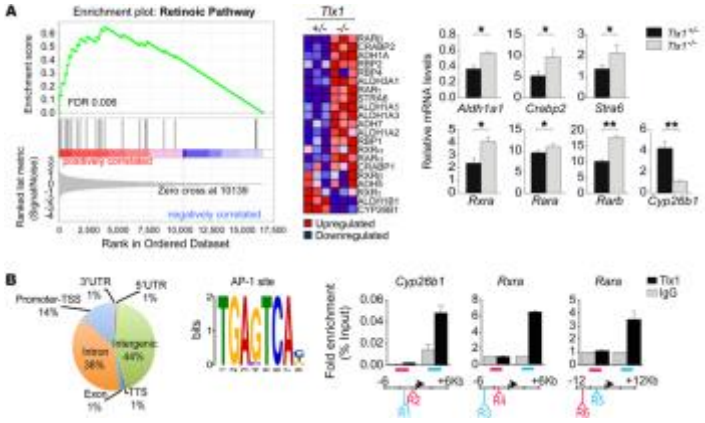

Figure 1. TLX1 controls RA signaling pathway. (**A**) GSEA enrichment plots and heat maps of differentially expressed genes belonging to the RA pathway associated with loss of *Tlx1*. The bar-code plot indicates the position of the genes on the expression data rank-sorted by its association with *Tlx1* mutants, with red and blue colors indicating over- and underexpression in the mRNA. Validation of RA-associated genes by qPCR was performed on *Tlx1*$^{+/-}$ and *Tlx1*$^{-/-}$ embryonic spleens. The means of triplicates ± SD are shown. *$P < 0.05$, **$P < 0.01$ (2-tailed Student's *t* test). Data are representative of 1 of 2 different validation experiments with 8–10 pooled spleens for each genotype. (**B**) TLX1 peak annotation relative to the indicated genomic feature. TLX1 ChIP-seq was performed in the eSMC line, and peak call was generated by comparison with an unrelated ChIP-seq experiment using rabbit IgG as control. MEME motif prediction of DNA sequences enriched in TLX1 ChIP-seq. ChIP-qPCR analysis of TLX1 binding in eSMC line. Positive (R1, R3, and R5) and negative (R2, R4, and R6) binding regions are indicated relative to transcription start site (TSS). Data are normalized to amplification of the input chromatin. Data are representative of 1 of 3 independent experiments.

leukemogenesis by altering the expression of genes involved in cell cycle regulation and thymocyte development (18, 19, 21, 24). At the molecular level, TLX1 can act as both an activator and a repressor of gene transcription depending on the cellular context and its interaction with transcriptional cofactors (25). For example, retinaldehyde dehydrogenase 1 (*Raldh1*, also known as *Aldh1a1*) is a gene that encodes a retinoic acid–synthesizing (RA-synthesizing) enzyme (26), and in mouse embryonic fibroblasts, TLX1 activates *Aldh1a1* expression (24, 25, 27). In contrast, in the developing mouse spleen, TLX1 represses *Aldh1a1* expression (25). At present, however, it remains unknown whether TLX1 plays a role in regulating retinoid signaling during spleen development, and whether deregulation in this pathway affects spleen organogenesis.

RA, the active metabolite of vitamin A, is an essential molecule required for vertebrate patterning and embryogenesis (15, 26, 28–31). RA binds to nuclear receptors (RARs) and regulates critical developmental pathways governing cellular proliferation, differentiation, organogenesis, and tissue homeostasis (32, 33). In the developing embryo, the activities of RA-synthesizing (RDHs, ALDHs) and degrading enzymes of cytochrome P450 family 26 (CYP26) regulate RA metabolism (31). Notably, elevated RA signaling in *Cyp26b1*$^{-/-}$ mutants causes aberrant cellular proliferation and differentiation, leading to several organ abnormalities including lymphatic vascular defects and altered germ cell development (33–36). Notably, RA controls the fate of germ cells in mice while SF-1 regulates RA metabolism during germ cell development (15, 37). Furthermore, elevated RA signaling in the form of teratogenic doses of RA in mice, rats, and nonhuman primates has also been associated with organ growth abnormalities (38–43).

Herein, we set out to uncover the molecular mechanism by which TLX1 regulates spleen development. Using gene expression profile analysis, we found that loss of *Tlx1* in the SPM causes upregulation of several genes involved in RA metabolism. Conversely, the expression of *Cyp26b1*, which encodes an enzyme involved in RA degradation, is markedly reduced in the embryonic splenic anlage of *Tlx1* mutant mice. Analysis of *Cyp26b1* or retinol dehydrogenase 10 (*Rdh10*) mutants, which respectively exhibit an excess or deficiency in RA signaling, revealed severe spleen hypoplasia or agenesis, demonstrating the importance of finely regulating RA metabolism to ensure proper spleen development. Interestingly, loss of *Sf-1* during spleen development also reduced *Tlx1* and *Cyp26b1* expression. Genome-wide analysis indicated that TLX1 binds the regulatory regions of RA-associated genes through the AP-1 site and cooperates with the AP-1 family of transcription factors to regulate gene expression. Importantly, pharmacological inhibition of RA signaling partially rescued the spleen phenotype of *Tlx1* mutants. Collectively, our findings unveil molecular interactions critical for spleen development and shed light onto the pathogenesis of congenital asplenia.

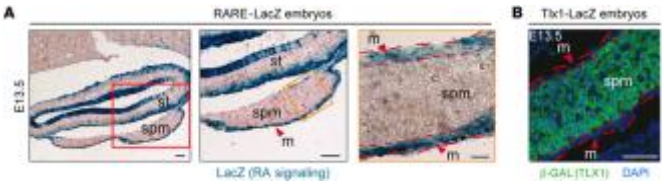

Figure 2. *Tlx1* expression is excluded from the domains of RA signaling. Transverse sections of RARE-LacZ embryos at E13.5 stained for LacZ to show RA signaling (**A**) and confocal images of E13.5 $Tlx1^{+/-}$ spleen sections to show TLX1 (β-GAL) (**B**). Scale bars: 50 μm and 25 μm. st, stomach; spm, splenic mesenchyme; m, mesothelium. Data are representative of 1 embryo of 5 embryos analyzed.

Results

Loss of Tlx1 deregulates the RA signaling pathway. We previously showed that loss of *Tlx1* causes defects in specification and proliferation of spleen mesenchymal progenitors (8). However, the mechanisms by which TLX1 coordinates the initiation and expansion of the splenic anlage remain unknown. To identify deregulated genes and signaling pathways associated with loss of *Tlx1*, we performed gene expression analysis using mRNA obtained from $Tlx1^{+/-}$ heterozygous and $Tlx1^{-/-}$ homozygous embryonic spleens at E13.5 (Figure 1A). This time point was chosen because it coincides with the appearance of the spleen defect in $Tlx1^{-/-}$ homozygous embryos. Gene ontology analysis revealed statistically significant differences in the expression of genes related to developmental processes including spleen organogenesis (Supplemental Figure 1; supplemental material available online with this article; doi:10.1172/JCI82956DS1). To identify deregulated pathways resulting from *Tlx1* loss, we took advantage of the Gene Set Enrichment Analysis (GSEA) tool, a computational method that detects modest but coordinated changes in the expression of groups of functionally related genes (44). Remarkably, we found a highly significant deregulation of the RA pathway (FDR = 0.006) (Figure 1A). Quantitative PCR (qPCR) validation analysis revealed that genes encoding for the RA-synthesizing enzymes (i.e., *Aldh1a1*), RA nuclear receptors (i.e., *Rara*, *Rarb*), and vitamin A/RA transporters (i.e., *Stra6/Crabp2*) were all upregulated as a result of *Tlx1* ablation (Figure 1A). Conversely, the expression of the RA-degrading enzyme *Cyp26b1* was significantly reduced in the absence of *Tlx1* (Figure 1A).

TLX1 binds genes associated with the RA pathway. To identify whether TLX1 binds RA-associated genes, we performed ChIP sequencing (ChIP-seq) in the embryonic spleen mesenchymal cell (eSMC) line. Analysis of the profile distribution revealed preferential binding of TLX1 to intergenic (44%) and intronic (38%) regions and, to a lesser extent, to promoter (14%) regions (Figure 1B). We then searched for putative TLX1-binding sites by motif discovery analysis using the multiple EM for motif elicitation (MEME) algorithm and found enrichment for an AP-1 site consensus element (Figure 1B), suggesting control of genes bearing the AP-1 motif (45). Confirming this finding, ChIP-qPCR analysis showed binding of TLX1 to *Cyp26b1*, *Rara*, and *Rxra* genomic regions carrying the AP-1 sequence (Figure 1B and Supplemental Sequences 1–5). Moreover, we found that the AP-1 sequence was present in several RA-associated genes deregulated in our GSEA analysis (Figure 1A and Supplemental Table 1). Consistent with TLX1 acting as either a cotranscriptional repressor or activator of gene transcription, cotransfection of *Tlx1* with *Jdp2* or *c-Jun* — 2 AP-1 family members with opposite transcriptional functions — synergistically modulates the transactivation of an AP-1 luciferase reporter system (Supplemental Figure 2A). Expression of *Jdp2* was strongly reduced in *Tlx1* mutant as compared with control embryonic spleens (Supplemental Figure 2B), and, in agreement with these data, ChIP-seq analysis followed by ChIP-qPCR revealed direct binding of TLX1 to the *Jdp2* locus (Supplemental Figure 2B). These findings raised the possibility that TLX1 and JDP2 may act in concert to regulate transcription. We therefore examined a possible physical association of TLX1 and JDP2, and found that these transcription factors interact in reciprocal coimmunoprecipitation assays (Supplemental Figure 2C), thus suggesting transcriptional coregulation of target genes, including RA-associated genes. Collectively, these findings demonstrate a direct transcriptional control of TLX1 on RA signaling during spleen organogenesis.

RA signaling and Tlx1 expression are mutually exclusive during spleen development. To determine whether and where RA signaling is active during normal spleen development, we analyzed WT RARE-*LacZ* transgenic embryos during the initial formation of the splenic anlage (Figure 2). In this mouse model, β-gal expression is under the control of an RA-responsive element (RARE), and, as a result, LacZ staining reveals the domains of active RA signaling (46). We found that at E11.5 RA activity is absent in the newly formed splenic anlage (Supplemental Figure 3). In contrast, RA activity is detectable at E13.5 and is confined to the outer mesothelium layer, whereas the inner SPM remains devoid of RA signaling (Figure 2A). Interestingly, staining of $Tlx1^{LacZ/+}$ heterozygous embryos, in which LacZ marks the domain of *Tlx1* expression, revealed that during normal spleen development, *Tlx1* is expressed only in the SPM (Figure 2B). In contrast, TLX1 is excluded from the outer mesothelial region exhibiting RA signaling (Figure 2A), thus indicating that TLX1 and RA are present in mutually exclusive domains during spleen development. Altogether, these results indicate that TLX1 may repress RA signaling in the SPM, possibly through the control of *Cyp26b1* expression and RA degradation.

Uncontrolled RA signaling causes spleen growth defects. Previous work has shown that *Cyp26b1* deficiency causes developmental defects consistent with excessive RA activity (34, 35, 39), demon-

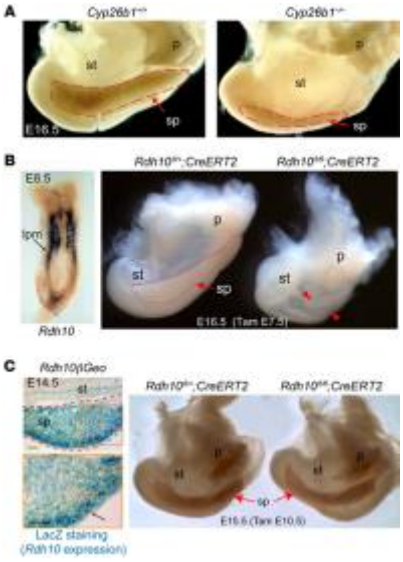

Figure 3. Spatiotemporal requirement of RA signaling during spleen development. (**A**) Gross morphology of abdominal organs from *Cyp26b1*$^{-/-}$ and *Cyp26b1*$^{+/+}$ embryos at E16.5. Data are representative of 1 embryo of 10 mutant and 8 control embryos analyzed from 4 different litters. (**B**) In situ hybridization for *Rdh10* at E8.5 (left) and gross morphology of E16.5 abdominal organs from *Rdh10*$^{fl/+}$*;CreERT2* embryos injected with tamoxifen at E7.5 (right). Data are representative of 1 embryo of 6 mutant and 6 control embryos analyzed from different litters and time points for each genotype. (**C**) Expression of *Rdh10* in the developing spleen as shown by LacZ staining of E14.5 spleens from *Rdh10βGeo* mice (left). Gross morphology of E15.5 abdominal organs from *Rdh10*$^{fl/+}$*;CreERT2* embryos injected with tamoxifen at E10.5 (right). Scale bars: 50 μm. Data are representative of 1 embryo of 15 mutant and 8 control embryos analyzed from 3 different litters. Dashed red lines indicate the developing spleen; red arrows indicate spleen normal situs. st, stomach; sp, spleen; p, pancreas; lpm, lateral plate mesoderm.

strating the critical role of this enzyme in regulating RA homeostasis during embryonic development. The finding that *Cyp26b1* is expressed during spleen development (47) and that it is strongly reduced in *Tlx1* mutant embryonic spleens (Figure 1A) prompted us to test the hypothesis that impaired CYP26B1 function causes spleen growth defects. Remarkably, analysis of *Cyp26b1* mutant embryos at E16.5 (Figure 3A) revealed the presence of only remnant splenic tissue when compared with littermate controls.

We then hypothesized that excessive RA signaling due to loss of *Cyp26b1* expression inhibits spleen development, and therefore sought to assess whether physiological levels of RA are required for the proper patterning of spleen descendants in the lateral plate mesoderm (LPM), from which the spleen is thought to arise. We first performed lineage-tracing experiments to unequivocally demonstrate the contribution of the LPM to the SPM by crossing R26YFP reporter mice to *Hoxb6-CreER* mice, in which tamoxifen-dependent Cre expression is directed to the LPM (48). Injection of *Hoxb6-CreER R26RYFP* pregnant females at E8.5 with a single dose of tamoxifen followed by immunofluorescence analysis revealed a large contribution of the YFP$^+$ LPM mesodermal cells to the developing SPM (Supplemental Figure 3).

Next, we crossed *Rdh10*$^{fl/fl}$ mice to the Cre-ERT2 tamoxifen-inducible transgenic line to conditionally ablate *Rdh10*, a critical enzyme involved in the first step of RA synthesis in the embryo (49, 50). Consistent with its expression in the LPM (Figure 3B), ablation of *Rdh10* by a single dose of tamoxifen at E7.5 caused spleen agenesis in mutant embryos compared with littermate controls (Figure 3B). Conversely, despite expression of *Rdh10* in developing spleen (Figure 3C), ablation of *Rdh10* by administration of tamoxifen at E10.5 during initial formation of the spleen primordium did not affect organogenesis (Figure 3C). Collectively, these findings demonstrate a differential and precise spatiotemporal requirement for RA during spleen development.

CYP26B1 in spleen mesenchymal cells is required to prevent aberrant RA signaling. To formally demonstrate that increased RA activity in the *Tlx1* mutant SPM is caused by reduced *Cyp26b1* expression, we exploited an in vitro system by coculturing RA reporter F9-LacZ cells (51) with an eSMC line that has been shown to mimic the native embryonic mesenchyme (9). Notably, silencing *Tlx1* in eSMCs via *shRNA* recapitulates our in vivo data by causing deregulated expression of several RA-associated genes, including *Cyp26b1* (Figure 4A and Supplemental Figure 4).

To assess the functional consequences of *Tlx1* and *Cyp26b1* deficiency for RA signaling, we cocultured RA reporter F9-LacZ cells with *shRNA-Tlx1* or *shRNA-Ctrl* control eSMCs, and performed LacZ staining to measure RA activity (Figure 4B). In the absence of TLX1, the number of LacZ$^+$ cells was significantly higher than among reporter cells cultured with *shRNA-Ctrl* control eSMCs (Figure 4B). Interestingly, rescue of *Cyp26b1* expression reduced the number of blue cells seen among *shRNA-Tlx1* eSMCs to none or a few, similar to what is seen in *shRNA-Ctrl* control eSMCs (Figure 4B). These findings demonstrate that loss of CYP26B1 function in *Tlx1* mutants causes increased RA signaling in the SPM.

To corroborate the role of CYP26B1 in limiting RA content and signaling in the SPM, we measured the expression of RA target genes under condition of CYP26B1 inhibition. RA-treated eSMCs cultured in the presence of the CYP26B1 inhibitor R116010 (52) displayed increased expression of RA-responsive genes (Supplemental Figure 3), thus demonstrating the critical role of CYP26B1 in restricting RA signaling in spleen mesenchymal cells.

TLX1 blocks RA-induced differentiation. Since our data demonstrated a role for TLX1 as a repressor of RA signaling, we next evaluated the effect of RA on the differentiation of F9 cells, a cellular system previously used to study RA-induced differentiation (53, 54). We found that the expression levels of *Lamb1* and *Col4a1*, 2 genes associated with RA-induced endodermal differentiation (53, 55), were significantly reduced in *Tlx1*-overexpressing F9 cells

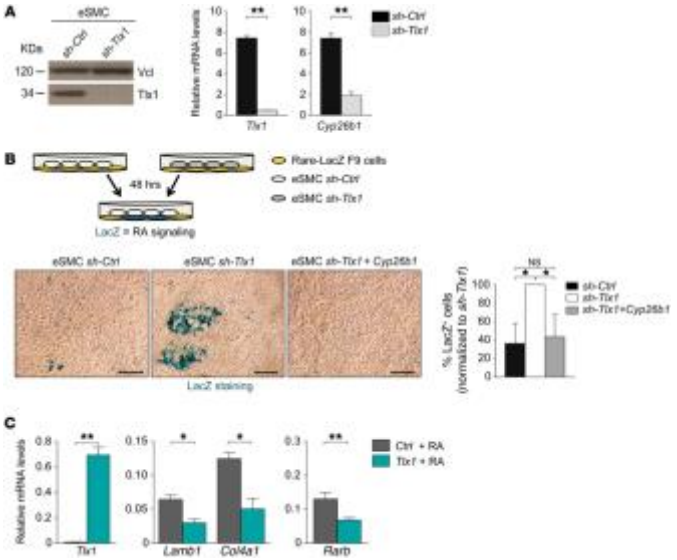

Figure 4. TLX1 controls RA activity. (**A**) Western blot analysis of TLX1 protein in eSMCs upon shRNA silencing of *Tlx1 (left)*. Anti-vinculin (Vcl) antibody is used as a loading control. Expression of *Tlx1* and *Cyp26b1* in *sh-Ctrl* and *sh-Tlx1* eSMCs (right). Data are representative of 3 independent experiments. (**B**) Scheme of the coculture experiments with RARE–LacZ F9 reporter cells and *sh-Ctrl* or *sh-Tlx1* eSMCs. Bright-field images of LacZ staining of F9-RARE-LacZ reporter cells cocultured for 48 hours with *sh-Ctrl* eSMCs (control), *sh-Tlx1* eSMCs (silenced), or *sh-Tlx1* eSMCs re-expressing *Cyp26b1*. Scale bars: 50 μm. Differences were measured by counting of the number of LacZ$^+$ cells (in blue) over total cells. Data are representative of 1 of 3 independent experiments. (**C**) RARE-F9 cells transiently expressing *Tlx1* or control vector were treated with RA and expression of indicated genes analyzed by qPCR 30 hours later. Data are representative of 1 of 3 independent experiments. (**A–C**)The means of triplicates ± SD are shown, $^*P < 0.05$ (**B** and **C**), $^{**}P < 0.01$ (**A** and **C**) (2-tailed Student's *t* test).

as compared with control cells (Figure 4C). Similarly, the expression of *Rarb,* a gene positively regulated by RA, was 50% lower in *Tlx1*-overexpressing cells than in control cells (Figure 4C), thus demonstrating that TLX1 counteracts RA-induced differentiation.

RA induces spleen growth arrest. GSEA analysis revealed enrichment for pathways associated with cell cycle control. Notably, the genes included in this signature were downregulated in *Tlx1* mutants (Supplemental Figure 5A). Consistent with this, we found that treatment of E13.5 primary spleen mesenchymal cells with RA significantly suppressed cellular proliferation compared with vehicle-treated cultures (Figure 5A). In line with this, RA treatment induced an upregulation of the cell cycle inhibitor *Cdkn2b/p15*. Notably, we found a significant upregulation of *Cdkn2b/p15* mRNA levels in *Tlx1* mutants as compared with control embryonic spleens (Figure 5A).

To assess the functional effects of RA exposure on spleen growth, we performed organotypic cultures. E13.5 WT littermate spleens were divided into 2 groups and cultured, on a collagen layer, in the presence of RA or vehicle. Quantitative analysis of spleen size revealed that RA exposure significantly inhibits growth, which is accompanied by reduced sprouting of mesenchymal cells into the collagen layer (Figure 5B, arrows). In line with these data, silencing of *Tlx1* causes G1 cell cycle arrest and deregulation of the RA signaling pathway (Supplemental Figure 4A and Supplemental Figure 5B). Altogether, these findings demonstrate that excessive RA signaling inhibits spleen organ expansion by reducing spleen mesenchymal cell proliferation.

Increased RA signaling induces premature differentiation and reduced vasculogenesis. Retinoid excess in humans and mice causes a wide spectrum of malformations associated with patterning defects, premature differentiation, and organ growth arrest (29, 35, 36, 38–40, 56). Consistent with this phenomenon, our GSEA revealed enrichment of signatures associated with markers of lymphoid stromal cell maturation and extracellular matrix. Particularly, genes that belong to these pathways were induced in *Tlx1* mutant as compared with control splenic anlage (Supplemental Figure 6). To test the possibility that increased RA activity in the

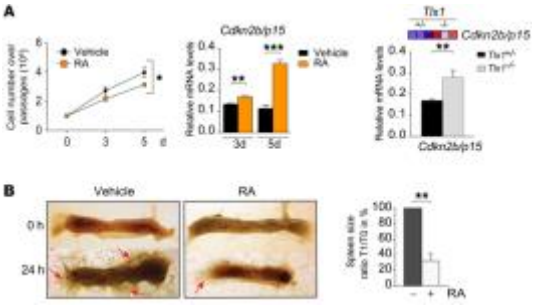

Figure 5. RA induces the expression of cell cycle inhibitors and growth arrest. (**A**) Growth curve analysis of primary E13.5 spleen mesenchymal cells treated with RA or control vehicle (left). The means of triplicates ± SD are shown, $^{*}P < 0.05$ (2-way ANOVA). Data are representative of 1 of 3 independent experiments. Expression of *Cdkn2b/p15* in primary E13.5 spleen mesenchymal cells treated for 3 or 5 days with RA or control vehicle (middle). The means of triplicates ± SD are shown, $^{**}P < 0.01$, $^{***}P < 0.001$ (2-tailed Student's *t* test). Data are representative of 1 of 2 independent experiments. Heat map and validation of *Cdkn2b/p15* expression by qPCR in E13.5 $Tlx1^{+/-}$ and $Tlx1^{-/-}$ spleens (right). The means of triplicates ± SD are shown, $^{**}P < 0.01$ (2-tailed Student's *t* test). Data are representative of 1 of 2 independent validation experiments. (**B**) Bright-field images of E13.5 explanted spleens cultured in the presence of RA or vehicle (DMSO). Arrows indicate mesenchymal cell sprouting. Quantification of the spleen size area (%) was calculated using ImageJ, as the ratio of spleen area at 24 hours versus 0 hours. The means of triplicates ± SD are shown, $^{**}P < 0.01$ (2-tailed Student's *t* test). Data are representative of 1 of 3 independent experiments with 8 explanted spleens for each condition.

Tlx1 mutant SPM results in premature cellular differentiation, we evaluated the expression of *Desmin*, a marker associated with maturation of spleen mesenchymal cells (57–59). *Desmin* was strongly upregulated at both the mRNA and the protein level in E13.5 *Tlx1* mutants as compared with control embryonic spleens (Figure 6A). Consistent with this observation, treatment of E14.5 primary spleen mesenchymal cells with RA induced a significant upregulation of *Desmin* expression (Figure 6A). In addition, we assessed the expression of ER-TR7, an antigen expressed by differentiating spleen and lymph node mesenchymal cells (60). Importantly, immunofluorescence analysis showed that ER-TR7 expression starts only postnatally in WT mice (Supplemental Figure 6B). However, ER-TR7 is prematurely expressed in *Tlx1* mutants as compared with controls (Supplemental Figure 6C). Finally, GSEA analysis revealed a significant increase in the expression of *Hox* genes that are known to be under the control of retinoid signaling during embryonic development (32) (Supplemental Figure 6D). Altogether, these findings indicate that the premature differentiation occurring in *Tlx1* mutants is caused, at least in part, by deregulation of RA signaling.

In addition to mesenchymal cells, the splenic anlage comprises endothelial cells that form an expanding vascular network. RA was shown to regulate the expression of *Vegf-a* (61), the major mitogen for endothelial cell proliferation and vessel network formation. Consistent with this principle, treatment of E14.5 primary spleen mesenchymal cells with RA reduced *Vegf-a* expression as compared with vehicle-treated cells (Figure 6B). Also, *Vegf-a* expression was strongly reduced in E13.5 *Tlx1* mutant as compared with controls, and this was accompanied by decreased microvessel density (Figure 6B). Moreover, TLX1 expression as indicated by β-gal staining of $Tlx1^{LacZ/+}$ knock-in embryos was not expressed in PECAM-1^{+} endothelial cells (Figure 6C), thus indicating a non–cell-autonomous role of TLX1 during vasculogenesis. These results are consistent with the idea that RA affects vasculogenesis in a paracrine fashion.

Inhibition of RA signaling partially rescues the spleen phenotype. We hypothesized that inhibition of RA signaling could potentially ameliorate the asplenic phenotype of *Tlx1* mutants. To test this idea, we crossed $Tlx1^{+/-}$ mice and treated pregnant females with BMS493, a pan-RAR antagonist (62, 63), during the initiation of spleen development at E10.5. We took advantage of *Tlx1* mutant mice expressing LacZ under the *Tlx1* endogenous promoter, in which LacZ staining marks the distribution of $TLX1^{+}$ spleen mesenchymal cells within the nascent splenic anlage. We observed that at E14.5, BMS493-treated *Tlx1* mutant spleens were mostly formed by 1 single splenic anlage and were more compact compared with untreated controls that exhibited multiple unjoined splenules/accessory spleens (Figure 7A). However, an evaluation of spleen size, as assessed by measurement of the surface of the $LacZ^{+}$ anlagen, did not reveal significant differences between homozygous mutant spleens from BMS493- and vehicle-treated mice (Figure 7A). Furthermore, qPCR analysis revealed that BMS493 treatment induced a significant rescue in the expression of *Vegf-a*, whereas *Desmin* expression was not rescued (Figure 7B). Importantly, the expression of 2 RA target genes — *Col4a1* and *Lamb1* — which are negatively regulated by RA in the SPM of *Tlx1* mutants, was completely recovered by RA signaling inhibition (Figure 7B). Similarly, the expression of *Rarb*, a gene positively regulated by RA, was also completely rescued by BMS493 treatment, thus demonstrating the presence of increased RA signaling in the absence of *Tlx1*. Altogether, these findings indicate that repression of RA signaling is required for condensation of spleen mesenchymal cells and organ morphogenesis.

SF-1 controls Tlx1 and RA metabolism in the SPM. Recent work by Zangen and collaborators reported that SF-1, which is required for human spleen development, transactivates the *TLX1* promoter (16). In addition, loss of *Sf-1* in mice causes a severe spleen hypoplasia defect (64). To test the hypothesis that *Sf-1* is genetically upstream of *Tlx1*, we performed gene expression analysis using mRNA obtained from $Sf1^{-/-}$ homozygous or control splenic anlagen at E14.5. Consistent with the hypothesis, we found a significant reduction of *Tlx1* mRNA levels in $Sf1^{-/-}$ mutants as compared with controls (Figure 8A). The expres-

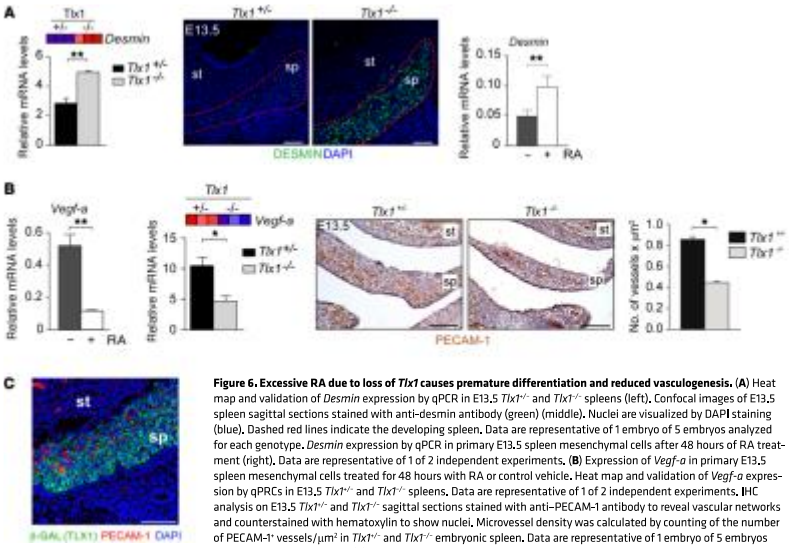

Figure 6. Excessive RA due to loss of *Tlx1* causes premature differentiation and reduced vasculogenesis. (**A**) Heat map and validation of *Desmin* expression by qPCR in E13.5 *Tlx1*$^{+/-}$ and *Tlx1*$^{-/-}$ spleens (left). Confocal images of E13.5 spleen sagittal sections stained with anti-desmin antibody (green) (middle). Nuclei are visualized by DAPI staining (blue). Dashed red lines indicate the developing spleen. Data are representative of 1 embryo of 5 embryos analyzed for each genotype. *Desmin* expression by qPCR in primary E13.5 spleen mesenchymal cells after 48 hours of RA treatment (right). Data are representative of 1 of 2 independent experiments. (**B**) Expression of *Vegf-a* in primary E13.5 spleen mesenchymal cells treated for 48 hours with RA or control vehicle. Heat map and validation of *Vegf-a* expression by qPRCs in E13.5 *Tlx1*$^{+/-}$ and *Tlx1*$^{-/-}$ spleens. Data are representative of 1 of 2 independent experiments. IHC analysis on E13.5 *Tlx1*$^{+/-}$ and *Tlx1*$^{-/-}$ sagittal sections stained with anti–PECAM-1 antibody to reveal vascular networks and counterstained with hematoxylin to show nuclei. Microvessel density was calculated by counting of the number of PECAM-1$^+$ vessels/μm^2 in *Tlx1*$^{+/-}$ and *Tlx1*$^{-/-}$ embryonic spleen. Data are representative of 1 embryo of 5 embryos analyzed for each genotype. (**C**) Representative confocal images of E13.5 *Tlx1*$^{+/-}$ and *Tlx1*$^{-/-}$ spleen sagittal sections stained with anti–PECAM-1 antibody (red) to reveal endothelial cells and anti–β-gal antibody (green) to show TLX1-expressing cells in *Tlx1-LacZ* knock-in embryos. Nuclei are visualized by DAPI staining (blue). Data are representative of 1 embryo of 5 embryos analyzed for each genotype. (**A** and **B**) The means of triplicates ± SD are shown. $^*P < 0.05$ (**B**), $^{**}P < 0.01$ (**A** and **B**) (2-tailed Student's *t* test). (**A**–**C**) Scale bars: 50 μm. st, stomach; sp, spleen.

sion of the RA-degrading enzyme *Cyp26b1* was also severely reduced in *Sf1*$^{-/-}$ mutants as compared with controls (Figure 8A). In agreement with this observation, we found that SF-1 transactivates the *Cyp26b1* promoter in a dose-dependent manner (Figure 8B). We then tested the possibility that, similar to TLX1, SF-1 may counteract the differentiation effects of RA. To this end, we treated F9 cells, transiently transfected with *Sf-1*, with RA and evaluated the expression of markers associated with cellular differentiation. Similarly to what we observed for *Tlx1*, overexpression of *Sf-1* significantly inhibited cellular differentiation as demonstrated by reduction of the expression *of Lamb1* and *Col4a1*, 2 genes associated with RA-induced endodermal differentiation (53, 55) (Figure 8C). Moreover, the expression of *Rarb*, a gene positively regulated by RA, was also significantly lower in *Sf-1*–expressing cells as compared with control cells (Figure 8C). Previous work showed that loss of *Sf-1* during spleen development causes reduced vasculogenesis (64). Consistent with this finding, we observed a significant reduction in *Vegf-a* mRNA levels in *Sf-1* mutants as compared with control embryonic splenic anlagen (Figure 8). Altogether these findings support a model in which SF-1 regulates *Tlx1* expression and RA metabolism to ensure spleen development.

Discussion

The lack of a spleen is often associated with deadly infections in humans. At present, the molecular mechanisms underlying asplenia remain mostly elusive. In the absence of *Tlx1*, spleen mesenchymal cells fail to proliferate and to form a discrete splenic primordium after E13.5 (6, 8, 11, 65). Our findings demonstrate that expression of *Tlx1* in the SPM is required to control excessive RA signaling in order to assure the proliferation of mesenchymal precursors and the formation of the splenic anlage. In support of this conclusion, we showed that loss of *Tlx1* leads to an increase in RA activity. This effect is due to reduced RA degradation caused by deregulated *Cyp26b1* expression and to increased nuclear receptor expression and activation. RA may diffuse or be transported within the nascent SPM, causing aberrant morphogenesis, premature differentiation, and vascular abnormalities. Furthermore, the finding that *Cyp26b1* mutant embryos exhibit only a remnant of splenic tissue clearly demonstrates the importance of restricting RA activity within the SPM to ensure proper spleen development. In support of this notion, re-expression of *Cyp26b1* in *Tlx1*-deficient mesenchymal cells restored RA signaling to control levels, indicating that uncontrolled RA signaling in *Tlx1* mutants is due to a deficit in CYP26B1 activity. While exces-

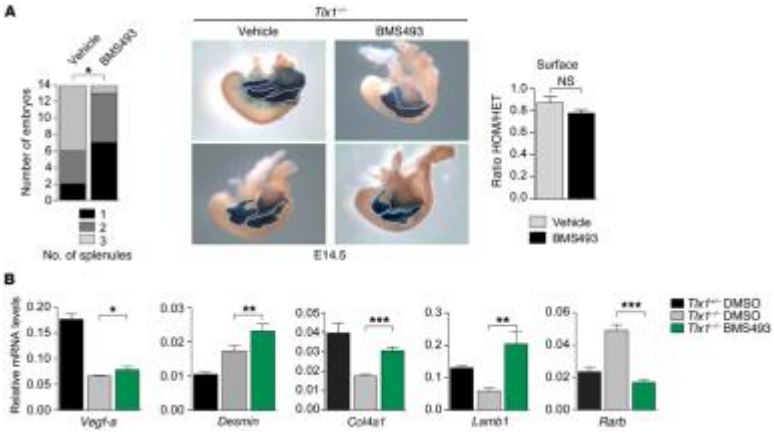

Figure 7. Inhibition of RA signaling partially rescues the spleen phenotype. (**A**) Partial rescue of spleen morphogenesis in E14.5 *Tlx1*$^{-/-}$ embryonic spleens treated with BMS493 or control vehicle at E10.5. Number of unjoined splenules (outlined in white) and surface area measurements were normalized to littermate controls. Statistical significance in the number of unjoined splenules was calculated using χ^2. $^*P < 0.05$. For the surface area measurement, the means of triplicates ± SD are shown. NS, not significant (2-tailed Student's *t* test). Data are from 15 (BMS493) and 14 (DMSO) treated embryonic spleens from 3 different litters. HOM, homozygous; HET, heterozygous. (**B**) Validation of *Vegf-a*, *collagen 4a1 (Col4a1)*, *laminin B1* (*Lamb1*), and *Rarb* expression by qPRCs in E14.5 *Tlx1*$^{+/-}$ and *Tlx1*$^{-/-}$ embryonic spleens treated with BMS493 or control vehicle. The means of triplicates ± SD are shown, $^*P < 0.05$, $^{**}P < 0.01$, $^{***}P < 0.001$ (2-tailed Student's *t* test). Data are representative of a pool of 12–16 embryonic spleens for each group from 4 different experiments.

sive RA signaling in *Cyp26b1* mutants is detrimental during the formation of the splenic primordium, loss of RA synthesis at this stage did not affect spleen development. Nevertheless, ablation of retinoid synthesis in the LPM from which spleen mesenchymal precursors originate caused spleen agenesis, indicating the presence of a spatiotemporal window in which retinoids are required during spleen organogenesis.

Excess of retinoids has been shown to cause several developmental anomalies, including abnormal morphogenesis and organ growth inhibition (38–40, 43, 66). Consistent with these observations, we showed that *Tlx1* mutant spleens exhibit reduced vasculogenesis and premature differentiation of mesenchymal progenitors. RA mediates these effects, since addition of RA to spleen organotypic cultures reduces *Vegf-a* expression while inducing *Desmin* and other markers normally expressed by mature lymphoid stromal cells (59). Also, *Tlx1* is not expressed in endothelial cells of the SPM, indicating a non–cell-autonomous role in the vasculogenesis defect. Thus, reduced CYP26B1-degrading activity within the SPM causes increased levels of RA signaling that affects endothelial cell proliferation in a paracrine fashion.

We have previously shown that loss of *Tlx1* leads to reduced proliferation of the SPM (8, 18). Consistent with this observation, we found that silencing *Tlx1* in spleen mesenchymal cells increases RA signaling and reduces proliferation by promoting G1 cell cycle arrest. The notion that RA-induced growth inhibition is associated with G1 cell cycle arrest in different cellular systems (67) suggests that RA may contribute to the proliferation defect observed in *Tlx1* mutant spleen. Supporting this hypothesis is the finding that *Cdkn2b/p15*, a gene that we showed to be induced by RA treatment in primary eSMCs, is significantly increased in *Tlx1*-deficient splenic anlage. However, the spleen phenotype of *Tlx1* mutants is only partially rescued upon inhibition of RA signaling in vivo. One explanation for this discrepancy may be the inefficient activity of the BMS493 inhibitor on RA signaling in vivo. In addition, TLX1 may control gene transcription and cellular proliferation independently of RA as previously demonstrated (17, 18). Indeed, while expression of *Col4a1*, *Lamb1*, and *Rarb* was significantly rescued upon RA signaling inhibition, *Vegf-a* transcription was only modestly reactivated. In addition, the expression of *Desmin* and *Cdkn2b/p15* (not shown) was not rescued upon RA inhibition.

At the molecular level, our ChIP-seq analysis revealed that TLX1 binds DNA preferentially through the AP-1 motif, a sequence found in the *Vegf-a* gene (61) and in several RA-associated genes, including *Cyp26b1*, *Rara*, and *Rxra*, which we found bound by TLX1. Among the TLX1 target genes, we also identified *Jdp2*, an AP-1 family transcription factor deregulated in the absence of *Tlx1* and known to repress RA-induced differentiation (68). As with JDP2, we showed that TLX1 also represses RA-induced differentiation and that TLX1 and JDP2 physically interact. These findings support a scenario in which reduced expression of these transcription factors within the SMP causes deregulation of genet-

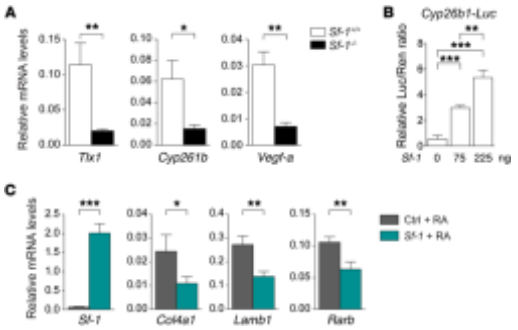

Figure 8. SF-1 controls *Tlx1* and RA metabolism. (**A**) Expression of *Tlx1*, *Cyp26b1*, and *Vegf-a* in E14.5 *Sf-1*$^{+/+}$ and *Sf-1*$^{-/-}$ embryonic spleens. Data are representative of 1 of 2 independent experiments with 4 pooled spleens for each genotype. (**B**) Luciferase activity on a *Cyp26b1* promoter reporter system was assessed at 48 hours in HEK293 cells transiently transfected with increasing concentrations of *Sf-1* expression vector. Data are representative of 1 of 3 different experiments. (**C**) RARE-F9 cells transiently expressing *Sf-1* or control vector were treated with RA and expression of indicated genes analyzed by qPCR 8 hours later. Data are representative of 1 of 3 independent experiments. (**A**–**C**) The means of triplicates ± SD are shown, *$P < 0.05$ (**A** and **C**), **$P < 0.01$ (**A**–**C**), ***$P < 0.001$ (**B** and **C**) (2-tailed Student's *t* test).

ic programs controlled by RA. Thus, we propose that, in addition to controlling RA metabolism in the SPM, TLX1 directly regulates RA target genes containing the AP-1 sequence. Accordingly, our microarray and ChIP-seq data indicate that TLX1 represses the activation of nuclear RARs by binding to their regulatory regions. In the absence of TLX1, the transcription of RARs would be derepressed, while uncontrolled RA in the SPM would favor the conversion of RARs from corepressors into coactivators and the subsequent induction of *c-Jun* and other RA-regulated genes. In support of this idea, *c-Jun*, which is induced by RA in an AP-1–dependent manner, is strongly upregulated in *Tlx1* mutant spleens compared with controls (not shown). In a similar manner, expression of *Desmin*, a marker associated with cellular differentiation positively regulated by RA and AP-1, is significantly increased in *Tlx1* mutant spleens compared with controls.

In this scenario, our data further support the previous hypothesis by Zangen and collaborators (16) and implicate SF-1 as an upstream regulator of *Tlx1* during spleen development. Our findings also indicate that SF-1 controls *Cyp26b1* expression independently of TLX1. Thus, we propose a model in which SF-1 is required to activate *Tlx1* transcription and both TLX1 and SF-1 independently control *Cyp26b1* expression and RA metabolism (Figure 9). Supporting a role for SF-1 in the control of RA activity is the demonstration that SF-1 regulates *Cyp26b1* expression during germ cell development (15). We showed that, similarly to what occurs with *Tlx1* mutants, loss of *Sf-1* causes reduced *Vegf-a* expression. Given that RA affects *Vegf-a* expression in spleen mesenchymal cells, it is likely that the severe vasculogenesis defect observed in *Sf-1*–deficient mice is caused, at least in part, by aberrant RA signaling (64).

Interestingly, although mice deficient for *Cyp26b1* have severe spleen hypoplasia, it has recently been reported that 2 siblings homozygous for a null allele of *CYP26B1* have normal spleen size (39) (S. Robertson, unpublished observations). At present, the reason for this discrepancy remains unclear, though it is possible that the human *CYP26B1*-null allele is associated with incomplete clinical penetrance or that other CYP family members compensate for *CYP26B1* deficiency in humans. Nevertheless, it is tentative to speculate that perturbations of *Tlx1* expression, both in mice and in humans, may deregulate critical downstream pathways, including retinoid signaling that affects spleen development. Interestingly, an excess of retinoids in animal models causes heterotaxy, a syndrome associated with congenital asplenia and vascular defects in humans (39, 40, 61). In conclusion, our findings reveal the important role of TLX1 in controlling RA signaling during spleen organogenesis and provide novel mechanistic insights underlying the pathogenesis of congenital asplenia.

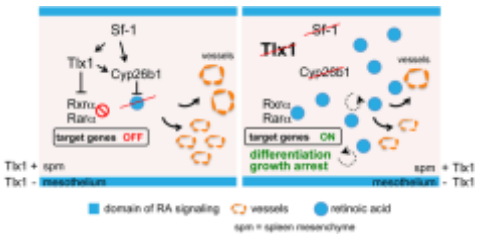

Figure 9. Proposed model for SF-1 and TLX1 function during spleen development. RA signaling starts at E13.5 and is confined in the outer mesothelial layer of the developing spleen, a domain negative for TLX1. On the contrary, SF-1 and TLX1 restrict RA signaling by promoting *Cyp26b1* expression and RA degradation, and repression of RA nuclear receptors in the inner mesenchyme. In the absence of *Sf-1* or *Tlx1* the expression of *Cyp26b1* is markedly reduced, thus causing increased RA content and activity. As a result, RA binds to nuclear receptors that activate RA-induced transcriptional programs. Under these conditions, RA signals in an autocrine (dashed arrows) and paracrine (solid arrows) fashion within the SPM, thus causing growth arrest due to premature cellular differentiation and reduced vasculogenesis. Thus, expression of SF-1 and TLX1 in the SPM is required to control RA signaling and ensure spleen development.

Methods

Mice. *Tlx1*$^{LacZ/+}$ (6), *Cyp26b1*$^{+/-}$ (33), *Rdh10*$^{fl/fl}$ (50), *RARE-hsp68-LacZ* (46), *Hoxb6-CreER* (48), *Rdh10βGeo* (50), *Sf-1*$^{+/-}$ (69–71), and *Cre-ERT2* mice have been previously described (72). *R26RYFP* mice (73) were used as a reporter strain of Cre activity. C57BL/6N and CD1 mice were purchased from Charles River, Italy. Mice were bred and maintained at San Raffaele Scientific Institute in pathogen-free rooms under barrier conditions, with constant temperature, food and water ad libitum, and light/dark cycles of 12 hours. Tamoxifen (5 mg) and progesterone (1 mg) were dissolved in corn oil and administered via oral gavage to pregnant mice at the desired embryonic stage of development.

Pregnant *Tlx1*$^{+/-}$ or *Tlx1*$^{-/-}$ mice were treated with RAR antagonist BMS493 (Tocris Bioscience) or vehicle (DMSO; Sigma-Aldrich) at the dose of 5 mg/kg in corn oil. Mice were mated overnight, and the day of vaginal plug detection was marked as E0.5. Treatment was given by oral gavage twice daily in 10- to 12-hour intervals from E10.5 until E13.5.

RNA isolation, qPCR, and microarray analysis. For gene expression profile analysis, total RNA was extracted from embryonic spleens harvested at E13.5 and E14.5, primary spleen mesenchymal cells (E14.5), and the established eSMC line with RNeasy Mini isolation kit (Qiagen). Reverse transcription of 1 μg of total RNA was performed using the ImProm II Reverse Transcription System kit with random primers (Promega Corp.). qPCRs were performed using the Universal Probe Library system on a LightCycler 480 (Roche). The Ct of *Rpl13a* (housekeeping) was subtracted from the Ct of the target gene, and the relative expression was calculated as $2^{-\Delta Ct}$. qPCRs were performed in triplicate and mean ± SD represented as relative expression. Primer sequences are described in Supplemental Table 2. Microarray analysis was performed using GeneChip Mouse Gene 1.0 ST Array from Affymetrix (GSE68519). Data were processed and normalized (GC robust multi-array average [GCRMA]) using GenePattern (74).

Chromatin immunoprecipitation. ChIP experiments were performed using the eSMC line according to a protocol described previously (8). In brief, 1×10^8 cells were cross-linked with 1% formaldehyde at room temperature followed by addition of glycine at a final concentration of 0.125 M. Chromatin was fragmented by sonication with Sonicator Ultrasonic Processor XL (Misonix Inc.) with a 3/16-in. (4.8-mm) microtip (419A Tapered Microtip; Gilson Inc.) at 30% of amplitude for 30 seconds and for 35 times with a 1-minute interval. Samples were immunoprecipitated with 4 μg of the antibodies anti-Tlx1 (rabbit polyclonal, SC-880X; Santa Cruz Biotechnology Inc.) and the normal rabbit serum IgG (ChromoPure 011-000-003; Jackson ImmunoResearch Laboratories Inc.). Immunoprecipitated DNA was purified using Qiaquick PCR Purification kit (Qiagen), suspended in 45 μl of Tris-HCl 10 mM, and amplified by qPCR on a LightCycler 480 using TaqMan chemistries (Roche). Regions within *Cyp26b1* (R1, R2), *Rxra* (R3, R4), *Rara* (R5, R6), and *Jdp2* (R7, R8, R9) were tested using primers designed using the UPL Assay Design Center (Roche) and are listed in Supplemental Table 3. For ChIP sequencing (ChIP-seq) analysis the purified DNA was quantified using Quant-iT PicoGreen dsDNA kit (Invitrogen). For each ChIP-seq assay 40 ng of DNA was used directly for cluster generation and sequencing analysis with the HiSeq 2000 following the protocol of the manufacturer (Illumina).

Sequencing and data analysis. Sequencing data (GSE81661) generated from the Illumina platforms were aligned to mouse reference genome (mm9) using Bowtie version 0.12.7. Only reads with unique alignment were retained for downstream analysis. Peak calling and bigWig files were generated using Model-Based Analysis for ChIP-seq (MACS) version 1.4. Only peaks with 10× -log *P* value ≥ 70 are considered for further processing. bigWig files were visualized using the University of California, Santa Cruz (UCSC) browser (http://genome.ucsc.edu). The list of mm9 annotated RefSeq genes used for the different analyses was downloaded from the UCSC database, and the data were processed by the MEME tool.

Immunofluorescence staining. E13.5 and E16.5 embryos and P1 spleens were harvested and fixed 30 minutes to 1 hour at 4°C with 4% (wt/vol) PFA (Sigma-Aldrich), then washed in PBS 1× and dehydrated overnight in 30% sucrose (Sigma-Aldrich) at 4°C. Samples were embedded in Tissue-Tek OCT compound (Bio-Optica) and frozen in an ethanol dry-ice bath. Eight- to ten-micrometer-thick sections were placed onto glass slides (Bio-Optica), fixed in cold acetone for 5 minutes, dried, and kept at –80°C until used. Slices were incubated 30 minutes with a blocking solution of PBS at 0.5% FBS and 0.5% Tween (PBS-T 0.05%), followed by anti-desmin (mouse IgG1; D1033, clone DE-U-10; 1:200 stock 8.8 μg/μl; Sigma-Aldrich), anti–β-gal (mouse IgG1; G8021, clone GAL-13; 1:100 stock 5 μg/μl; Sigma-Aldrich), anti–CD31/PECAM-1 (PE rat IgG2a; 553373, clone MEC 13.3; 1:100 stock 0.2 μg/μl; BD), and anti–ER-TR7 (rat IgG2a; BM4018, clone ER-TR7; 1:200 stock 0.4 mg/ml; Acris) specific antibodies. Secondary anti-mouse Alexa Fluor 488 (1:500 stock 2 μg/μl; A10684; Invitrogen) or anti-rat Alexa Fluor 488 (1:500 stock 2 μg/μl; A21208; Invitrogen) antibody was diluted in PBS-T 0.05% blocking solution and incubated for 30 minutes. Nuclei were visualized with DAPI (Fluka), and mounting was performed with Mowiol (Calbiochem). Images were acquired using an Ultraview Leica TCS SP2 laser confocal microscope. Digital images were recorded in separately scanned channels with no overlap in detection of emission from the respective fluorochromes. Final image processing was performed with Adobe Photoshop and Illustrator.

IHC staining. E13.5 embryos were harvested and fixed overnight at 4°C with 4% (wt/vol) PFA and processed into paraffin through graded alcohol series. Five- to eight-micrometer-thick sections were placed onto glass slides, dried overnight at 40°C–42°C, and kept at room temperature until used. Slices were deparaffinized, quenched for 5 minutes in 3% (vol/vol) hydrogen peroxide, and incubated with blocking solution of 3% of BSA (Sigma-Aldrich) in TBS (VWR) for 10 minutes at room temperature. Sections were stained with anti–CD31/PECAM-1 (rabbit polyclonal; 1:200 stock 200 μg/ml; RB-10333; Thermo Scientific) antibody overnight at 4°C. Immunolabeling was performed using Vectastain Elite ABC kit (Vector Laboratories) according to the manufacturer's instructions. Slides were counterstained in Gill's Hematoxylin (Sigma-Aldrich) and next mounted with xylene (Carlo Erba). Images were acquired using Aperio Scan Scope slide scanner (Leica Biosystems), and quantification of the microvessel density was performed with ImageJ software. Final image processing was performed with Adobe Photoshop and Illustrator.

Cell cultures, silencing, and transfections. The embryonic spleen mesenchymal cell (eSMC) line, the F9-RARE-LacZ reporter cell line, and the embryonic endothelial cell line were previously described (9, 51, 75). Primary embryonic spleen mesenchymal cells were generated from E13.5 embryonic spleens. Cells were grown at 37°C, 5% CO_2 in DMEM (Gibco) supplemented with 10% heat-inactivated FBS (Euroclone), 2 mM L-glutamine (L-Glu; Gibco), and 100 U/ml penicillin and 100 μg/ml streptomycin (Pen/Strep; Gibco). 293T (9) and NIH3T3 (8) cells were grown in Iscove's modified Dulbecco's medium (IMDM; Gibco) or in DMEM (Gibco), respectively, supplemented with 10% heat-inactivated FBS,

L-Glu, and Pen/Strep. Embryonic endothelial cells were grown in 0.1% gelatin (Sigma-Aldrich) precoated dishes in DMEM supplemented with 20% FBS, L-Glu, Pen/Strep, 1 mM Na pyruvate (Gibco; Thermo Fisher Scientific), 100 μg/ml heparin (Sigma-Aldrich), and 5 μg/ml endothelial cell growth supplement (ECGS; Sigma-Aldrich). For silencing experiments, lentiviral particles were produced and used following the manufacturer's instructions using the lentiviral plasmid pLKO.1-puro containing 2 different shRNA target sequences against murine Tlx1 or the scrambled sequence (Sigma-Aldrich). The shRNA-Tlx1 sequence was CCGGCGGTATCGACCAGATCCTCAACTCGAGTTGAGGATCTGGTCGATACCGTTTTTG; the control shRNA-scrambled sequence was a non-target shRNA. Selection of infected cells was performed in puromycin (Sigma-Aldrich), and cells were kept under culture conditions described above during all experiments.

For transfection experiments, cells were transfected using Lipofectamine 2000 (Invitrogen) or Amaxa MEF2 Nucleofector Kit (Lonza) with the following vectors: *pCMV-Cyp26b1* (76), *pcDNA3-Tlx1* (8), *pcDNA3-Jun* (77), *pcDNA3-SF-1* (78), *pcDNA4-Jdp2*, and *pAP1-Luc* (53, 55). The *Cyp26b1promo-Luc* vector was generated by cloning of 4,000 bp of the mouse *Cyp26b1* proximal promoter isolated by PCR from genomic DNA into a pGL3 luciferase reporter vector (Promega Corp.). Sequencing was performed to verify accuracy of the insert. Luciferase activity was assayed with a dual luciferase assay system (Promega Corp.), and activities were standardized against the internal control, Renilla luciferase or β-gal.

In situ hybridization. Whole-mount in situ hybridization for *Rdh10* was performed as previously described (49, 79) using digoxigenin-labeled probe with hybridization detected via NBT-BCIP or BM-purple (Roche).

Western blot analysis and immunoprecipitation assay. Cells were lysed in RIPA buffer (5 mM Tris-HCl pH 8.0, 150 mM NaCl, 0.1% SDS, 1% NP-40, 0.5% NaDOC) containing protease inhibitor cocktail (Roche). Protein concentration was determined by the Bradford assay following the manufacturer's instructions (Bio-Rad). Proteins were transferred onto a PVDF membrane (Immobilon-O; Millipore) and blocked in 5% skim milk, and immunoblotting was performed with anti–Hox11/Tlx1 (1:500 stock 200 μg/ml; SC-880; Santa Cruz Biotechnology Inc.) and anti-vinculin (1:10,000; V4505, clone VIN-11-5; Sigma-Aldrich) primary antibodies. Binding of HRP-labeled anti-rabbit or -mouse secondary antibodies (NA934 or NA931, respectively; GE Healthcare) was detected with the SuperSignal West Pico Chemiluminescent kit (Thermo Scientific). Immunoprecipitation was performed as previously described (80, 81). In brief, cells were harvested using PRO-PREP Protein Extraction Solution (iNtRON Biotechnology). The preparation of cell lysates, SDS-PAGE (8% or 10% gel), and Western blotting were performed as described elsewhere (80). In the case of sequential immunoprecipitation and Western blot analysis, 293T cells were transfected with pcDNA4-JDP2 or pcDNA3-TLX1 by Lipofectamine 2000 (Invitrogen), and after 48 hours, the cell lysates of each transformant were prepared for the sequential immunoprecipitation and Western blotting as described elsewhere (80). Each supernatant was precleared with protein A/G beads (Millipore), and incubated with antibodies specific for JDP2 (2) or TLX1 (1:550 stock 200 μl/ml; SC-880; Santa Cruz Biotechnology Inc.) at 4°C for 16 hours. The beads were preblocked with 1% BSA before being added to samples and then incubated at 4°C for 4 hours with rotation. The beads were pelleted, washed by chilled PBS, and loaded to Western blotting.

Proliferation assay. For assaying proliferation of primary and immortal eSMCs, 5×10^3 cells per well were seeded in a 96-well plate. Primary spleen mesenchymal cells were obtained by trypsin digestion of pooled E14.5 spleens. Sixteen to eighteen hours after plating, cells were treated with 1 μM RA (in DMSO; Sigma-Aldrich) and 1 μM R116010 (in ethanol [EtOH]; ref. 52; provided by Miguel Torres, Centro Nacional de Investigaciones Cardiovasculares, Madrid, Spain). In controls and cultures treated for 24, 48, 72, or 96 hours, cells were fixed with 100 μl of Diff-Quick Fix solution (Medion Diagnostics) for 3 minutes at room temperature and then stained with 100 μl of Crystal Violet (Dade Behring) for 5 minutes at room temperature. Cells were washed with tap water and allowed to dry, and then 50 μl/well of Dissolving Solution (0.1% SDS, 50% EtOH, 0.25 M Tris-HCl pH 7.7, in 10 ml of ddH_2O) was added. Optical absorbance was read at 570 nm with Microplate Reader Model 680 (Bio-Rad), and the data were analyzed with Microsoft Excel and GraphPad Prism 5.0c (GraphPad Software).

Coculture and organotypic experiments. SMC shRNA-Scramble, shRNA-Tlx1, or shRNA-Tlx1/rescue-Cyp26b1 cells were seeded in a poly-L-Lysine–coated 12-well plate (Costar) with F9-RARE-LacZ cell lines in a 1:1 ratio (10^5 cells per well for each cell line). Coculture experiments were conducted in triplicate, and cells were maintained in complete DMEM with 5% CO_2 at 37°C for 48 hours. Then LacZ staining or β-gal activity assays on the cocultured cells were performed. For organotypic experiments, embryonic spleens were microdissected from E13.5 CD1 embryos and embedded in 600 μl of 1.6% type I rat tail collagen solution (SERVA) in MEM and 16 mM sodium bicarbonate, using 12-well plates. Littermate spleens were divided into 2 groups, and after collagen polymerization, 1 ml of complete DMEM with 1 μM RA or vehicle (DMSO) was added to each well. All cultures were incubated at 5% CO_2 at 37°C for 24 hours. Images were taken using Nikon Digital Camera DXM1200 mounted on a Nikon Eclipse TE200 microscope using the Nikon ACT-1 program. To further quantify the spleen areas, the images were analyzed with ImageJ software.

LacZ staining. RARE-*LacZ* embryos were collected at E11.5 and E13.5 and fixed for 1 hour at 4°C in PBS containing 4% formaldehyde, 0.8% glutaraldehyde, 0.02% NP-40, and 1 mM $MgCl_2$. After brief washing in PBS, embryos were stained overnight at 37°C in PBS 1× supplemented with 5-bromo-4-chloro-3-indolyl-D-galactopiranoside (X-Gal; 400 mg/ml) in 0.1 mM $MgCl_2$, 20 mM potassium ferrocyanide, and 20 mM potassium ferricyanide. After the staining, embryos were incubated overnight at 4°C in PBS 1× containing 30% sucrose, and the day after, they were equilibrated for 20–30 minutes at room temperature in OCT-Killik (Bio-Optica) and then embedded in OCT-Killik. For the LacZ staining of the cocultured experiments, cells were fixed with LacZ fixing solution (0.5% glutaraldehyde, 0.1 M $MgCl_2$, 5 mM EGTA pH 7.5), washed with LacZ washing buffer (0.2% Nonidet-P40, 2 mM $MgCl_2$, 0.01% NaDOC in PBS 1× without $MgCl_2$ and $CaCl_2$), and then incubated overnight at 37°C in the dark with LacZ Staining solution (1 mg/ml X-Gal, 5 mM potassium ferrocyanide, and 5 mM potassium ferricyanide in LacZ washing buffer solution). Images were captured as previously described, and to further quantify the number of $LacZ^+$ cells, the count of resulting blue cells was done with ImageJ software. To perform the β-gal activity assay the cocultured cells were lysed with Lysis Buffers (Promega Corp.) for 20 minutes at room temperature in agitation. After, 20 μl/well of cell lysates were transferred into a 96-well plate (Costar), and 140 μl/well of ONPG-MIX was added. The ONPG-MIX contained 1.4 μl/well of Mg^{2+} 100× (0.1 M $MgCl_2$, 4.5 M

b-MeEtOH), 104 μl/well of 0.1 M sodium phosphate solution pH 7.5 (0.06 M Na_2HPO_4 eptahydrate, 0.04 M NaH_2PO_4), and 34.6 μl/well of ONPG solution (3.6 mg/ml in 0.1 M sodium phosphate solution pH 7.5). The absorbance was measured with the Microplate Reader Model 680 (Bio-Rad) at 415 nm, and the data were analyzed using Microsoft Excel.

Statistics. Statistical analysis using a 2-tailed unpaired Student's *t* test or 2-way ANOVA or χ^2 test, as indicated, was performed with GraphPad Prism and values expressed as mean ± SD. Differences were considered statistically significant at *P* less than 0.05.

Study approval. All animal experiments were conducted in accordance with protocols approved by the IACUC of San Raffaele Scientific Institute.

Author contributions

EL, DF, LC, F Bernassola, and AB designed and performed experiments. KW and KKY performed immunoprecipitation experiments. LLS, NEBT, and PAT performed *Rdh10* experiments. D Penkov, GL, D Pasini, and GT analyzed microarray and ChIP-seq data. NC and AD performed cloning experiments. KN, MW, F Blasi, KK, GM, and PAT provided reagents. EL and AB analyzed data, prepared figures, and wrote the manuscript with the contribution of PAT, and AB directed the study.

Acknowledgments

The authors are grateful to laboratory members for technical assistance and helpful suggestions. We are grateful to J. Rossant for providing the RARE-*LacZ* transgenic mice, Hiroshi Hamada for providing the *Cyp26b1* mice, and Susan Mackem for providing the *Hoxb6-CreERT* mice. We are thankful to Daniela Talarico for comments on the manuscript. This work was supported by Associazione Italiana Ricerca sul Cancro Start-Up Grant 4780, grant IG 14511, and Special Program Molecular Clinical Oncology 5 per mille 9965, to A. Brendolan; Marie Curie Foundation IRG-2007 208932, to A. Brendolan; the Stowers Institute for Medical Research, to P.A. Trainor; the Taiwan government MOST-104-2320-B-037-033-My2, MOST-104-2314-B-037-002, NHRI-EX104-10416SI, and KMU-TP104A04, E24, G03, G04, to K.K. Yokoyama; Slovenian Research Agency project J7-7226, to G. Majdic; and the Russian Science Foundation (14-35-00026), to D. Penkov for ChIP-seq.

Address correspondence to: Andrea Brendolan, Laboratory of Lymphoid Organ Development, Division Experimental Oncology, DIBIT-1, 3A2, San Raffaele Scientific Institute, Via Olgettina 60, 20132 Milan, Italy. Phone: 39.02.26434719; E-mail: brendolan.andrea@hsr.it.

1. Ejstrud P, Kristensen B, Hansen JB, Madsen KM, Schonheyder HC, Sorensen HT. Risk and patterns of bacteraemia after splenectomy: a population-based study. *Scand J Infect Dis*. 2000;32(5):521–525.
2. Bisharat N, Omari H, Lavi I, Raz R. Risk of infection and death among post-splenectomy patients. *J Infect*. 2001;43(3):182–186.
3. Thomsen RW, et al. Risk for hospital contact with infection in patients with splenectomy: a population-based cohort study. *Ann Intern Med*. 2009;151(8):546–555.
4. Ram S, Lewis LA, Rice PA. Infections of people with complement deficiencies and patients who have undergone splenectomy. *Clin Microbiol Rev*. 2010;23(4):740–780.
5. Kristinsson SY, Gridley G, Hoover RN, Check D, Landgren O. Long-term risks after splenectomy among 8,149 cancer-free American veterans: a cohort study with up to 27 years follow-up. *Haematologica*. 2014;99(2):392–398.
6. Dear TN, et al. The Hox11 gene is essential for cell survival during spleen development. *Development*. 1995;121(9):2909–2915.
7. Burn SF, et al. The dynamics of spleen morphogenesis. *Dev Biol*. 2008;318(2):303–311.
8. Brendolan A, et al. A Pbx1-dependent genetic and transcriptional network regulates spleen ontogeny. *Development*. 2005;132(13):3113–3126.
9. Koss M, et al. Congenital asplenia in mice and humans with mutations in a Pbx/Nkx2-5/p15 module. *Dev Cell*. 2012;22(5):913–926.
10. Brendolan A, Rosado MM, Carsetti R, Selleri L, Dear TN. Development and function of the mammalian spleen. *Bioessays*. 2007;29(2):166–177.
11. Roberts CW, Shutter JR, Korsmeyer SJ. Hox11 controls the genesis of the spleen. *Nature*. 1994;368(6473):747–749.
12. Mahlaoui N, et al. Isolated congenital asplenia: a French nationwide retrospective survey of 20 cases. *J Pediatr*. 2011;158(1):142–148.
13. Bolze A, et al. Ribosomal protein SA haploinsufficiency in humans with isolated congenital asplenia. *Science*. 2013;340(6135):976–978.
14. Unolt M, et al. Transposition of great arteries: new insights into the pathogenesis. *Front Pediatr*. 2013;1:11.
15. Kashimada K, et al. Antagonistic regulation of Cyp26b1 by transcription factors SOX9/SF1 and FOXL2 during gonadal development in mice. *FASEB J*. 2011;25(10):3561–3569.
16. Zangen D, et al. Testicular differentiation factor SF-1 is required for human spleen development. *J Clin Invest*. 2014;124(5):2071–2075.
17. Kawabe T, Muslin AJ, Korsmeyer SJ. HOX11 interacts with protein phosphatases PP2A and PP1 and disrupts a G2/M cell-cycle checkpoint. *Nature*. 1997;385(6615):454–458.
18. Riz I, Hawley RG. G1/S transcriptional networks modulated by the HOX11/TLX1 oncogene of T-cell acute lymphoblastic leukemia. *Oncogene*. 2005;24(36):5561–5575.
19. Owens BM, Hawley TS, Spain LM, Kerkel KA, Hawley RG. TLX1/HOX11-mediated disruption of primary thymocyte differentiation prior to the $CD4^-CD8^+$ double-positive stage. *Br J Haematol*. 2006;132(2):216–229.
20. Riz I, et al. TLX1/HOX11-induced hematopoietic differentiation blockade. *Oncogene*. 2007;26(28):4115–4123.
21. De Keersmaecker K, et al. The TLX1 oncogene drives aneuploidy in T cell transformation. *Nat Med*. 2010;16(11):1321–1327.
22. Dadi S, et al. TLX homeodomain oncogenes mediate T cell maturation arrest in T-ALL via interaction with ETS1 and suppression of TCRalpha gene expression. *Cancer Cell*. 2012;21(4):563–576.
23. Kanzler B, Dear TN. Hox11 acts cell autonomously in spleen development and its absence results in altered cell fate of mesenchymal spleen precursors. *Dev Biol*. 2001;234(1):231–243.
24. Riz I, Hawley TS, Johnston H, Hawley RG. Role of TLX1 in T-cell acute lymphoblastic leukaemia pathogenesis. *Br J Haematol*. 2009;145(1):140–143.
25. Rice KL, Izon DJ, Ford J, Boodhoo A, Kees UR, Greene WK. Overexpression of stem cell associated ALDH1A1, a target of the leukemogenic transcription factor TLX1/HOX11, inhibits lymphopoiesis and promotes myelopoiesis in murine hematopoietic progenitors. *Leuk Res*. 2008;32(6):873–883.
26. Niederreither K, Dolle P. Retinoic acid in development: towards an integrated view. *Genetics*. 2008;9(7):541–553.
27. Greene WK, Bahn S, Masson N, Rabbitts TH. The T-cell oncogenic protein HOX11 activates Aldh1 expression in NIH 3T3 cells but represses its expression in mouse spleen development. *Mol Cell Biol*. 1998;18(12):7030–7037.
28. Duester G. Retinoic acid synthesis and signaling during early organogenesis. *Cell*. 2008;134(6):921–931.
29. Niederreither K, Vermot J, Messaddeq N, Schuhbaur B, Chambon P, Dolle P. Embryonic retinoic acid synthesis is essential for heart morphogenesis in the mouse. *Development*. 2001;128(7):1019–1031.
30. Vermot J, Gallego Llamas J, Fraulob V, Niederreither K, Chambon P, Dolle P. Retinoic acid controls the bilateral symmetry of somite formation in the mouse embryo. *Science*. 2005;308(5721):563–566.
31. Rhinn M, Dolle P. Retinoic acid signalling during development. *Development*. 2012;139(5):843–858.
32. Cunningham TJ, Duester G. Mechanisms of retinoic acid signalling and its roles in organ and limb development. *Mol Cell Biol*. 2015;16(2):110–123.
33. Yashiro K, et al. Regulation of retinoic acid distribution is required for proximodistal patterning and outgrowth of the developing mouse limb.

Dev Cell. 2004;6(3):411–422.
34. Sakai Y, et al. The retinoic acid-inactivating enzyme CYP26 is essential for establishing an uneven distribution of retinoic acid along the anterio-posterior axis within the mouse embryo. *Genes Dev*. 2001;15(2):213–225.
35. Uehara M, Yashiro K, Takaoka K, Yamamoto M, Hamada H. Removal of maternal retinoic acid by embryonic CYP26 is required for correct Nodal expression during early embryonic patterning. *Genes Dev*. 2009;23(14):1689–1698.
36. Bowles J, et al. Control of retinoid levels by CYP26B1 is important for lymphatic vascular development in the mouse embryo. *Dev Biol*. 2014;386(1):25–33.
37. Bowles J, et al. Retinoid signaling determines germ cell fate in mice. *Science*. 2006;312(5773):596–600.
38. Makori N, Peterson PE, Lantz K, Hendrickx AG. Exposure of cynomolgus monkey embryos to retinoic acid causes thymic defects: effects on peripheral lymphoid organ development. *J Med Primatol*. 2002;31(2):91–97.
39. Laue K, et al. Craniosynostosis and multiple skeletal anomalies in humans and zebrafish result from a defect in the localized degradation of retinoic acid. *Am J Hum Genet*. 2011;89(5):595–606.
40. Lee LM, et al. A paradoxical teratogenic mechanism for retinoic acid. *Proc Natl Acad Sci U S A*. 2012;109(34):13668–13673.
41. Garnaas MK, et al. Rargb regulates organ laterality in a zebrafish model of right atrial isomerism. *Dev Biol*. 2012;372(2):178–189.
42. Oh SP, Li E. The signaling pathway mediated by the type IIB activin receptor controls axial patterning and lateral asymmetry in the mouse. *Genes Dev*. 1997;11(14):1812–1826.
43. Wasiak S, Lohnes D. Retinoic acid affects left-right patterning. *Dev Biol*. 1999;215(2):332–342.
44. Subramanian A, et al. Gene set enrichment analysis: a knowledge-based approach for interpreting genome-wide expression profiles. *Proc Natl Acad Sci U S A*. 2005;102(43):15545–15550.
45. Eferl R, Wagner EF. AP-1: a double-edged sword in tumorigenesis. *Cancer*. 2003;3(11):859–868.
46. Rossant J, Zirngibl R, Cado D, Shago M, Giguere V. Expression of a retinoic acid response element-hsplacZ transgene defines specific domains of transcriptional activity during mouse embryogenesis. *Genes Dev*. 1991;5(8):1333–1344.
47. Abu-Abed S, MacLean G, Fraulob V, Chambon P, Petkovich M, Dolle P. Differential expression of the retinoic acid-metabolizing enzymes CYP26A1 and CYP26B1 during murine organogenesis. *Mech Dev*. 2002;110(1–2):173–177.
48. Nguyen MT, Zhu J, Nakamura E, Bao X, Mackem S. Tamoxifen-dependent, inducible Hoxb6CreERT recombinase function in lateral plate and limb mesoderm, CNS isthmic organizer, posterior trunk neural crest, hindgut, and tailbud. *Dev Dyn*. 2009;238(2):467–474.
49. Sandell LL, et al. RDH10 is essential for synthesis of embryonic retinoic acid and is required for limb, craniofacial, and organ development. *Genes Dev*. 2007;21(9):1113–1124.
50. Sandell LL, Lynn ML, Inman KE, McDowell W, Trainor PA. RDH10 oxidation of Vitamin A is a critical control step in synthesis of retinoic acid during mouse embryogenesis. *PLoS One*. 2012;7(2):e30698.
51. Wagner M, Han B, Jessell TM. Regional differences in retinoid release from embryonic neural tissue detected by an in vitro reporter assay. *Development*. 1992;116(1):55–66.
52. Van Heusden J, et al. Inhibition of all-TRANS-retinoic acid metabolism by R116010 induces antitumour activity. *Br J Cancer*. 2002;86(4):605–611.
53. Jin C, et al. JDP2, a repressor of AP-1, recruits a histone deacetylase 3 complex to inhibit the retinoic acid-induced differentiation of F9 cells. *Mol Cell Biol*. 2002;22(13):4815–4826.
54. Su D, Gudas LJ. Gene expression profiling elucidates a specific role for RARgamma in the retinoic acid-induced differentiation of F9 teratocarcinoma stem cells. *Biochem Pharmacol*. 2008;75(5):1129–1160.
55. Jin C, Li H, Ugai H, Murata T, Yokoyama KK. Transcriptional regulation of the c-jun gene by AP-1 repressor protein JDP2 during the differentiation of F9 cells. *Nucleic Acids Res Suppl*. 2002;(2):97–98.
56. Gutierrez-Mazariegos J, Theodosiou M, Campo-Paysaa F, Schubert M. Vitamin A: a multifunctional tool for development. *Semin Cell Dev Biol*. 2011;22(6):603–610.
57. Bajenoff M, et al. Stromal cell networks regulate lymphocyte entry, migration, and territoriality in lymph nodes. *Immunity*. 2006;25(6):989–1001.
58. Mueller SN, Germain RN. Stromal cell contributions to the homeostasis and functionality of the immune system. *Immunology*. 2009;9(9):618–629.
59. Castagnaro L, et al. Nkx2-5(+)islet1(+) mesenchymal precursors generate distinct spleen stromal cell subsets and participate in restoring stromal network integrity. *Immunity*. 2013;38(4):782–791.
60. Katakai T, Hara T, Sugai M, Gonda H, Shimizu A. Lymph node fibroblastic reticular cells construct the stromal reticulum via contact with lymphocytes. *J Exp Med*. 2004;200(6):783–795.
61. Lai L, Bohnsack BL, Niederreither K, Hirschi KK. Retinoic acid regulates endothelial cell proliferation during vasculogenesis. *Development*. 2003;130(26):6465–6474.
62. Chen F, Cao Y, Qian J, Shao F, Niederreither K, Cardoso WV. A retinoic acid-dependent network in the foregut controls formation of the mouse lung primordium. *J Clin Invest*. 2010;120(6):2040–2048.
63. van de Pavert SA, et al. Maternal retinoids control type 3 innate lymphoid cells and set the offspring immunity. *Nature*. 2014;508(7494):123–127.
64. Morohashi K, et al. Structural and functional abnormalities in the spleen of an mFtz-F1 gene-disrupted mouse. *Blood*. 1999;93(5):1586–1594.
65. Roberts CW, Sonder AM, Lumsden A, Korsmeyer SJ. Development expression of Hox11 and specification of splenic cell fate. *Am J Pathol*. 1995;146(5):1089–1101.
66. Chazaud C, Chambon P, Dolle P. Retinoic acid is required in the mouse embryo for left-right asymmetry determination and heart morphogenesis. *Development*. 1999;126(12):2589–2596.
67. Wang L, Mear JP, Kuan CY, Colbert MC. Retinoic acid induces CDK inhibitors and growth arrest specific (Gas) genes in neural crest cells. *Dev Growth Differ*. 2005;47(3):119–130.
68. Jin C, et al. Regulation of histone acetylation and nucleosome assembly by transcription factor JDP2. *Nat Struct Mol Biol*. 2006;13(4):331–338.
69. Budefeld T, Grgurevic N, Tobet SA, Majdic G. Sex differences in brain developing in the presence or absence of gonads. *Dev Neurobiol*. 2008;68(7):981–995.
70. Majdic G, et al. Knockout mice lacking steroidogenic factor 1 are a novel genetic model of hypothalamic obesity. *Endocrinology*. 2002;143(2):607–614.
71. Luo X, Ikeda Y, Parker KL. A cell-specific nuclear receptor is essential for adrenal and gonadal development and sexual differentiation. *Cell*. 1994;77(4):481–490.
72. Ruzankina Y, et al. Deletion of the developmentally essential gene ATR in adult mice leads to age-related phenotypes and stem cell loss. *Cell Stem Cell*. 2007;1(1):113–126.
73. Soriano P. Generalized lacZ expression with the ROSA26 Cre reporter strain. *Nat Genet*. 1999;21(1):70–71.
74. Reich M, Liefeld T, Gould J, Lerner J, Tamayo P, Mesirov JP. GenePattern 2. *Nat Genet*. 2006;38(5):500–501.
75. Balconi G, Spagnuolo R, Dejana E. Development of endothelial cell lines from embryonic stem cells: A tool for studying genetically manipulated endothelial cells in vitro. *Arterioscler Thromb Vasc Biol*. 2000;20(6):1443–1451.
76. Takeuchi H, Yokota A, Ohoka Y, Iwata M. Cyp26b1 regulates retinoic acid-dependent signals in T cells and its expression is inhibited by transforming growth factor-β. *PLoS One*. 2011;6(1):e16089.
77. Bakiri L, Matsuo K, Wisniewska M, Wagner EF, Yaniv M. Promoter specificity and biological activity of tethered AP-1 dimers. *Mol Cell Biol*. 2002;22(13):4952–4964.
78. Schepers G, Wilson M, Wilhelm D, Koopman P. SOX8 is expressed during testis differentiation in mice and synergizes with SF1 to activate the Amh promoter in vitro. *J Biol Chem*. 2003;278(30):28101–28108.
79. Nagy A, Gertsenstein M, Vintersten K, Behringer R. In situ hybridization of mouse embryo and tissue sections with radiolabeled RNA probes. *CSH Protoc*. 2007;2007:pdb.prot4821.
80. Pan J, et al. Suppression of cell-cycle progression by Jun dimerization protein-2 (JDP2) involves downregulation of cyclin-A2. *Oncogene*. 2010;29(47):6245–6256.
81. Aronheim A, Zandi E, Hennemann H, Elledge SJ, Karin M. Isolation of an AP-1 repressor by a novel method for detecting protein-protein interactions. *Mol Cell Biol*. 1997;17(6):3094–3102.

CHAPTER 5. A Retinoic Acid-dependent Stroma-Leukaemia Crosstalk Promotes Tissue Remodelling And Chronic Lymphocytic Leukaemia Progression

D. Farinello[1,2] and M. Wozinska[1,2], E. Lenti[1,2], L. Genovese[1,2], S. Bianchessi[1,2], EPM. Migliori[1,2], N. Sacchetti[1,2], A. di Lillo[1,2], R. Valsecchi, Andreas Aghatangelidis, Cristina Scielzo, Claudia de Lalla, Laura Mauri, Sandro Sonnino, Lydia Scarfò, Dejan Lazarevic, Sabrina Bascones Gleave, Rosa bernardi, Maurilio Ponzoni, Andrea Cerutti, Linda Pattini, MTS. Bertilaccio[1], F. Caligaris-Cappio[1,4], P. Ghia[1,3] and A. Brendolan[1,2].

[1] San Raffaele Scientific Institute, Division of Experimental Oncology, Istituto di Ricovero e Cura a Carattere Scientifico (IRCCS), San Raffaele Scientific Institute, Milan, Italy, [2]Unit of Lymphoid Organ Development, [3]Unit of B-cell Neoplasia.20132 Milan, Italy F.C.C. is presently scientific director of AIRC (Associazione Italiana per la Ricerca sul Cancro), 20123 Milan, Italy

Manuscript in preparation

MATERIALS AND METHODS

Mice

C57BL6 *Eμ-TCL1*, *Rag2*$^{-/-}\gamma_c^{-/-}$[1] and *Pdgfrα*$^{gfp/+}$ mice have been previously described [1] [2] [3]. Animals were maintained in a specific pathogen-free animal facility and treated in accordance with European Union and Institutional Animal Care and Use Committee guidelines.

For leukemia propagation, EμTCL1 mice were euthanized when CD19$^+$CD5$^+$ cells reached 90% in PB. A total of 1x10^7 leukemic cells purified form the spleen were injected intraperitoneally into syngeneic C57BL6/N or Rag2$^{-/-}\gamma_c^{-/-}$ recipients. Treatment with the BMS493 inhibitor was performed by oral gavage at 5mg/Kg dosage (in corn oil) 3 times a week for 6 consecutive weeks. For *ex vivo* organ cultures, animals were euthanized when terminally sick.

Labeling of B-lymphocytes with CellTracker™ Green CMFDA Dye (ThermoFisher Scientific) was performed by incubating 1x10^7 cells /mL for 20 minutes at 37°C according to manufacture instructions. Labeled cells were injected intraperitoneally and mice sacrificed at the indicated time points. Vitamin A Deficient mice were generated as previously described [4].

HPLC/UV analysis of retinyl ester (RE) and retinol (ROL)

Vitamin A depletion was assessed by measurement of retinol and retynil palmitate with UV-HPLC as previously described [5]. Solvents and controls were purchased from Sigma-Aldrich. 300-500mg of tissue were frozen immediately after harvesting and were kept at -80°C until

assay. Samples were extracted as previously described with some modifications Immediately before the analysis, 5µl of internal standard (IS, 20µM retinyl acetate) were added to each sample. Then tissues were homogenized on ice using a Heavy Duo Stirrer motorized potter in 1.5ml of cold 0.9% NaCl. 1.5 ml of 0.025 M KOH in ethanol was added to tissue homogenates and mixed at 1100 rpm, RT for 30 minutes. Then 5 ml hexane was added to the aqueous ethanol phase. The samples were vortexed and centrifuged for 10 min at 1200 rpm. The hexane phase containing ROL and RE was recovered. The extraction was repeated twice, the hexane phase collected and dryed under nitrogen. ROL/RE extracts were resuspended in 500µl acetonitrile. 100µl portions were analyzed by high pressure liquid chromatography (HPLC). Separations were obtained on a LiChrospher 100 RP18 column (5 µm, 250 × 4 mm; Merck) and were quantified by UV absorbance at 325 nm. Elution was carried out at a flow rate of 1 mL/min, with gradient formed by the solvent A, consisting of water, solvent B, consisting of acetonitrile, and solvent C consisting of acetonitrile with 0.1% dichloromethane. The gradient elution program was as follows: 19 min 30% A and 70% B, 11 min linear gradient to 11% A and 89% B, 1 min 11% A and 89% B, 1 min linear gradient to 100% B, 8 min to 100%, 2 min linear gradient to 100% C, 8 min linear gradient to 100% B, 5 min linear gradient 30% A and 70% B.

Immunofluorescence staining

Tissues were harvested and fixed for 5 minute in 4% (w/v) PFA (Sigma-Aldrich), then washed in PBS 1X and dehydrated overnight in 30% sucrose (Sigma-Aldrich) at 4°C. Samples were embedded in Tissue-

Tek OCT compound (Bio-optica) and frozen in ethanol dry-ice bath (using Dehyol 95 (Bio-optica)). 8-10 μm thick sections were placed onto glass slides (Bio-optica), fixed in cold acetone for 5 minutes, dried, and kept at -80°C until used. Slides were incubated 30 minutes with a blocking solution of PBS at 0.5%FBS and 0.05% Tween (VWR) (PBS-T 0.05%), followed by primary specific antibodies. Primary antibodies, secondary antibodies and streptavidin reagents (listed in supplementary materials) were diluted in blocking solution PBS-T 0.05% and incubated for 1hour and 30 minutes, respectively. For anti-mouse and biotin-conjugated primary antibodies, additional incubation with MoM (Vector Lab) and Avidin/Biotin blocking solution (Vector Lab), respectively, were performed following the manufacturer's instructions. Nuclei were visualized with DAPI (Fluka), and mounting was performed with Mowiol (Calbiochem). For detection of MAdCAM-1, CXCL13 and gp38 antibodies Tyramide Signal Amplification kit (Perkin Elmer) was used. For CXCL13 stainings on human samples, goat anti-human CXCL13 (BLC/BCA-1), clone AF801 (R&D Systems) was used. To visualize proliferating cells, Click-iT® EdU Imaging Kits (Invitrogen) was employed accordingly to manufacturer's protocol. Confocal images were acquired using Leica TCS SP2 and Leica TCS SP8 microscopes. Digital images were recorded in separately scanned channels with no overlap in detection of emissions from the respective fluorochromes. Final image processing was performed with Adobe Illustrator CS4 and Adobe Photoshop CS4.

Isolation, purification and characterization of B cells

Eμ-TCL1, transplanted and control mouse tissues (peripheral blood, lymph nodes, omentum, mesentery and femoral bone marrow) were collected from mice either alive (PB) or euthanized (other tissues). Solid tissues were smashed and filtered on a 40μm cell strainer (Corning). Single-cell suspensions were washed in PBS and erythrocytes were depleted using an ammonium chloride solution (ACK) lysis buffer (NH_4Cl 0.15M, $KHCO_3$ 10mM, Na_2EDTA 0.1 mM, pH 7.4). For flow cytometry analyses, samples were incubated for 15 minutes at RT with Mouse BD Fc Block™ (purified rat anti-mouse CD16/CD32; BD Bioscience Pharmingen). Then cells were washed and incubated for 15 minutes at 4°C with conjugated antibodies (Supplementary table 1) and finally data were acquired on FACSCanto™ II (BD Biosciences) and analyzed using FlowJo software (Tree Star). For culture experiments, B-lymphocytes were collected from the spleen, purified and enriched by negative depletion (EasySep™ Mouse B Cell Enrichment Kit; StemCell Technologies). The purity of all B-cell samples was always more than 90%.

Leukemic cells were purified immediately after blood withdrawal, by negative depletion using the RosetteSep B-lymphocyte enrichment kit (StemCell Technologies). The purity of all preparations was always more than 99% and the cells co-expressed CD19 and CD5 on their cell surface as checked by flow cytometry (FC500; Beckman Coulter); preparations were virtually devoid of natural killer cells, T lymphocytes, and monocytes. Human primary samples were obtained from RAI stage 0-1CLL patients, after informed consent as approved by the Institutional committee (protocol VIVI-CLL) of San Raffaele

Scientific Institute (Milan, Italy in accordance with the Declaration of Helsinki).

Cell cultures and treatments

A mouse spleen-derived stromal cell line (mSSC) expressing *yfp* was generated as previously described from Nkx2-5Cre;R26YFP mice [6]. F9-RARE-LacZ cell line was previously described [7] [8]. Cells were cultured at 37°C, 5% CO_2 in DMEM (Gibco) supplemented with 10% heat-inactivated FBS (Euroclone), 2mM L-glutamine (L-Glu; Gibco), 100U/ml penicillin and 100µg/ml streptomycin (Pen/Strep; Gibco).

For experiments in Vitamin A deficient medium, the FBS serum was substituted with B27 supplement normal and without retinyl acetate (B27-normal and B27-vitA^-; Invitrogen).

Stromal cells were treated for 24 or 48 hrs with different stimuli: 1µM all-trans Retinoic Acid (in DMSO; Sigma-Aldrich), 1µM BMS493 (in DMSO; Tocris Bioscience [9]) or vehicle (DMSO).

In vitro co-culture system and GEP

Co-culture experiments were performed using purified B-lymphocytes in combination with either mSSC or F9-RARE LacZ reporter cell line. For the co-culture experiments with F9-RARE LacZ reporter cell line, $1x10^7$ B-lymphocytes were seeded on top of $2.5x10^5$ of F9-RARE LacZ cells in poly-L-Lysine-coated 48-well plate (Costar) [7] [8]. After 48 hours, floating cells were discarded while remaining adherent cells were lysed and β-gal activity assay was assessed. Co-culture experiments were conducted in triplicate, and cells were maintained in

complete DMEM with 5% CO_2 at 37°C. Assessment of βgal activity was performed as previously described [7].

For microarray analysis, $2x10^7$ purified B-lymphocytes ($20x10^6$ cells) were seeded on top of $7.5x10^5$ mSSC in 60mm dishes (Costar). After 40-48hrs, floating B-lymphocytes were collected with the supernatant by gently flushing, instead stromal cells and stroma-adherent B lymphocytes were separated by sorting using MoFlo™ XDP (Beckman Coulter) cell sorter. mRNA from all cell populations was further analyzed by Microarray or qPCR analysis. Total RNA was extracted from murine and human samples (murine and human purified B-lymphocytes and murine tissues) with RNeasy Micro or Mini kit (Qiagen). Reverse transcription of 0.2-2μg of total RNA was performed with the ImProm-II Reverse Transcription System kit with random primers (Promega). qPCRs were performed using Universal Probe Library system (Roche) on a LightCycler480 (Roche). The C_t of *Rpl13* or *GAPDH* (housekeeping genes for mouse and human, respectively) was subtracted from the C_t of the target gene, and the relative expression was calculated as $2^{-\Delta C_t}$. qPCRs were performed in triplicate or quadruplicates and mean ± SD represented as relative expression (primer sequences are described in Table 1). For microarray analysis, cRNA preparation and amplification was performed using Illumina® TotalPrep™ RNA Amplification Kit, and then the analysis was performed using Illumina® Whole-Genome Gene Expression Direct Hybridization Assay system (Illumina).

For RNA-seq analysis, RNeasy Mini kit (Qiagen) was used to extract RNA from cells. Small aliquots were used to check the quality of the RNA with Agilent RNA 6000 Nano chip, and run on Bioanalyzer 2100

(Agilent). Briefly, library preparation was performed using the Illumina TrueSeq Stranded mRNA kit (Illumina), starting from 300 ng of total RNA. After barcoding, the RNA libraries were pooled, denatured and diluted to an 8 pM final concentration. Cluster formation was performed on cBot (Illumina) using flow cell v.3. The SBS (sequencing by synthesis) was performed according to TruSeq SR protocol (Illumina) for the HiSeq 2500 (Illumina) set to 100 cycles, yielding an average of $18x10^6$ clusters for each sample. Raw sequences (fastq) were filtered for good quality scores using FastQC software (REF: Andrews S. (2010). FastQC: a quality control tool for high throughput sequence data. Available online at: http://www.bioinformatics.babraham.ac.uk/projects/fastqc).

Sequences obtained were aligned to the Mouse genome (mm10 release) using STAR aligner (version 2.3.0e_r291) [10]. Only uniquely mapped reads were used to estimate gene counts using the reported Ensembl gene annotations (v85) using *Rsubread* Bioconductor package [11]. Subsequent to mapping the gene count, data were normalized using the "weighted trimmed mean of M-values" described elsewhere [12]. After normalization, differential gene expression was performed using the *limma* package in R [13].

For spheroid formation, immortalized Stromal cells (iSC) and leukemic B-lymphocytes were used. Specifically, iSCs and Leukemic B-cells were mixed in a ratio 1:20 (specifically $4x10^6$ cells and $80x10^6$ cells, respectively), pelleted and re-suspended in 1ml of 0.9% type I rat tail collagen solution. This solution was prepared, on ice, with the following components: 360µl of DMEM, 14µl of PBS 10X, 3µl of NaOH 1M and 125µl of Collagen I (Corning), and was used

immediately after the preparation. 5µl drops of the resulting cell suspension were spotted on the lid of a petri dish, as hanging drops, and were incubated for 20-25 minutes in humidified incubator with 5% CO_2 at 37°C, to favor collagen polymerization. Next, the polymerized cells-collagen drops were transferred into a petri dish with 10ml of DMEM. After 24 hrs, the organoids were formed by collagen contraction [14].

For BMS493 treatment experiments: mSSCs and murine leukemic cells were pre-treated individually before the organoids formation for 24hrs with 1µM of BMS493 (in DMSO; Sigma) and vehicle (DMSO). Then the organoids were prepared, as previously described, and BMS453 or vehicle treatment was repeated for the next 48 hrs, with one administration per day. At the end of the treatments, pools of 4 organoids were digested in 60µl of 0.225 mg/ml Liberase (Roche) solution for 10 minutes at 37°C, agitating. Digested organoids were analyzed at FACS, counting live cells (DAPI negative) and further analysis was performed using FlowJo software (Tree Star).

Statistical analysis

Illumina microarray data were processed in the R environment. Normalization was obtained with the *lumi* package [Du P et al 2008, PMID: 18467348], and differential analysis was performed by applying a permutation-based non-parametric method implemented in the RankProd package [15]. Differential expressed genes were selected according to the threshold FDR q-value <0.05.

Statistical analysis using a 2-tailed unpaired student's *t* test or 2-way Anova or Log-rank (Mantel-Cox) test was performed with GraphPad Prism 5.0c (GraphPad Software), and values were expressed as mean ±

SD. Differences were considered statistically significant at p less than 0.05.

Study approval

All CLL cells and tissues biopsies were obtained with the approval of the institutional review board at San Raffaele Hospital (Milan, Italy). Informed consent was obtained in accordance with the Declaration of Helsinki.

RESULTS

Leukemic cells expand within follicular areas in contact with FDC networks

Recent work in mice demonstrated that upon injection into wild-type recipients, *Eμ-TCL1* B-CLL cells migrate to follicles in a CXCR5-dependent manner and engage a cross-talk with FDCs via LTβR, resulting in CXCL13 secretion, leukemia activation and proliferation [16]. However, in this mouse model that recapitulates the progressive form of human CLL, it remains unknown whether FDC-CLL interactions persist at later stages, and FDCs are involved in disease expansion. To test this, we first injected labeled *Eμ-TCL1* leukemic cells into wild type recipients and analyzed their distribution relative to FDC networks. Forty-eight hours post injection, leukemic cells localized within the $CD35^+$ FDC networks, and in the outer follicular region in proximity to the marginal zone (Figure S1A). We then assessed leukemic distribution relative to FDC networks at later time points. To this end, we injected CD45.2 $CD19^+CD5^+$ leukemic cells into CD45.1 wild-type recipients and analyzed leukemia dissemination in the spleen at one and two weeks after adoptive transfer. Interestingly, one week after transplantation we found that leukemic cells were increased in number and localized predominantly to the B-cell follicle contacting $CD35^+$ FDC networks, and the outer follicular region adjacent to the marginal zone (Figure 1). Interestingly, two weeks later, leukemic cells were still mainly expanding in the white pulp, particularly within $CD35^+$ FDC networks (Figure 2B). At two weeks, we also found few clusters of leukemic cells at the border of the T- and B-cell zone and in the red pulp area (not shown). These findings clearly

demonstrate that *Eμ-TCL1* leukemic cells localized within the FDC networks of the B-cell zone during disease onset.

Remodeling of stromal cells and the extracellular matrix correlates with leukemia progression in *Eμ-TCL1* mice

To address whether FDCs networks are maintained during tumor development, we assessed the presence and distribution of these specialized stromal cells in *Eμ-TCL1* transgenic mice and in wild-type mice transplanted with *Eμ-TCL1* leukemic cells, at different stages of disease progression. Confocal mosaic imaging demonstrated a splenic progressive loss of $CD35^+$ FDCs networks during disease evolution (Figure 2A). This phenotype was already evident in mice with intermediate (10-20%) leukemia infiltration, and it was more pronounced in mice with advance leukemia accumulation (50-60%) that for the large majority showed absence or rare CD35+ FDC networks, with only few mice that had disorganized but distinct CD35+ FDCs clusters (Figure 2A). Consistent with the disruption of the follicular stromal architecture, Ki67+ B-cell networks also gradually disappear along with disease evolution (Figure 2B). We then aimed at testing whether loss of FDCs may in part result from altered lymphotoxin (LT)-signaling that is known to be crucial to maintain FDC networks [17]. To this end, we performed qPCR analysis on purified *Eμ-TCL1* leukemic cells and found that, whereas *Ltβ* expression does not significantly change as compared to control B cells, the mRNA levels of *Ltα* are strongly reduced (Figure S1B). Altogether, these findings are coherent with the observation in human CLL, that FDC networks differ according to the growth pattern of the tumor, and

are disorganized and gradually lost during CLL progression [18] [19].

In addition, we uncovered that remodeling of the splenic stromal cell compartment during disease progression of *Eμ-TCL1* mice correlates with increased deposition of collagen I (COLL-I), collagen IV (COLL-IV) and nidogen-2 (NID-2). This was particularly evident in the areas corresponding to FDC networks that are largely devoid of collagen/nidogen deposition (Figure 2C, arrowheads). In these mice, we also found disease evolution was associated with disorganized NID-2 distribution at the edge between the marginal zone and the white pulp (Figure S2A). In addition, analysis of podoplanin (PDPN), a marker of the T-cell zone FRCs revealed that the area occupied by $PDPN^+$ stromal cells was strongly reduced in leukemia-bearing mice as compared to controls (Fig S2B). Overall, these data demonstrate that disease progression is associated with structural alterations of the ECM along with the cellular components of the stromal compartment. These findings are in line with previous work showing that remodeling of stromal/ECM compartment occurs in mice depleted of splenic FDCs [20].

Leukemic cells promote CXCL13 in non-hematopoietic stromal cells different from FDCs

FDCs are the major stromal cell type secreting CXCL13, a B-cell chemoattractant promoting the homing of the $CXCR5^+$ B-cells to the follicle [21]. Based on this notion, we hypothesized that loss of FDCs during leukemia progression may cause a contraction of the $CXCL13^+$ domains. To test this, we first performed confocal mosaic imaging to

analyze the distribution of CXCL13 in the spleen of *Eμ-TCL1* mice with low, intermediate and high leukemia infiltration. The analysis revealed that CXCL13 distribution did not diminish during leukemogenesis, and in some cases increased despite the gradual loss of $CD35^+$ FDC networks (Figure 3A). We then analyzed transplanted mice with low, intermediate and high leukemia splenic infiltration, and found a significant increase in CXCL13 signal localized throughout the entire white pulp, and in the outer region of the follicle corresponding to the area occupied by marginal reticular cells (MRCs) (Figure 3A, bottom panels). In transgenic mice with intermediate and high infiltration the distribution pattern of CXCL13 was more disorganized and less rounded as compared to that of transplanted mice (Figure 3A, upper panels).

In the spleen, $MAdCAM\text{-}1^+$ marginal reticular cells (MRCs) localize at the edge of the B-cell follicles and produce CXCL13 [22]. We analyzed the spleen of transplanted mice and found a disorganized reticular expansion of $MAdCAM\text{-}1^+$ stromal cells in the area corresponding to the MRC layer (Figure S2B). Of note, by employing an *in vitro* co-culture system, we showed that murine CLL cells, but not control B cells, up-regulate *Madcam-1* expression in stromal cells (Figure S2C). Altogether, these findings demonstrate that CLL cells induce a profound remodeling of the stromal compartment including the MRC pool.

To address whether CXCL13 is also present in stromal cells, we performed immunohistochemistry analysis and found $CXCL13^+$ non-hematopoietic stromal cells in LN biopsies of CLL patients (Figure S3).

Altogether, these findings demonstrate that CLL cells induce a profound remodeling of stromal cells including the MRC pool, and that CXCL13 can be also expressed in non-hematopoietic cells of human CLL biopsies beside macrophages (Burkle, Niedermeier et al. 2007).

To assess whether murine CLL cells can induce CXCL13 in stromal cells, we injected *Eμ-TCL1* leukemic cells into *Rag2*$^{-/-}\gamma c^{-/-}$ mice lacking CXCL13 and mature FDCs [23]. We found that, besides being capable inducing the formation of small foci of CD35^{+} FDC networks, to a higher extent, leukemic cells promoted the formation of large clusters of CXCL13^{+} stromal cells (Figure 3B). Based on this, we assessed whether the increase in CXCL13 signal observed during leukemogenesis may result from the expansion of CXCL13^{+} stromal cells different from FDCs, or from induction of CXCL13 expression in non-hematopoietic stromal cells that previously did not express the chemokine. To this end, we took advantage of the *Pdgfrα*$^{gfp/+}$ knock-in mouse model in which the *Pdgfrα* promoter drives the expression of nuclear GFP [3]. In this model, a large majority of FRCs and MRCs, and a fraction of FDCs can be visualized by nuclear GFP expression, thus allowing a more precise visualization of stromal cells. We transplanted *Pdgfrα*$^{gfp/+}$ mice with *Eμ-TCL1* leukemic cells, and then injected them with 5-ethynyl-2 deoxyuridine (EdU) to assess proliferation. The immunofluorescence analysis on the spleen revealed that the number of CXCL13^{+}GFP^{+} cells increased during disease progression; however, this was not associated with a statistically significant increase in proliferation of preexisting GFP^{+} stromal cells (Figure 3C). In line with this, we observed that despite the increase in

spleen cellularity observed in mice with high leukemia infiltration, the density of GFP^+ stromal cells per mm^2 diminished instead of increasing, further pointing towards a mechanism of induction CXCL13 expression rather than to an increase in stromal cell proliferation (Figure 3C).

These data indicate that leukemic blasts induce a chemokine-rich stromal microenvironment that favors the recruitment and accumulation of neoplastic cells in peripheral lymphoid tissues.

Fat-associated lymphoid clusters are niches that support leukemia expansion in the peritoneal cavity

Fat-associated lymphoid clusters (FALCs) are atypical lymphoid tissues of the mesentery and omentum [24]. Recent work showed that FALCs are induced by inflammation and contain different cell subsets including B-1 and $CXCL13^+$ non-hematopoietic stromal cells [25]. Given that leukemic cells from *Eμ-TCL1* mice share features of B-1 cells, we hypothesized that peritoneal FALCs may represent supportive niches for CLL expansion. To test this, we first assessed the homing of leukemic cells to the omental FALCs by injecting green-labeled *Eμ-TCL1* leukemic cells into the tail vein of wild-type recipients. Immunofluorescence confocal analysis performed 48 hrs post injection revealed a substantial accumulation of CLL cells in this site (Figure 4A). We then analyzed the peritoneal cavity of *Eμ-TCL1* transgenic mice with a high percentage of leukemia cells in their peripheral blood. In these mice, we found an increased number of mesenteric FALCs containing a high percentage of $CD19^+CD5^+$ leukemic cells as compared to control mice in which mesenteric FALCs were barely detected (Figure 4C). Moreover, FALCs from *Eμ-TCL1* mice were

significantly larger and characterized by a considerable expansion of $CXCL13^+$ stromal cells distributed within a network of collagen IV (Figure 4B and C, left panel). These findings indicate that in this mouse model, peritoneal FALCs are supportive niches for the growth of leukemia.

Leukemic cells induce stromal remodeling through retinoid signaling

To investigate the mechanisms underlying remodeling of the stromal microenvironment during CLL progression, we performed a microarray analysis using mRNA purified from a murine spleen stromal cell line cultured for 48 hrs with either *Eμ-TCL1* leukemia or control splenic B cells. Up-regulated transcripts in stromal cells cultured with CLL B cells revealed significant enrichment for interferon regulatory factor (IRF) targets, genes related to extracellular region, exosomes and inflammatory responses (Figure 5A, bottom panels). Up-regulated IRF targets contain the *bone marrow stromal cell antigen 2* (BST2) gene, a membrane protein expressed in bone marrow stromal cell lines that was reported to support the stromal cell-dependent growth of the murine pre-B-cell line DW34 [26]. Stromal cells co-cultured with leukemia showed also the over-expression of *actin alpha 2 smooth muscle* (Acta2/αSMA), a mesenchymal marker characteristic of cancer associated fibroblasts (CAFs) [27]. Among deregulated genes annotated for extracellular region, we also discovered the up-regulation of *Aldh1a1, Cyp1b1*, and *Aldh3a1*, all genes encoding for retinoic acid (RA)-synthetizing enzymes (Figure S4). Differentially expressed genes were overall found significantly enriched for extracellular matrix

(ECM) genes as annotated in the Matrisome-DB atlas, which represents an effort toward the characterization of global composition of the ECM, collecting not only structural components but also genes encoding proteins that can interact with ECM or be involved in its remodeling [28]. They are categorized in *core matrisome* genes, comprising ECM glycoproteins, collagens and proteoglycans and *ECM-associated proteins* including ECM-affiliated proteins, ECM regulators and secreted factors (Figure 5A).
Consistent with the EdU labeling results, we found down-regulation of gene-signatures related to cell cycle and cell division, indicating that leukemic cells do not promote stromal cell proliferation (Figure 5A, bottom panels).

Retinoids have been implicated in regulating different cellular processes and target genes, including *Cxcl13* expression in stromal progenitors [29] [30]. Based on these findings, we hypothesized that during leukemogenesis, enhanced RA-activity in the microenvironment may contribute, at least in part, to induce *Cxcl13* in stromal cells. We first evaluated whether CLL cells could modulate the RA-signaling in the microenvironment by exploiting an *in vitro* system, in which F9 cells, expressing LacZ under the RA responsive elements (RARE) are cultured with leukemia or control cells (Figure 5B). We found that βgal activity, indicative of the RA-signaling activation, was significantly higher in the presence of leukemic, as compared to control B-cells (Figure 5B, left panel). To confirm that this effect was RA-dependent, we treated the cultures with the RA-signaling inhibitor BMS493 [9],

and found that this significantly abrogated βgal activity (Figure 5B, right panel).

Given the induction of CXCL13 observed *in vivo*, we tested the possibility that retinoids released by stromal cells upon leukemia interaction activate the expression of *Cxcl13* in stromal cells in an autocrine manner. Gene expression profile analysis revealed a significant increase in *Cxcl13* mRNA levels in stromal cells cultured with leukemia as compared to control cells (Figure 5C). Notably, treatment with the RA-signaling inhibitor BMS493 abrogated the induction of *Cxcl13* and *Rarβ,* a known target of the RA-signaling (Figure 5C). To corroborate these findings in a more controlled setting, we cultured stromal cells in a vitamin A deficient media, either in the presence or absence of exogenous RA. Under these conditions, we found significant induction of *Cxcl13* and *Rarb* expression by RA, which was blocked by BMS493 treatment (Figure 5D).

Recent work showed that RA can activate *Madcam-1* promoter [31] (showed that RA increases Madcam1), and in line with this, we found a significant up-regulation of *Madcam-1* expression upon RA treatment; again, this effect was blocked by BMS493 (Figure S5B). We then sought to test whether RA inhibition can affect the distribution of CXCL13 and MAdCAM-1 proteins *in vivo*. To this end, we assessed CXCL13 and MAdCAM-1 in the spleen of wild-type mice following exposure to BMS493. The analysis revealed a modest but consistent reduction of CXCL13 distribution particularly in the outer follicular region corresponding to the MRC layer that appeared more disorganized as compared to controls (Figure S5A, upper panels). In this region, the distribution of MAdCAM-1 was similar to controls;

however, in BMS-treated mice we observed loss of MAdCAM-1 in the region corresponding to FDCs (Figure S5A, lower panels).
Together, these findings indicate that leukemia promote a retinoic acid-enrich microenvironment that contribute to stromal remodeling.

Antagonizing RA-signaling in stromal cells restore the expression a large fraction of genes induced by leukemic cells

To assess the effect of RA-signaling inhibition in stromal cells, we performed RNA-seq on cells treated with BMS493 or control vehicle (Figure 6A). Transcriptome analysis revealed a significant down-regulation in the expression of genes involved in cellular adhesion, ECM-receptor interactions, and migration (Figure 6A). Among the deregulated signatures, we validated a set of genes involved in cellular adhesion (e.g. *Vcam-1* and *Itgα1);* migration (e.g. *Cxcl12);* and genes involved in stromal cell activation (e.g. *Acta2/αSma)* (Figure S6). Ablation of the RA-signaling also significantly reduced the expression of genes involved in ECM remodeling, including *Loxl2, Lama5*, *Nidogen2*, *Col1a1*, *Col3a1*, and *Col4a6* (Figure S6). Notably, we found that 30% of the genes deregulated in stromal cells after leukemia co-culture were modulated in the opposite manner following BMS493 treatment of stromal cells (Figure 6B), confirming that in these cells, retinoids control a large subset of genes involved in different biological processes.

Based on the transcriptomic analysis of murine stromal cells treated with BMS493, we decided to functionally validate the possibility to alter stroma-leukemia cell adhesion through inhibition of retinoid-

signaling. To this end, we first quantified the number of *Eμ-TCL1* CLL cells adherent to a monolayer of BMS493-treated murine stromal cells (Figure 6C). Quantification analysis revealed that RA-signaling inhibition reduces adhesion of CLL cells to the stroma as compared to control (Figure 6C). To further test this under conditions that more closely mimic the native lymphoid compartment, we set up a 3D co-culture model, in which stromal and leukemic cells treated with BMS493 or control vehicle, were aggregated to form a lymphoid cluster (Figure 6D). Under these conditions, we observed that while the overall number of stromal cells did not significantly change during the 3D co-culture period, the number of CLL cells that took part to the lymphoid aggregate was significantly reduced upon BMS493 treatment (Figure 6D). These functional data are consistent with the RNA-seq results, and indicate that retinoid-signaling strengthen stroma-leukemia interactions by promoting cell adhesion.

Increased expression of RA nuclear receptors correlates with worse prognosis in murine and human CLL

Previous work showed that RA induces the expression of different target genes including RA-nuclear receptors [32] [7]. Based on these findings, we hypothesized that increased RA synthesis in the microenvironment may promote induction of RA-associated genes in responder murine CLL cells. To test this hypothesis, we first performed gene expression profile (GEP) analysis of genes belonging to the RA pathway in leukemic cells freshly isolated from the spleen of *Eμ-TCL1* mice. Among different genes tested, we found that expression of *Rarγ2*

was significantly increased in leukemia as compared to control B cells (Figure S7A).

We then analyzed expression of RA-nuclear receptors in a previously published data set of CLL patient samples [33], and found that leukemic cells express higher levels of *RXRα* as compared to control B cells (Figure S7B, left panel). Additionally, we screened a pool of 60 CLL cases with different genomic aberrations, and found a significant increase in *RXRα* expression in patients with del(17p) and/or del(11q) deletions and worse prognosis, as compared to those with del(13q) and better outcome (Figure S7B, right panel). Moreover, we found *RXRα* expression is independent from other parameters such as IGHV gene mutational status, CD38 and ZAP70 (Figure S7C). These data demonstrate that RA nuclear receptors are up-regulated in CLL, and that their expression levels identify a subset of patients with bad prognosis.

Targeting the RA-signaling pathway as therapeutic strategy in CLL

Taken together our data suggest that inhibition of the RA-signaling might affect disease progression by interfering with the chemokine networks and with the stroma/ECM-leukemia interactions. To test this possibility, we exploited three different approaches to block RA signaling *in vivo*. First, we generated vitamin A deficient (VAD) mice, and transplanted them at 2 months of age with *Eμ-TCL1* leukemic cells. We observed that leukemia engraftment was strongly suppressed in the spleen and bone marrow (BM) of VAD mice, as compared to mice fed with a control diet (data not shown). We then established a more

physiological model, in which retinoids were gradually depleted over time. To this end, we fed 2 months old *Eμ-TCL1* mice with VAD or control diet before leukemia onset. Long-term survival analysis revealed that VAD *Eμ-TCL1* mice survived longer (Figure 7A, left panel), and this corresponded to significantly reduced levels of retinoic acid precursors as compared to control mice (Figure 7A, right panel).

Lastly, we aimed to establish the therapeutic potential of retinoid-antagonist therapy on leukemia progression. To this end, we treated wild-type mice with the BMS493 or control vehicle after transplantation of leukemic cells. We found that inhibition of RA-signaling significantly delayed leukemia onset and reduced tumor expansion as compared to control by interfering with the accumulation of leukemic cells in the spleen, bone marrow, peritoneal cavity and peripheral blood (Figure 7B). Notably, annexin V and Ki67 staining did not reveal differences in apoptosis or proliferation respectively in mice treated as compared to controls (Figure 7C).

Interestingly, gross morphology analysis revealed that inhibition of RA-signaling significantly suppressed induction of mesenteric FALCs in transplanted mice. Altogether, these findings demonstrate that retinoid-signaling might be a therapeutic target suitable to control disease onset and progression.

FIGURE LEGENDS

Figure 1. *Eμ-TCL1* leukemic cells localize and expand within FDC networks.

Representative confocal images of the spleen from CD45.1 wild-type mice transplanted with CD45.2 *Eμ-TCL1* leukemic cells. Tissues were harvested at 7 and 15 days post leukemia injection and stained with CD35 (green) to visualized FDC networks, CD45.2 (red) to detect leukemic cells, and collagen IV to label the ECM. Scale bars indicate 50μm. Each staining is representative of five mice analyzed.

Figure 2. Disease progression is associated with loss of FDC networks and germinal centers.

A) Representative confocal mosaic images of spleen sections from transgenic *Eμ-TCL1* (upper images) and leukemia-transplanted mice (lower images). Tissues isolated from mice with low (<5%), intermediate (10-20%) and high (>60%) leukemia infiltration were stained for CD35 (green) to visualized FDCs.

B) Representative confocal images of wild-type mice transplanted with *Eμ-TCL1* CLL cells. Tissues were stained with CD35 and Ki67 to visualized germinal centers in mice with different percentage of leukemia infiltration.

C) Representative images of the spleen from wild-type and transgenic *Eμ-TCL1* mice with intermediate infiltration of leukemia. with Scale bars indicate 200μm (A), and 50μm (B). Each staining is representative of four to five mice analyzed.

Figure 3. Leukemia development induces CXCL13 in stromal cells

different from FDCs.

A) Representative confocal mosaic images of the spleen from transgenic *Eμ-TCL1* (upper images) and leukemia-transplanted mice (lower images). Tissues were stained for CXCL13 to visualized stromal cells. Each staining is representative of four to five mice analyzed.

B) Representative confocal images of spleen sections from *Rag2*$^{-/-}\gamma c^{-/-}$ mice injected with leukemic cells, and stained three-weeks after with CD35 (green) or CXCL13 (red) to visualized stromal cells. Each staining is representative of three mice analyzed.

C) Representative confocal images of the spleen from *Pdgfrα*$^{GFP/+}$ mice injected with EdU to assess proliferation at different stages of leukemia development. Tissues were stained for GFP (green) to visualized PDGFRα^{+} stromal cells, and CXCL13 (red). Graphs represent: i) the number of EdU^{+}PDGFRα^{+} proliferating stromal cells; ii) the number of CXCL13^{+} PDGFRα^{+} stromal cells; and iii) the number (density) of PDGFRα^{+} stromal cells. Each count represents the mean ± SD of cells from seven to ten fields analyzed for each tissue.

*** $p<0.001$. Scale bars indicate 200μm (A) and 50μm (B and C). Each staining is representative of one out of three to five mice analyzed.

Figure 4. Fat-associated lymphoid clusters support leukemia expansion in the peritoneal cavity.

A) Representative confocal images of omental FALCs from wild type mice injected with CMFDA-labeled *Eμ-TCL1* leukemic B-cells (green) and stained for collagen IV (red).

B-C) Representative bright-field images, flow cytometry plots showing

CD5 and CD19 staining, and representative confocal images stained for CXCL13 and Coll-IV of control or leukemic *Eμ-TCL1* mice. Scale bars represent 50μm. Data are representative of one out of five mice analyzed.

Figure 5. Leukemic cells promote *Cxcl13* expression through retinoid-signaling.

A) Experimental design of stromal cells cultured with leukemia or control B-cells. Illumina microarray heat maps, and annotations of stromal-associated genes are shown.

B) Experimental design of RA-reporter cells cultured with CLL B-cells or control cells (left). RA-signaling was measured by quantifying the β-gal activity (absorbance after ONPG staining) (left) after co-cultures and treatments with vehicle (DMSO) or with BMS493 (right). Data are representative of six independent experiments.

C) qPCR analysis of *Cxcl13* expression on stromal cells cultured with CTRL or CLL B-cells, and after treatment with DMSO or BMS493. Expression of *Rarβ* after BMS493 treatment was used as control.

D) Representative qPCR analysis of *Cxcl13* expression on mRNA from stromal cells cultured in vitamin A deficient media and treated with vehicle (DMSO), retinoic acid (RA), or BMS493. Expression of *Rarβ* after BMS493 treatment was used as control. qPCRs data are representative of one out of three independent experiments. The mean of triplicates and ± SD are shown, * $p < 0.05$, ** $p < 0.01$, *** $p < 0.001$.

Figure 6. Inhibition of the RA-signaling pathway in stromal cells affects multiple biological processes.

A) Experimental design of RNA-seq analysis performed on mRNA obtained from stromal cells treated with either vehicle (DMSO) or BMS493 (left), and most down-regulated gene-signatures (right).
B) Interpolation of gene expression profiles between microarray and and RNA-seq data.
C) Quantification of leukemic cell adherence to stromal cells after BMS493 or vehicle (DMSO) treatment.
D) Aggregation of stroma and leukemic cells in spheroid assay. The percentage of aggregation results from the number of leukemic cells that contribute to spheroid formation after treatment with BMS493 or vehicle (DMSO). Data are from one out of four to five independent experiments. The mean of triplicates and ± SD are shown, * $p < 0.05$, ** $p < 0.01$.

Figure 7. Targeting Ra-signaling controls disease development.
A) Survival curve for *Eμ-TCL1* mice (n. 10 each group) fed with vitamin A deficient (VitA-) or control (VitA+) diet. Quantification of the RA-precursors retinol and retinyl palmitate in the liver of selected *Eμ-TCL1* VitA+ or VitA- mice. Statistical analysis was performed using the Mantel-Cox log rank.
B) Analysis of leukemia progression over time in CLL transplanted mice (n.11) treated with vehicle (DMSO) or BMS493. Flow cytometry analysis of leukemia cell infiltration in different tissues at 20 or 30 days after BMS493 treatment. * $p < 0.05$, ** $p < 0.01$, *** $p < 0.001$.
C) Percentage of annexin V^+ and $Ki67^+$ leukemic cells from the spleen and bone marrow (BM) at 20 or 30 days after the indicated treatment. * $p < 0.05$, ** $p < 0.01$, *** $p < 0.001$.

Figure S1. Leukemic cells localize in the follicular region after transplantation.

A) Representative confocal images of the spleen from wild-type mice transplanted with CMFDA labeled *Eμ-TCL1* leukemic B-cells (green). Mice were sacrificed and analyzed 48 hours (panel A) after leukemia injection. Tissues were stained for laminin (blue) to visualize the ECM, CD35 (red) to indicate FDC networks, and CXCL13 (red) a marker for FDCs and MRCs.

B) Representative qPCR analysis of *Ltβ and Ltα* expression in leukemia and control B cells.

Data are the mean values of four to five mice analyzed. The mean of triplicates and ± SD are shown, *** $p < 0.001$.

Figure S2. ECM and follicular-zone remodeling accompanies leukemia development.

A) Representative confocal images of the spleen from transgenic *Eμ-TCL1* mice with low, intermediate and high infiltration of leukemic cells. Tissues were stained for NID-2 (green) to visualize the ECM. Data are representative of one out of five mice analyzed for each condition. Scale bars represent 100μm.

B) Representative confocal images of the spleen from transplanted or transgenic *Eμ-TCL1* mice with high infiltration of leukemic cells. Tissues were stained for podoplanin (green) to visualize the T-zone stromal cells, and nidogen-2 to (red) to label the ECM. Data are representative of one out of five mice analyzed for each condition. Scale bars represent 100μm.

C) Representative confocal images of the spleen from transplanted mice with high infiltration of leukemic cells in the spleen. Tissues were stained for MAdCAM-1 to visualize MRCs (green). Nuclei are visualized with DAPI staining (blue). Scale bars indicate 50μm and 25μm. Representative qPCR analysis of *Madcam-1* expression in stromal cells cultured with CTRL and CLL B-cells (left). Data are representative of three independent experiments. The mean of triplicates and ± SD are shown, ** $p < 0.01$.

Figure S3. CXCL13 protein in the lymph node of CLL patients and expression of RA-associated genes in human CLL cells.

Representative images of lymph node sections obtained from CLL patients and immunostained for CXCL13 (brown). Original magnification: 40x and 100x (insets).

Figure S4. Leukemic cells induce the expression of genes involved in RA-synthesis and tissue remodeling.

List of selected gene-signatures deregulated in stromal cells after the co-culture with B-CLL or CTRL B cells. In red are highlighted *Cyp1b1* and *Aldh1a1* two genes involved in RA synthesis that were validated by qPCR analysis. Data are from one out of four independent experiments with similar results. The mean of triplicates and ± SD are shown,

** $p < 0.01$.

Figure S5. The RA-signaling inhibition affects CXCL13 and MAdCAM-1 distribution.

A) Representative confocal images of the spleen from wild-type mice treated with either DMSO (left) or BMS493 (right). Tissue sections were stained for laminin (gray) and CXCL13 (red, upper panels) or MAdCAM-1 (red, lower panels). Yellow arrowheads indicate the MRC layer; white dash-line indicate MAdCAM-1^+ staining corresponding to the FDCs. Images are representative of one out of three mice analyzed. Scale bars indicate 50μm.

B) Representative qPCR analysis of *Madcam-1* expression on mRNA from stromal cells cultured in vitamin A deficient media and treated with vehicle (DMSO), retinoic acid (RA), or BMS493. Data are from one out of three independent experiments with similar results.

The mean of triplicates and ± SD are shown, *** $p < 0.001$.

Figure S6. Inhibition of RA-signaling in stromal cells causes down-modulation of genes involved in stromal cell activation and tissue remodeling.

qPCR analysis for validation of RNA-seq data. Expression levels of selected stromal gene-signatures after vehicle (DMSO) or BMS493 treatment. Data are representative of four independent experiments; * $p < 0.05$, ** $p < 0.01$, *** $p < 0.001$.

Figure S7. Increased expression of RA-nuclear receptors in hCLL cells correlates with bad prognosis.

A) qPCR analysis of *Rarγ*2 expression in control B and *Eμ-TCL1* leukemic cells. Data are representative of one out of five mice analyzed. The mean of triplicates and ± SD are shown, * $p < 0.05$.

B-C) Relative *RXRα* expression data of purified B-cells from healthy

donors and CLL patients (panel B, left) from public repository. Correlation analysis of *RXRα* expression from purified CLL cells from patients with different genetic aberrations (panel B, right), mutational status, CD38 and ZAP70 expression. The mean of triplicates and ± SD are shown, * $p < 0.05$ and *** $p < 0.001$

Figure 1.

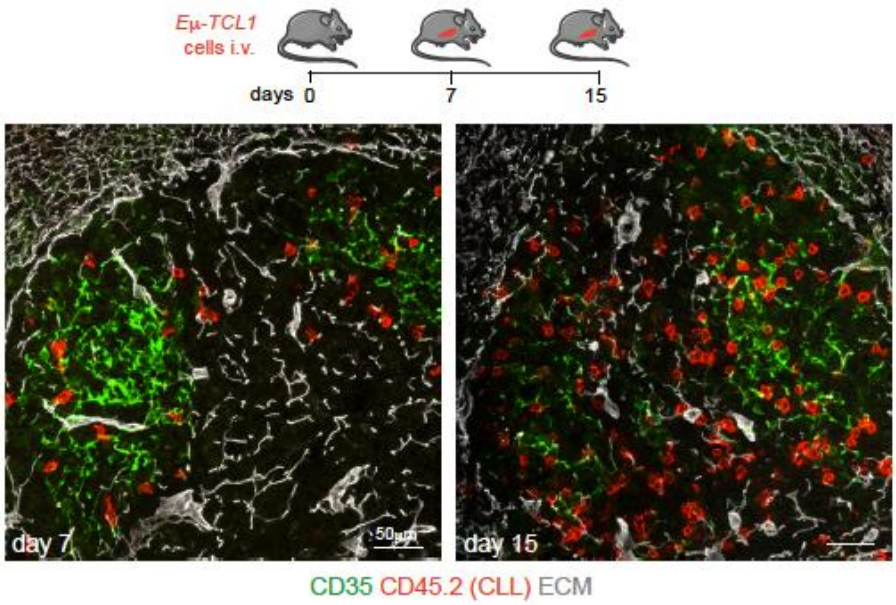

Figure 2.

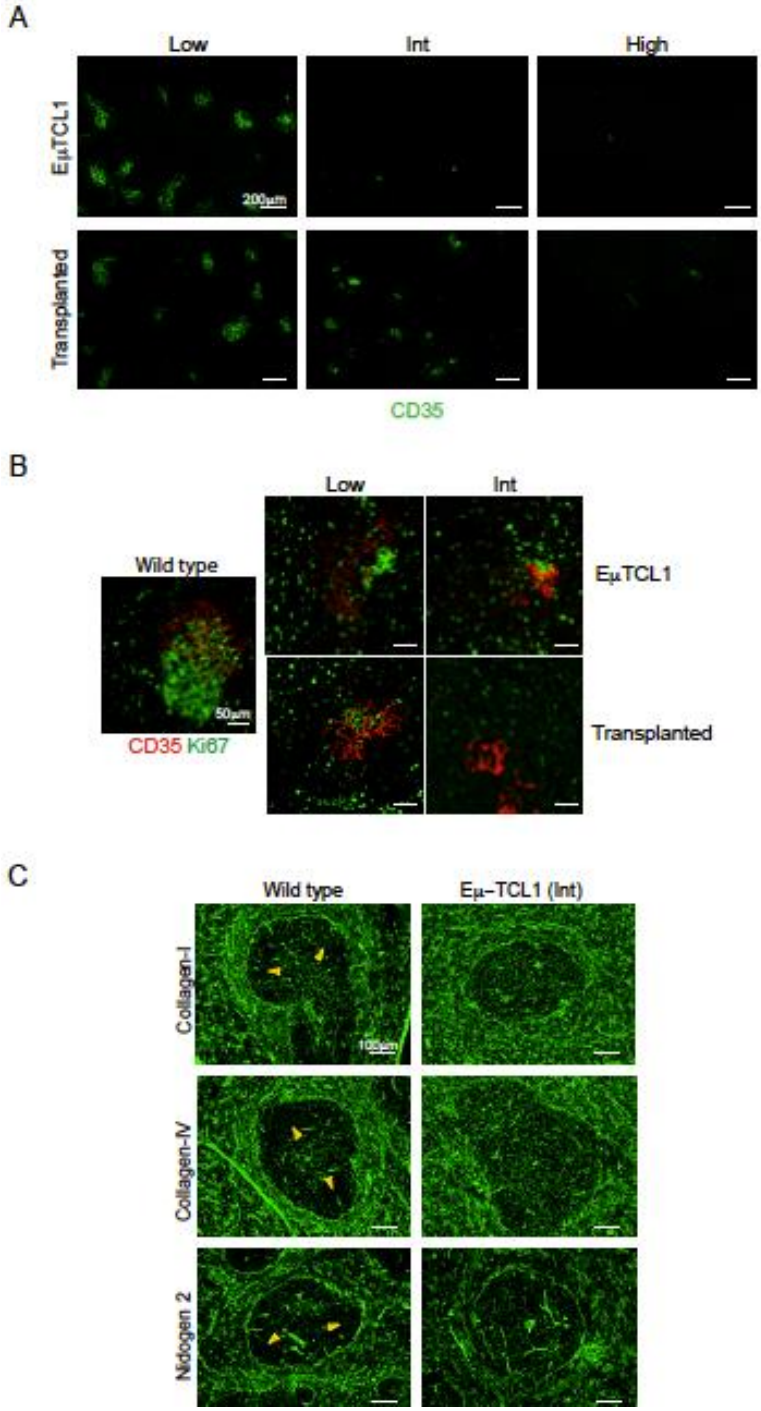
A
Low
Int
High
EμTCL1
Transplanted
200μm
CD35
B
Low
Int
Wild type
EμTCL1
Transplanted
50μm
CD35 Ki67
C
Wild type
Eμ–TCL1 (Int)
Collagen-I
Collagen-IV
Nidogen 2
100μm

Figure 3.

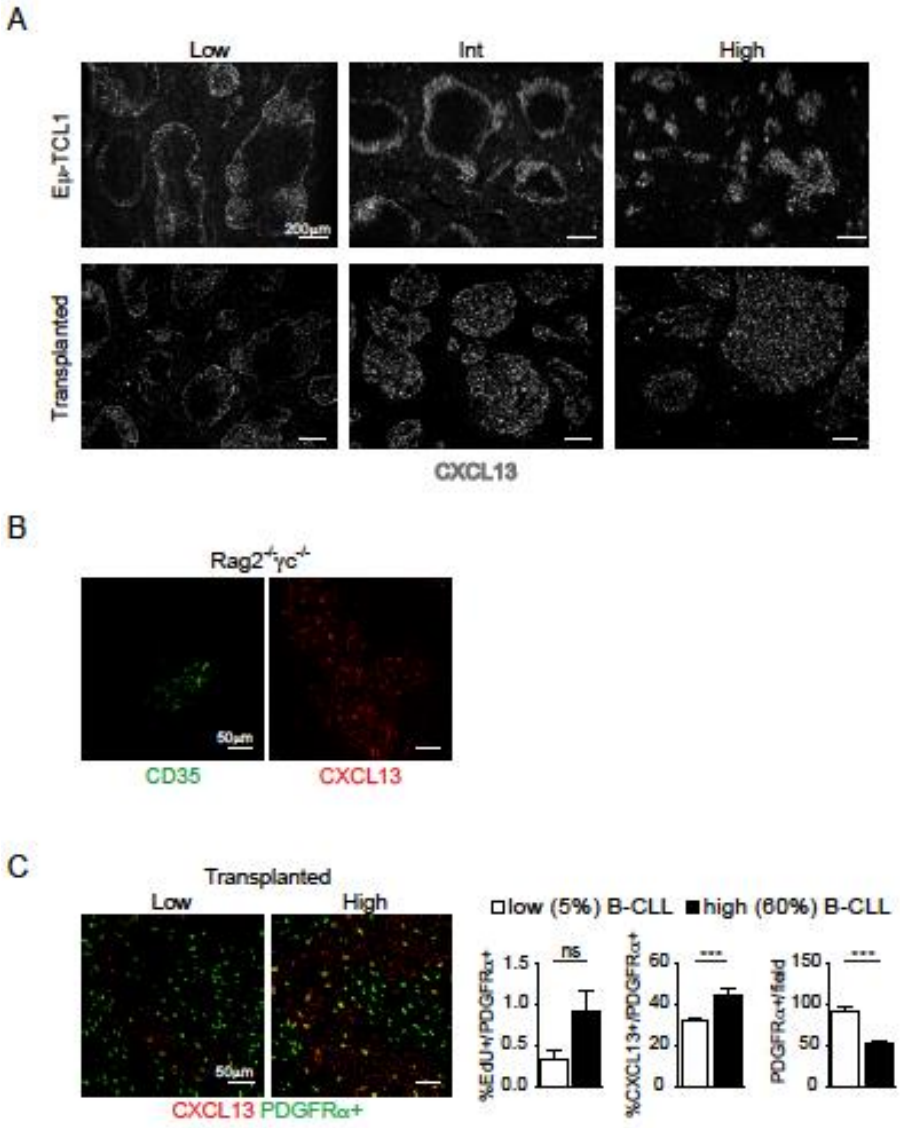
A
Low
Int
High
Eμ-TCL1
Transplanted
200μm
CXCL13
B
Rag2-/-γc-/-
50μm
CD35
CXCL13
C
Transplanted
Low
High
50μm
CXCL13 PDGFRα+
low (5%) B-CLL
high (60%) B-CLL
%EdU+/PDGFRα+
ns
%CXCL13+/PDGFRα+
***
PDGFRα+/field
***

Figure 4.

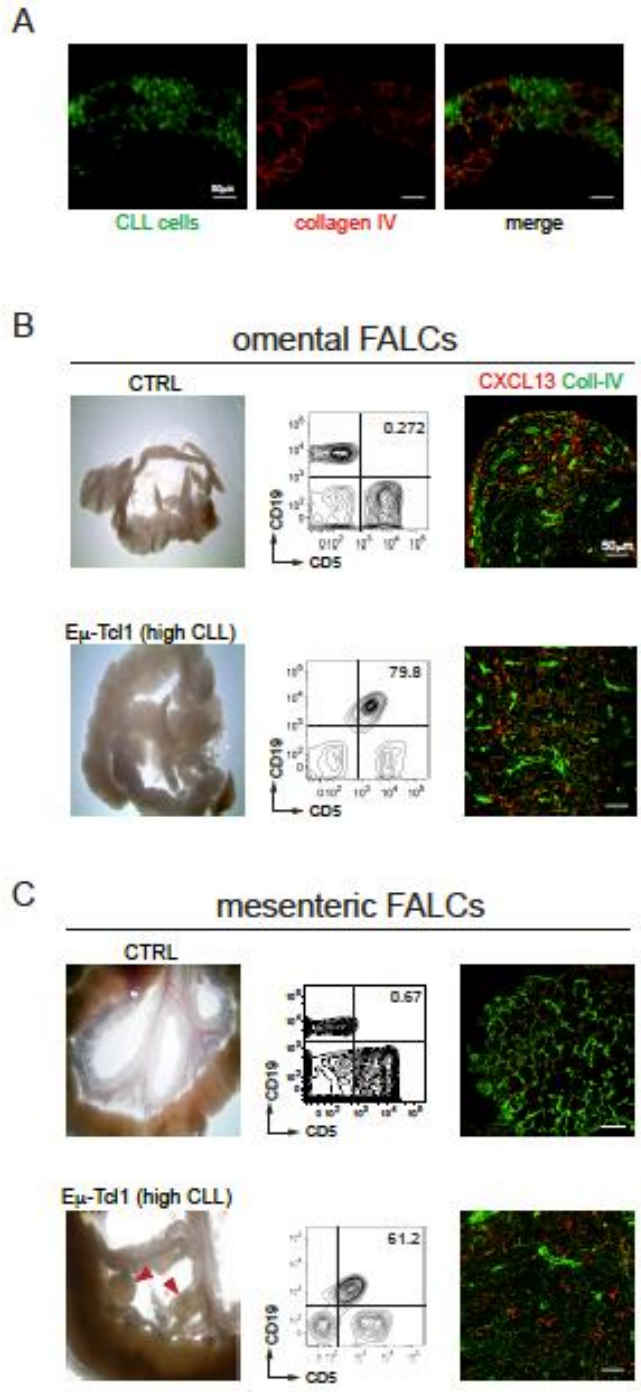
A
CLL cells
collagen IV
merge
B
omental FALCs
CTRL
CXCL13 Coll-IV
0.272
CD19
CD5
Eμ-Tcl1 (high CLL)
79.8
C
mesenteric FALCs
CTRL
0.67
Eμ-Tcl1 (high CLL)
61.2

Figure 5.

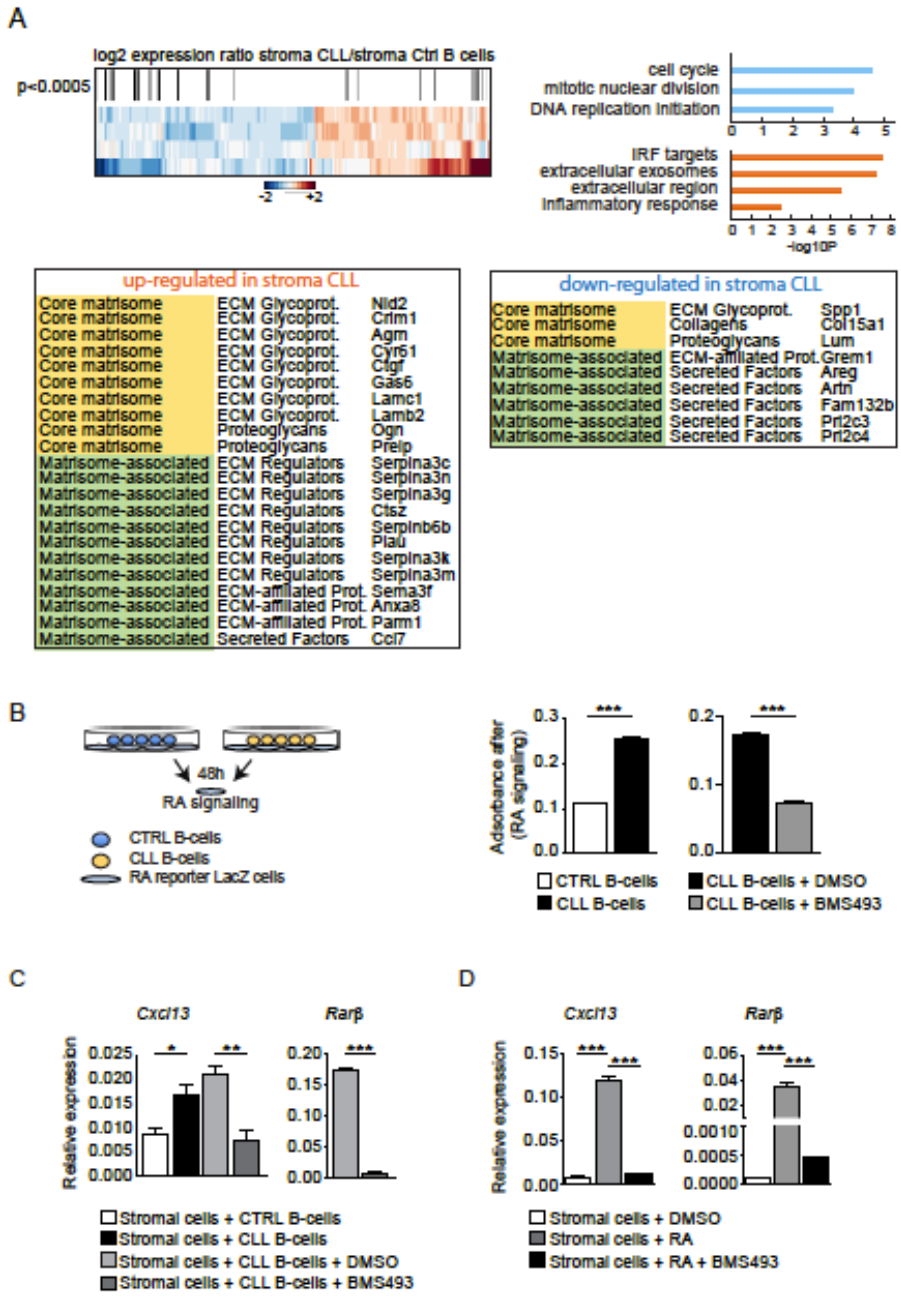
A
log2 expression ratio stroma CLL/stroma Ctrl B cells
p<0.0005
-2
+2
cell cycle
mitotic nuclear division
DNA replication initiation
IRF targets
extracellular exosomes
extracellular region
inflammatory response
-log10P
up-regulated in stroma CLL
Core matrisome ECM Glycoprot. Nid2
Core matrisome ECM Glycoprot. Crlm1
Core matrisome ECM Glycoprot. Agrn
Core matrisome ECM Glycoprot. Cyr61
Core matrisome ECM Glycoprot. Ctgf
Core matrisome ECM Glycoprot. Gas6
Core matrisome ECM Glycoprot. Lamc1
Core matrisome ECM Glycoprot. Lamb2
Core matrisome Proteoglycans Ogn
Core matrisome Proteoglycans Prelp
Matrisome-associated ECM Regulators Serpina3c
Matrisome-associated ECM Regulators Serpina3n
Matrisome-associated ECM Regulators Serpina3g
Matrisome-associated ECM Regulators Ctsz
Matrisome-associated ECM Regulators Serpinb6b
Matrisome-associated ECM Regulators Plau
Matrisome-associated ECM Regulators Serpina3k
Matrisome-associated ECM Regulators Serpina3m
Matrisome-associated ECM-affilated Prot. Sema3f
Matrisome-associated ECM-affilated Prot. Anxa8
Matrisome-associated ECM-affilated Prot. Parm1
Matrisome-associated Secreted Factors Ccl7
down-regulated in stroma CLL
Core matrisome ECM Glycoprot. Spp1
Core matrisome Collagens Col15a1
Core matrisome Proteoglycans Lum
Matrisome-associated ECM-affilated Prot. Grem1
Matrisome-associated Secreted Factors Areg
Matrisome-associated Secreted Factors Artn
Matrisome-associated Secreted Factors Fam132b
Matrisome-associated Secreted Factors Prl2c3
Matrisome-associated Secreted Factors Prl2c4
B
48h
RA signaling
CTRL B-cells
CLL B-cells
RA reporter LacZ cells
Adsorbance after (RA signaling)
CTRL B-cells
CLL B-cells
CLL B-cells + DMSO
CLL B-cells + BMS493
C
Cxcl13
Rarβ
Relative expression
Stromal cells + CTRL B-cells
Stromal cells + CLL B-cells
Stromal cells + CLL B-cells + DMSO
Stromal cells + CLL B-cells + BMS493
D
Cxcl13
Rarβ
Relative expression
Stromal cells + DMSO
Stromal cells + RA
Stromal cells + RA + BMS493

Figure 6.

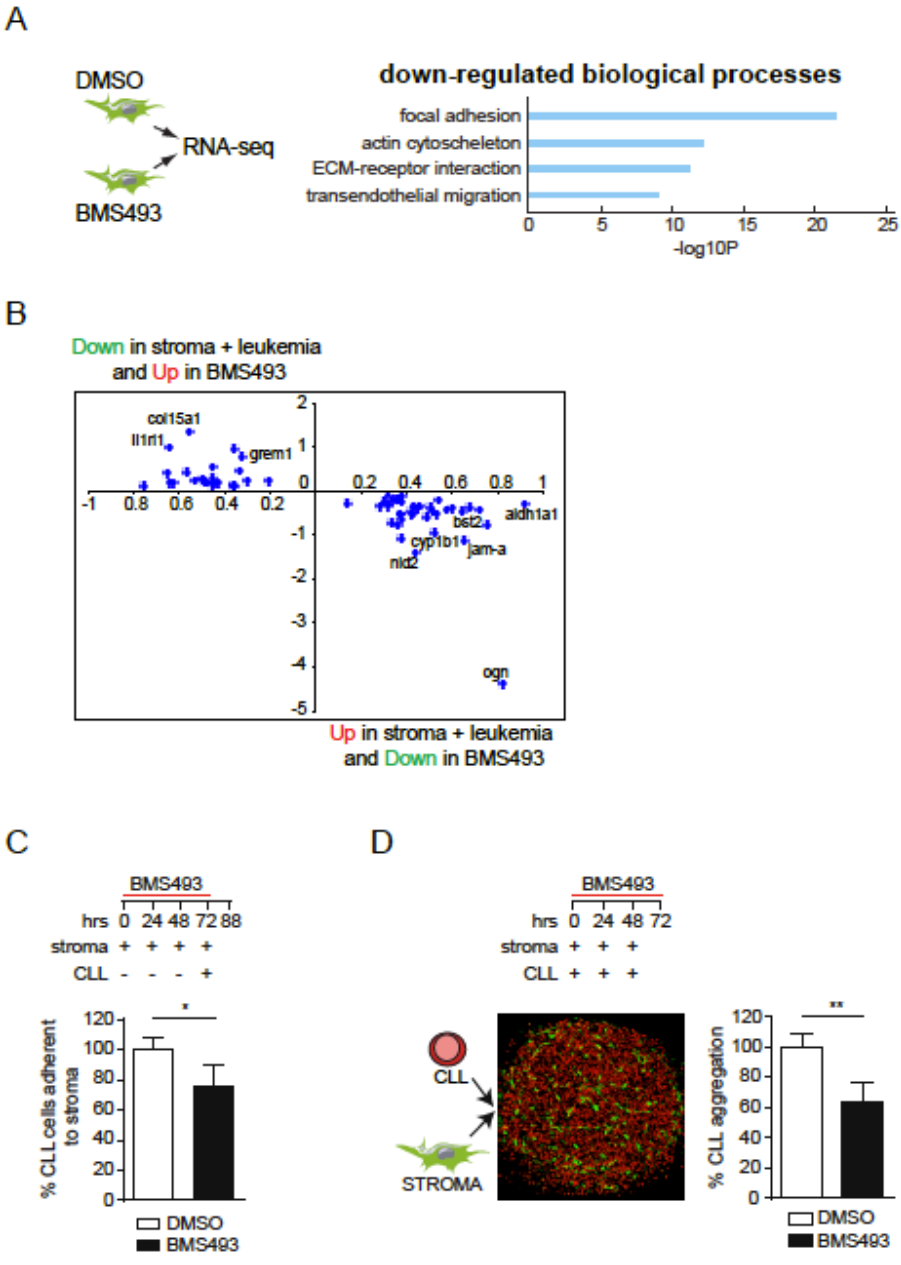
A
DMSO
RNA-seq
BMS493
down-regulated biological processes
focal adhesion
actin cytoscheleton
ECM-receptor interaction
transendothelial migration
0
5
10
15
20
25
-log10P
B
Down in stroma + leukemia
and Up in BMS493
col15a1
il1rl1
grem1
bst2
aldh1a1
cyp1b1
jam-a
nid2
ogn
Up in stroma + leukemia
and Down in BMS493
C
BMS493
hrs 0 24 48 72 88
stroma + + + +
CLL - - - +
% CLL cells adherent to stroma
DMSO
BMS493
D
BMS493
hrs 0 24 48 72
stroma + + +
CLL + + +
CLL
STROMA
% CLL aggregation
DMSO
BMS493

Figure 7.

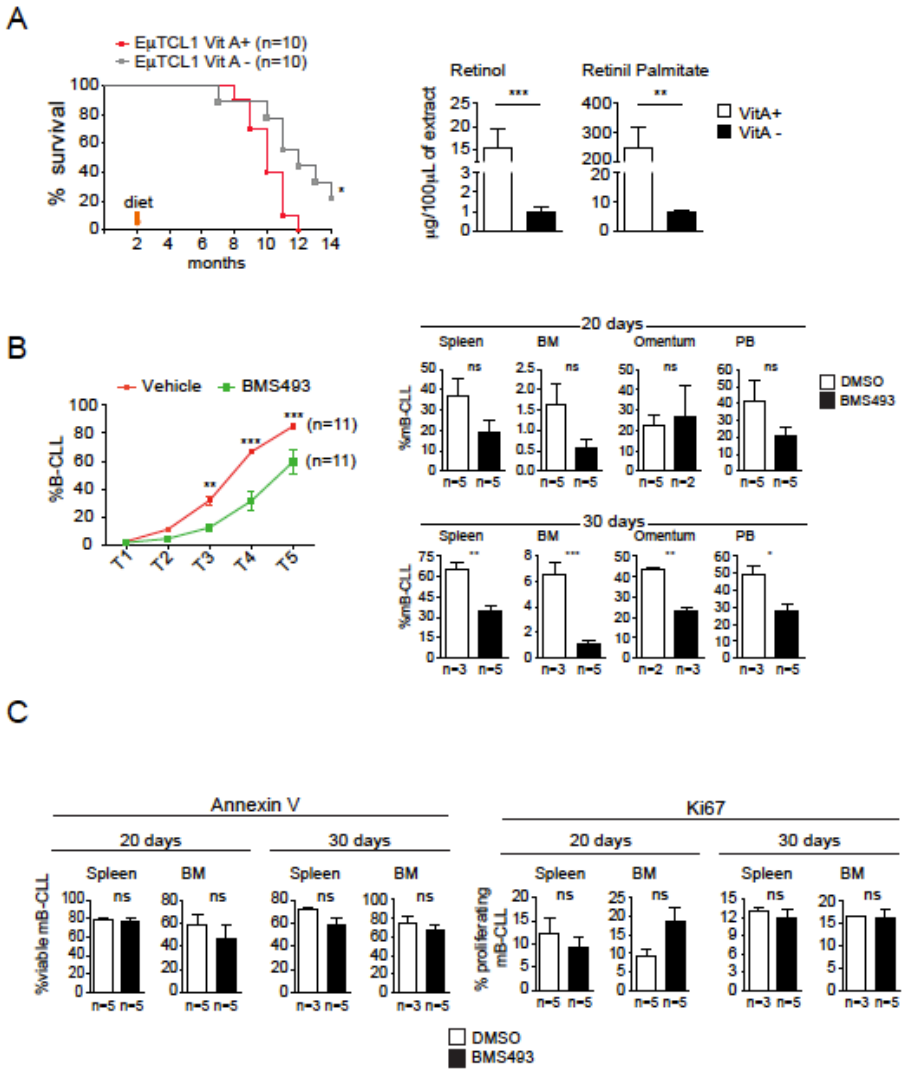
A
EμTCL1 Vit A+ (n=10)
EμTCL1 Vit A - (n=10)
% survival
diet
months
Retinol
Retinil Palmitate
μg/100μL of extract
VitA+
VitA -
B
Vehicle
BMS493
%B-CLL
(n=11)
(n=11)
20 days
30 days
Spleen
BM
Omentum
PB
%mB-CLL
DMSO
BMS493
C
Annexin V
Ki67
20 days
30 days
%viable mB-CLL
% proliferating mB-CLL
DMSO
BMS493

Figure S1.

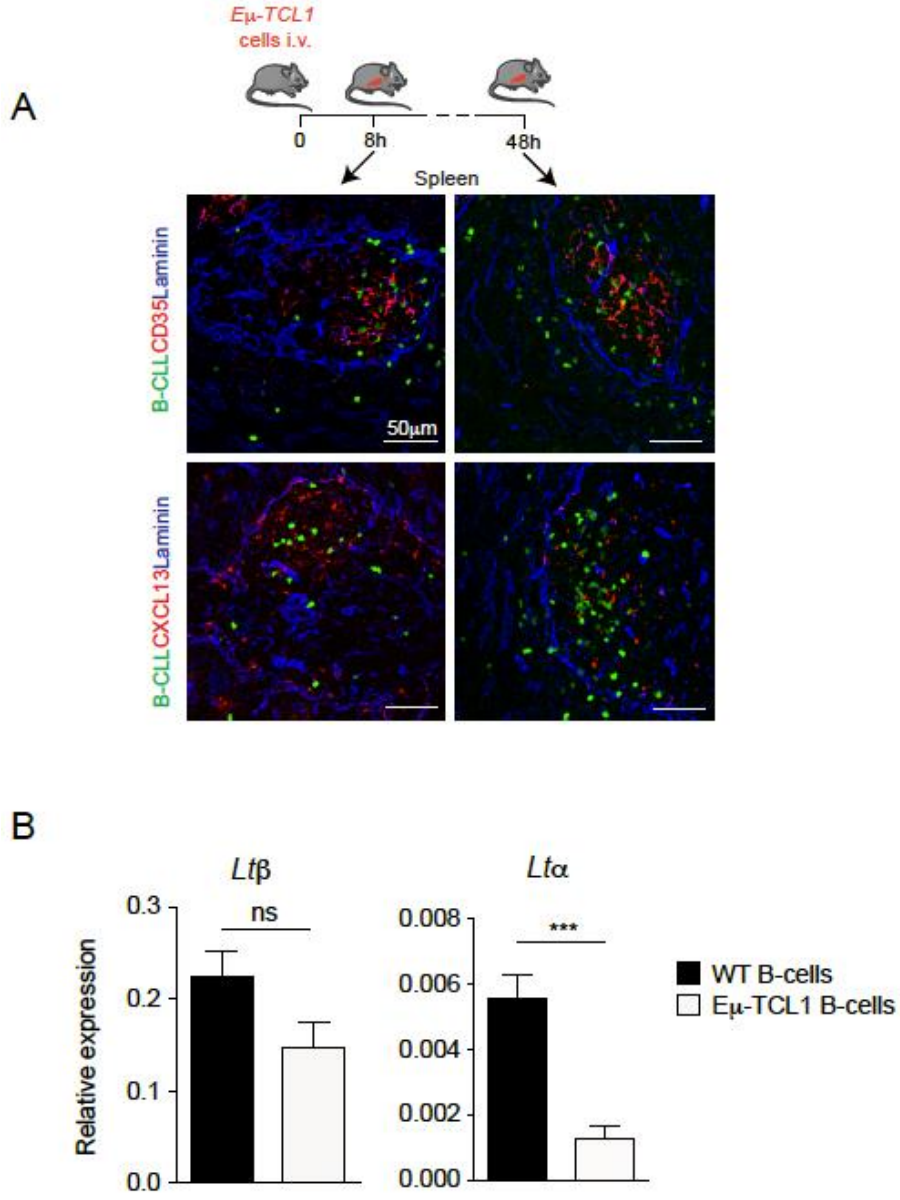
A
Eμ-TCL1
cells i.v.
0
8h
48h
Spleen
B-CLL CD35 Laminin
B-CLL CXCL13 Laminin
50μm
B
Ltβ
Ltα
ns
***
Relative expression
0.3
0.2
0.1
0.0
0.008
0.006
0.004
0.002
0.000
WT B-cells
Eμ-TCL1 B-cells

Figure S2.

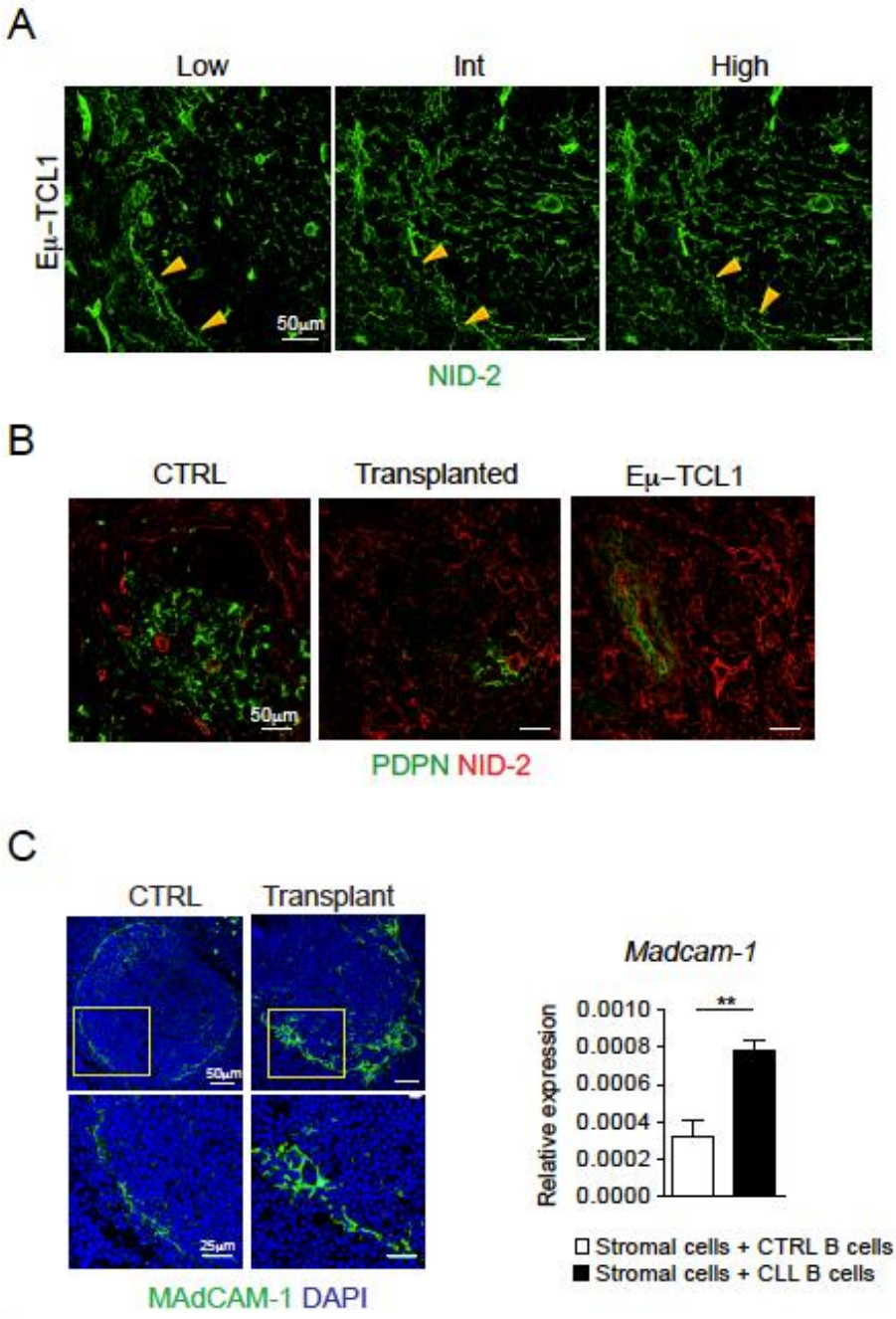
A
Low
Int
High
Eμ–TCL1
50μm
NID-2
B
CTRL
Transplanted
Eμ–TCL1
50μm
PDPN NID-2
C
CTRL
Transplant
50μm
25μm
MAdCAM-1 DAPI
Madcam-1
**
Relative expression
0.0010
0.0008
0.0006
0.0004
0.0002
0.0000
Stromal cells + CTRL B cells
Stromal cells + CLL B cells

Figure S3.

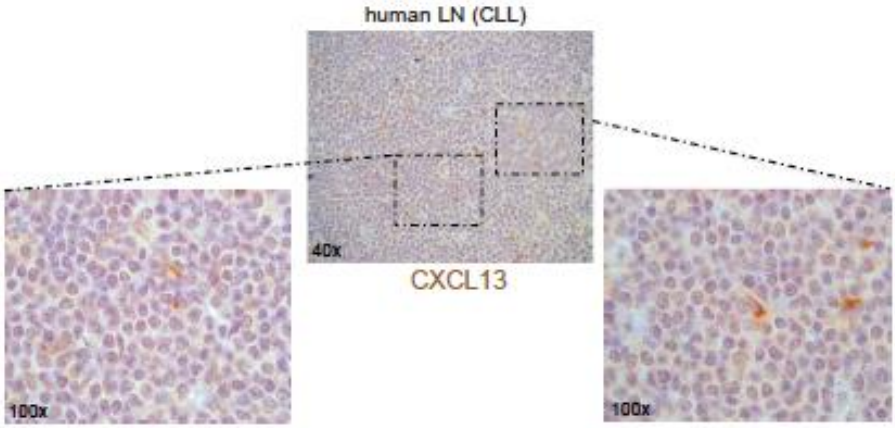

Figure S4.

Vgll4	Nid2	C3,
Bst2	Crim1	Cd59a
Ifit3	Agrn	Cd74
Isg15	Cyr61	Crim1
Psmb10	Gas6	F11r
Lgals3bp	Acta2	Gadd45g
Vamp5	Ogn	Hp
Psme1	Prelp	Ier3
Aldh1a1	Serpina3n	Il6st
Usp18	Serpinb6b	Lamb2
Cyp1b1	Plau	Rgs16
Actg2	Sema3f	Trex1

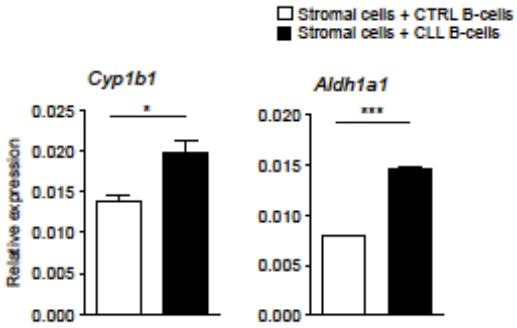

Figure S5.

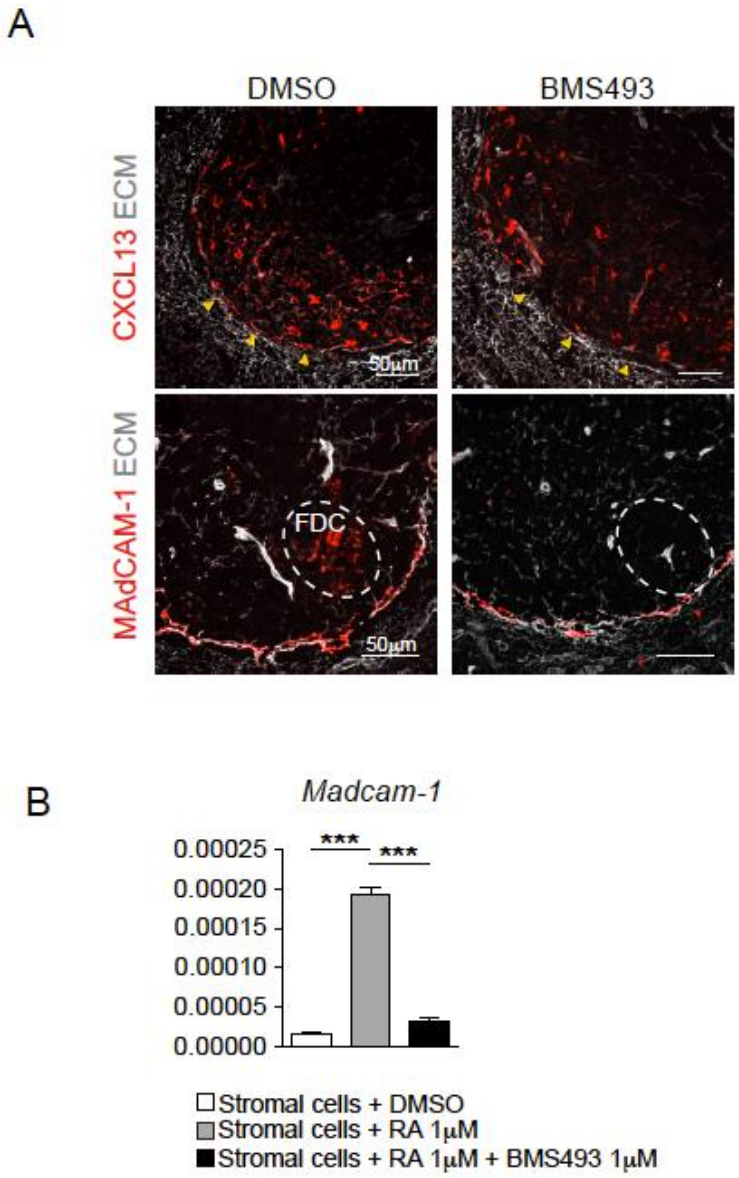
A
DMSO
BMS493
CXCL13 ECM
MAdCAM-1 ECM
FDC
50µm
50µm
B
Madcam-1
0.00025
0.00020
0.00015
0.00010
0.00005
0.00000
***
***
Stromal cells + DMSO
Stromal cells + RA 1µM
Stromal cells + RA 1µM + BMS493 1µM

Figure S6.

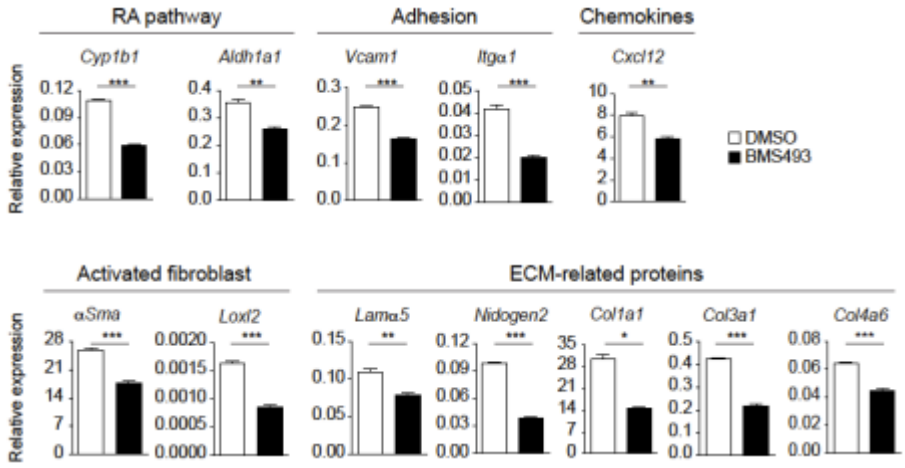
RA pathway
Adhesion
Chemokines
Cyp1b1
Aldh1a1
Vcam1
Itgα1
Cxcl12
Relative expression
DMSO
BMS493
Activated fibroblast
ECM-related proteins
αSma
Loxl2
Lamα5
Nidogen2
Col1a1
Col3a1
Col4a6

Figure S7.

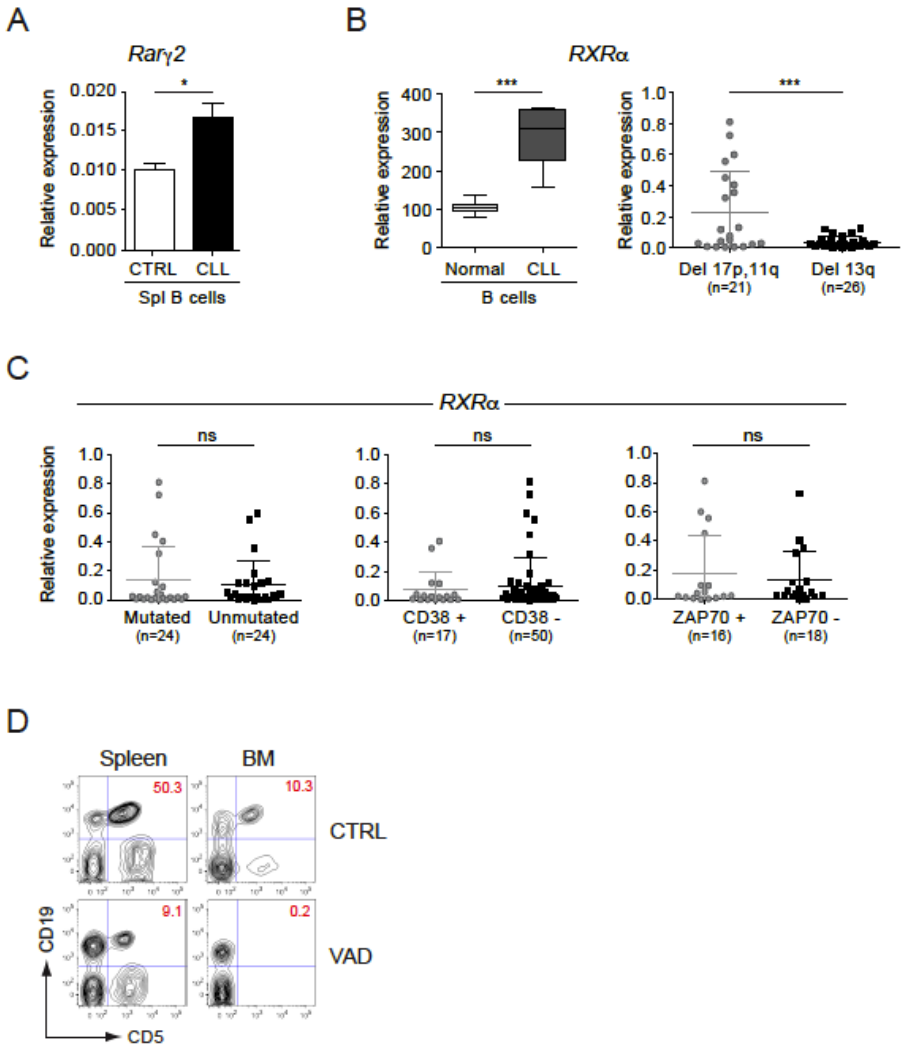
A
Rarγ2
Relative expression
0.020
0.015
0.010
0.005
0.000
*
CTRL
CLL
Spl B cells
B
RXRα
Relative expression
400
300
200
100
0
***
Normal
CLL
B cells
1.0
0.8
0.6
0.4
0.2
0.0
***
Del 17p,11q
(n=21)
Del 13q
(n=26)
C
RXRα
Relative expression
ns
Mutated
(n=24)
Unmutated
(n=24)
CD38 +
(n=17)
CD38 -
(n=50)
ZAP70 +
(n=16)
ZAP70 -
(n=18)
D
Spleen
BM
50.3
10.3
CTRL
9.1
0.2
VAD
CD19
CD5

Antigen	Species	Conjugation	Company	Dilution factor	Clone / cat. #
BP-3	Mouse	PE	BD pharmingen	1:100	552814
CD19	Rat	PE	BD pharmingen	1:50	1D3 / 553786
CD3	Hamster	PE	BD pharmingen	1:100	145-2C11 / 553064
CD35	Rat	biotinilated	BD pharmingen	1:100	8C12 / 553816
Collagen IV	Rabbit	-	Abcam	1:500	Ab19808
CXCL13	Goat	-	R&D systems	1:100	AF470
Podoplanin	Syrian Hamster	-	eBioscience	1:200	8.1.1 / 14-53814
Nidogen 2	Rabbit	-	Abcam	1:500	Ab14513
Laminin	Rabbit	-	Sigma Aldrich	1:300	L9393
MadCAM-1	Rat	biotinilated	BD pharmingen	1:50	MECA-367 / 553808
MOMA-1	Rat	biotinilated	Abcam	1:500	Ab51814
Collagen I	Rabbit	-	Abcam	1:500	Ab34710
CD21/35	Rabbit	PE	eBioscience	1:100	eBio4E3 / 12-0212
CD45.2	Mouse	PE	Biolegend	1:200	104
F4/80	Rat	APC	Biolegend	1:200	123115

MOMA-1	Rat	biotinilated	Abcam	1:500	Ab51814
ER-TR7	Rat		Acris (Duotech)	1:500	BM4018

Supplementary table 1

Antigen	Fluorochrome	Company	Dilution factor	Clone / cat. #
Anti-Syrian Hamster	Biotinylated	Vector	1:500	BA9100
Anti-goat	Biotinylated	Vector	1:500	BA-5000
Anti-rabbit	Alexa Fluor 546	Invitrogen	1:500	A-11035
Anti-rabbit	Alexa Fluor 488	Invitrogen	1:500	A-21441
Anti-rabbit	Alexa Fluor 647	Invitrogen	1:500	A-31573
Anti-rat	Alexa Fluor 488	Invitrogen	1:500	A21208
Streptavidin	HRP	Perkin Elmer	1:500	NEL750
Streptavidin	Alexa Fluor 546	Invitrogen	1:500	S11225
Streptavidin	Alexa Fluor 488	Invitrogen	1:500	S11223
Streptavidin	Alexa Fluor 647	Invitrogen	1:500	S21374

Supplementary table 2

Antigen	Fluorochrome	Company	Volume/ sample	Clone / cat. #
Anti-CD19	PE-Cy7	Biolegend	1 μL	6D5

Anti-CD5	APC	BD Pharmingen	1 μL	53-7.3
Anti-Ki67	FITC	BD Pharmingen	12 μL	556026
Anti-CD45.2	FITC	BD Pharmingen	1 μL	104
Anti-CD3	PE	eBioscience	1 μL	145-2C11 / 553064
Annexin V	APC		5 μL	550475
Anti-CD5	FITC	BD Pharmingen	1 μL	53-7.3

Supplementary table 3

Gene name	Forward primer	Reverse primer	Probe #
Aldh1a1	caccatggatgcttcagaga	actttcccaccattgagtgc	84
Cyp1b1	ggaaaccacgcttcatcg	aggacggagaagagtagcagaa	49
Cxcl13	cagaatgaggctcagcacag	atgggcttccagaataccg	34
Cyp26b1	acatccaccgcaacaagc	gggcaggtagctctcaagtg	41
Madcam-1	gggcaggtgaccaatctgta	ataggacgacggtggagga	72
Rarβ	tgaggctcagcacagcaa	atgggcttccagaataccg	63
Rarγ1	tttccaccaggtccctcac	ctgtccagtgggtttccaag	64
Rarγ2	tcgccggacttgagtcttt	ctggtgctctgtgtctccac	104
Rpl13a	ccctccaccctatgacaaga	gtaggcttcagccgaacaac	108
Acta2	agagacaccaccggacatct	caagggatcacttcaatttgtg	58
Col1a1	acctaagggtaccgctgga	gagctccagcttctccatctt	18
Col3a1	acctcctggtgctcttggt	cacgctctccaggtcgtc	58
Col4a6	cagcctctggatcggatact	actagggactggcctccac	3
Lama5	gagtctgtgcgagctgtgg	tcgccagacggtaccaag	80

Loxl2	agcttttcttctgggcaacc	ctccatccttgtcctgtgct	104
RXRα (human)	aagcggatcccacacttct	gaaggaggcgatgagcag	18
GAPDH (human)	agccacatcgctcagacac	gcccaatacgaccaaatcc	60

Supplementary table 4

5.1 MANUSCRIPT BIBLIOGRAPHY

1. Bichi, R., et al., *Human chronic lymphocytic leukemia modeled in mouse by targeted TCL1 expression.* Proc Natl Acad Sci U S A, 2002. **99**(10): p. 6955-60.
2. Goldman, J.P., et al., *Enhanced human cell engraftment in mice deficient in RAG2 and the common cytokine receptor gamma chain.* Br J Haematol, 1998. **103**(2): p. 335-42.
3. Hamilton, T.G., et al., *Evolutionary divergence of platelet-derived growth factor alpha receptor signaling mechanisms.* Mol Cell Biol, 2003. **23**(11): p. 4013-25.
4. Maruya, M., et al., *Vitamin A-dependent transcriptional activation of the nuclear factor of activated T cells c1 (NFATc1) is critical for the development and survival of B1 cells.* Proc Natl Acad Sci U S A, 2011. **108**(2): p. 722-7.
5. Kane, M.A., A.E. Folias, and J.L. Napoli, *HPLC/UV quantitation of retinal, retinol, and retinyl esters in serum and tissues.* Anal Biochem, 2008. **378**(1): p. 71-9.
6. Castagnaro, L., et al., *Nkx2-5(+)islet1(+) mesenchymal precursors generate distinct spleen stromal cell subsets and participate in restoring stromal network integrity.* Immunity, 2013. **38**(4): p. 782-91.
7. Lenti, E., et al., *Transcription factor TLX1 controls retinoic acid signaling to ensure spleen development.* J Clin Invest, 2016. **126**(7): p. 2452-64.
8. Wagner, M., *Detection and measurement of retinoic acid production by isolated tissues using retinoic acid-sensitive reporter cell lines.* Methods Mol Biol, 1998. **89**: p. 41-53.
9. Chen, F., et al., *Inhibition of Tgf beta signaling by endogenous retinoic acid is essential for primary lung bud induction.* Development, 2007. **134**(16): p. 2969-79.
10. Dobin, A., et al., *STAR: ultrafast universal RNA-seq aligner.* Bioinformatics, 2013. **29**(1): p. 15-21.
11. Liao, Y., G.K. Smyth, and W. Shi, *The Subread aligner: fast, accurate and scalable read mapping by seed-and-vote.* Nucleic Acids Res, 2013. **41**(10): p. e108.
12. Robinson, M.D., D.J. McCarthy, and G.K. Smyth, *edgeR: a Bioconductor package for differential expression analysis of*

digital gene expression data. Bioinformatics, 2010. **26**(1): p. 139-40.
13. Ritchie, M.E., et al., *limma powers differential expression analyses for RNA-sequencing and microarray studies.* Nucleic Acids Res, 2015. **43**(7): p. e47.
14. Zhu, Y.K., et al., *Contraction of fibroblast-containing collagen gels: initial collagen concentration regulates the degree of contraction and cell survival.* In Vitro Cell Dev Biol Anim, 2001. **37**(1): p. 10-6.
15. Hong, F., et al., *RankProd: a bioconductor package for detecting differentially expressed genes in meta-analysis.* Bioinformatics, 2006. **22**(22): p. 2825-7.
16. Heinig, K., et al., *Access to follicular dendritic cells is a pivotal step in murine chronic lymphocytic leukemia B-cell activation and proliferation.* Cancer Discov, 2014. **4**(12): p. 1448-65.
17. Lu, T.T. and J.L. Browning, *Role of the Lymphotoxin/LIGHT System in the Development and Maintenance of Reticular Networks and Vasculature in Lymphoid Tissues.* Front Immunol, 2014. **5**: p. 47.
18. Bagdi, E., et al., *Follicular dendritic cells in reactive and neoplastic lymphoid tissues: a reevaluation of staining patterns of CD21, CD23, and CD35 antibodies in paraffin sections after wet heat-induced epitope retrieval.* Appl Immunohistochem Mol Morphol, 2001. **9**(2): p. 117-24.
19. Tandon, B., et al., *Chronic lymphocytic leukemia/small lymphocytic lymphoma: another neoplasm related to the B-cell follicle?* Leuk Lymphoma, 2015. **56**(12): p. 3378-86.
20. Wang, X., et al., *Follicular dendritic cells help establish follicle identity and promote B cell retention in germinal centers.* J Exp Med, 2011. **208**(12): p. 2497-510.
21. Ansel, K.M., et al., *A chemokine-driven positive feedback loop organizes lymphoid follicles.* Nature, 2000. **406**(6793): p. 309-14.
22. Buckley, C.D., et al., *Stromal cells in chronic inflammation and tertiary lymphoid organ formation.* Annu Rev Immunol, 2015. **33**: p. 715-45.
23. Krautler, N.J., et al., *Follicular dendritic cells emerge from ubiquitous perivascular precursors.* Cell, 2012. **150**(1): p. 194-206.

24. Cruz-Migoni, S. and J. Caamano, *Fat-Associated Lymphoid Clusters in Inflammation and Immunity.* Front Immunol, 2016. **7**: p. 612.
25. Benezech, C., et al., *Inflammation-induced formation of fat-associated lymphoid clusters.* Nat Immunol, 2015. **16**(8): p. 819-28.
26. Ishikawa, J., et al., *Molecular cloning and chromosomal mapping of a bone marrow stromal cell surface gene, BST2, that may be involved in pre-B-cell growth.* Genomics, 1995. **26**(3): p. 527-34.
27. Xing, F., J. Saidou, and K. Watabe, *Cancer associated fibroblasts (CAFs) in tumor microenvironment.* Front Biosci (Landmark Ed), 2010. **15**: p. 166-79.
28. Naba, A., et al., *The extracellular matrix: Tools and insights for the "omics" era.* Matrix Biol, 2016. **49**: p. 10-24.
29. van de Pavert, S.A., et al., *Chemokine CXCL13 is essential for lymph node initiation and is induced by retinoic acid and neuronal stimulation.* Nat Immunol, 2009. **10**(11): p. 1193-9.
30. Guo, Y., et al., *A retinoic acid--rich tumor microenvironment provides clonal survival cues for tumor-specific CD8(+) T cells.* Cancer Res, 2012. **72**(20): p. 5230-9.
31. Guerra-Perez, N., et al., *Retinoic acid imprints a mucosal-like phenotype on dendritic cells with an increased ability to fuel HIV-1 infection.* J Immunol, 2015. **194**(5): p. 2415-23.
32. Ozpolat, B., K. Mehta, and G. Lopez-Berestein, *Regulation of a highly specific retinoic acid-4-hydroxylase (CYP26A1) enzyme and all-trans-retinoic acid metabolism in human intestinal, liver, endothelial, and acute promyelocytic leukemia cells.* Leuk Lymphoma, 2005. **46**(10): p. 1497-506.
33. Seifert, M., et al., *Cellular origin and pathophysiology of chronic lymphocytic leukemia.* J Exp Med, 2012. **209**(12): p. 2183-98.

CHAPTER 6. FINAL CONCLUSIONS

6.1 SUMMARY

In chronic lymphocytic leukemia (CLL), the non-hematopoietic stromal microenvironment plays a critical role in promoting tumor cell activation, survival and expansion. However, the nature of stromal cells and signaling pathways involved remain largely unknown. Using the *Eμ-TCL1* mouse model, which recapitulates the progressive form of human CLL (hCLL), we show that leukemia development induces a dynamic remodeling of the stromal compartment characterized by loss of follicular dendritic cells (FDCs) maturation markers, and expansion of a $CXCL13^{+}$ stromal cell subset. Gene expression profile analysis revealed that leukemia promotes tissue remodeling and chemokine secretion by inducing retinoid synthesis and signaling in stromal cells. We found that mouse and human leukemia cells could be distinguished from normal B-cells by their increased expression of *Rarγ2* and *RXRα,* respectively. Notably, reducing retinoic acid precursors from the diet or inhibiting RA-signaling through retinoid-antagonist therapy prolong survival by preventing accumulation of leukemia cells into peripheral lymphoid tissues. These findings establish a role for retinoids in CLL pathogenesis, and provide new therapeutic strategies to target the stromal microenvironment and to control disease progression.

6.2 CONCLUSIONS

In mouse and human CLL, the crosstalk between leukemia and the surrounding microenvironment promotes tumor cell survival and disease progression [1] [2] [3]. Our findings using *Eμ-TCL1* mice which recapitulates the progressive form of human CLL reveal that leukemia development is associated with profound changes in the composition and distribution of stromal cells and their associated ECM, and that the RA-signaling pathway contributes to such changes. Our data demonstrate that CLL-FDC interactions persist within the B-cell zone, and that this causes disorganization and gradual loss of $CD35^+$ FDC networks during diseases progression. We show that these stromal alterations are already present in the large majority of mice with an intermediate percentage of leukemic cell infiltration. These findings indicate that, at least in this mouse model, leukemia modifies the follicular stromal microenvironment at early stages of disease evolution, and suggest that mature $CD35^+$ FDCs are dispensable for CLL progression, and may play a role only in the early phase disease, as previously proposed [4]. Our findings are also consistent with the notion that disruption and loss of FDC networks occurs in a large fraction of human cases of progressive CLL [5] [6].

Previous work showed that ablation of FDCs is associated with a reduction of the $CXCL13^+$ domains, with only the outermost region of the B-cell zone showing CXCL13 signal after FDC depletion [7]. Unexpectedly, we found that loss of $CD35^+$ FDCs is associated with an increase in CXCL13 distribution. This is particularly evident in transplanted mice, in which $CXCL13^+$ stromal cells are spread

throughout the white pulp, including the outer follicular region corresponding to the MRC layer. Expansion of $CXCL13^+$ stromal cells results from induction of CXCL13 in stromal cells previously negative for this chemokine, rather than to an increase in stromal proliferation. However, we cannot exclude the possibility that a slow-rate proliferation of $CXCL13^+$ stromal cells takes place during disease progression and may contribute to CXCL13 expansion. Notably, FDCs and CXCL13 maintenance relies on the continuous homeostatic signaling through the LTβR and TNFR1 [8]. Our findings show that while *Ltβ* expression is similar between CLL and control spleen B cells, the expression of *Ltα* was significantly reduced in *Eμ-TCL1* CLL cells. This reduction may cause an insufficient stimulation of the LTβR and a defect in FDC maintenance. Alternatively, FDCs may undergo phenotypic alterations under the pressure of leukemia-derived factors, and may loose differentiation markers such as CD35. Nevertheless, our data support a scenario in which leukemic cells induce CXCL13 in cells different from mature FDCs. Of note, recent work showed that during inflammation, B-cell follicles expanding into the T-cell zone convert pre-existing stromal cells, positioned at the B-T border, into $CXCL13^+$ secreting cells [9]. These cells, different from conventional T-zone FRCs, were termed versatile stromal cells. A similar mechanism might operate during CLL progression, where leukemic cells expanding into the T-cell zone change the phenotype of local stromal cells. In support of this hypothesis, we found that concomitantly with the increase in $CXCL13^+$ stromal cells, the distribution of $PDPN^+$ FRCs is significantly reduced in mice with high splenic infiltration of leukemia. In contrast to what we found in *Eμ-TCL1* mice, previous work in

Eμ–Myc transgenic mice, a model for MYC-driven lymphomagenesis, showed that lymphoma cells migrate to and interact preferentially with T-zone stromal cells [10]. These findings clearly indicate that unique stromal niches characterize different lymphoid malignancies.

Our data also show that in addition to stromal remodeling, leukemia development in *Eμ-TCL1* mice is characterized by an increase in ECM deposition and an overall disorganization of its architecture. ECM deposition and remodeling is already evident in mice with an intermediate percentage of leukemia infiltration, and in the areas of the B-cell zone corresponding to the FDC networks that are normally devoid of collages and nidogens [9]. Of note, recent work using *lpr/lpr/sparc* deficient mice, a mouse model that more closely recapitulates the indolent instead of the progressive form of CLL, showed that lymphomagenesis is associated with reduced collagen IV deposition [11]. These differences likely reflect the distinctive behavior of the leukemia in different mouse models. Notably, efficient collagen signaling was shown to be a driving factor in malignant Hodgkin/Reed-Sternberg cells in human Hodgkin lymphoma [12]. Although it remains unclear whether lymphoid tissues from CLL cases with different prognosis have a distinctive stromal/ECM organization, recent work showed a positive correlation between poor outcome and advanced grade of BM reticulin fibrosis in the microenvironment of CLL patients carrying the 11q deletion [13] [14]. Notably, altered stroma/ECM composition may also contribute to the immunosuppression described in *Eμ-TCL1* mice [15]. This hypothesis is in line with recent data demonstrating that following exposure to cancer-derived factors LN

stromal cells undergo remodeling and exhibit features of immunosuppression [16]. Altogether, these findings strenthen the notion that defective stroma/ECM composition and organization may contribute to cancer progression [17].

Consistent with the notion that leukemic cells modify the microenvironment, GEP analysis of stromal cells cultured with *Eμ-TCL1* leukemic cells revealed deregulation of genes involved in inflammation and stroma/extracellular matrix remodeling. Among those genes, we found up-regulation of *αSma/Acta2*, a marker of activated and cancer-associated fibroblasts, and *Nidogen-2*, *Lamb2* and *Prelp,* which encode for ECM-associated proteins. Notably, NID-2 was indeed found increased in the follicular areas of leukemic mice. In addition, PRELP and its family member FMOD are two ECM secreted glycoproteins overexpressed in CLL cells, and whose role in CLL remains unknown [18] [19]. Our GEP analysis also revealed that *Eμ-TCL1* leukemic cells stimulate RA synthesis and signaling in stromal cells of the microenvironment, and that RA-signaling is involved in stroma/ECM remodeling. During lymph node development, retinoids regulate *Cxcl13* expression in stromal progenitors, and in line with this, we found that treatment of our stromal cell line with RA induces *Cxcl13* expression. Our work demonstrates that the CLL-dependent induction of *Cxcl13* in stromal cells is indeed retinoid-dependent. Consistent with this, inhibition of RA-signaling causes a slight but consistent reduction and disorganization of CXCL13 distribution. Based on these findings, we suggest that RA acts in an autocrine fashion in stromal cells to stimulate chemokine secretion, possibly in combination with other

pathways such as toll-like receptor signaling, as previously demonstrated [20]. In addition, we propose that RA may function in a paracrine manner to activate target genes in both neoplastic and other non-tumoral cells of the microenvironment. Although future work is required to further support this hypothesis, our findings reveal that mouse and human leukemic cells could be distinguished from normal B-cells by their increased expression of *Rarγ2* and *RXRα* respectively, thus indicating they are equipped with the machinery to activate target genes upon ligand-binding. At present, the meaning of the correlation between increase expression of *RXRα* in a subset of patients carrying high-risk genetic aberrations and bad prognosis remains unclear. Nevertheless, emerging data point to a critical contribution of RXRα in lymphoid malignancies [21]. In support of this, loss of *Rxrα* protects mice from developing leukemia [22]. It is worth mentioning that RXRα is a dimerization partner for other nuclear receptors such LXRs, VDRs and PPARs, and thus it might be involved in the regulation of other signaling pathways implicated in CLL.

Given that retinoids have been shown to affect multiple biological processes including chemokine secretion, cell adhesion and stroma/ECM remodeling, we hypothesized that inhibition of RA-signaling could be a strategy to reduce chemokine expression and modulate stroma-leukemia interactions at multiple levels. Indeed, murine stromal cells treated with the RA-signaling inhibitor showed repression of genes involved in adhesion, ECM-cell interactions, migration and tissue remodeling. Interestingly, our findings indicate that 30% of the genes deregulated in stromal cells after leukemia co-

culture are controlled by RA-signaling. As predicted from the RNA-seq data, retinoid-antagonist therapy reduces the adhesion and aggregation of *Eμ-TCL1* CLL cells to stromal cells, and in line with this, inhibition of RA-signaling *in vivo* prolongs survival by preventing the accumulation and expansion of leukemic cells in lymphoid tissues. Our findings also reveal that FALCs represent additional leukemia-supportive niches, and that retinoid-antagonist therapy prevents FALC formation, and consequently the expansion of leukemia in the peritoneal cavity. At present, the role of retinoids in FALC development remains unclear. Still, given the high retinoids content of the peritoneal adipose tissue, it is possible that RA-signaling is required to induce *Cxcl13* expression and consequently FALC formation. Of note, peritoneal infiltration and enlargement of abdominal LNs occurs in CLL and other blood malignancies [23]. Although several reports have linked omental FALCs with solid tumor metastasis, it is unknown whether FALCs are induced in human CLL, and function as supportive niches promoting disease progression.

In conclusion, our findings indicate that retinoid-signaling plays an important role in the pathogenesis of murine CLL, and that retinoid-antagonist therapy may represent an effective strategy to target CLL-microenvironmental interactions at multiple levels in order to control disease progression.

6.3 FUTURE PERSPECTIVES

Combined therapies aiming to target cancer cells and the microenvironment are currently studied for enhancing therapeutic

efficacy. Although limited, there are examples of this kind of combined therapies, across different type of cancers [24].

The inhibition of hyaluronan synthesis in combination with cyclophosphamide exacerbates the immune-response against colorectal carcinoma [25]. In melanoma, curcumin-mediated tumour microenvironment targeting combined with tumour vaccines increases efficacy of cancer rejection [26]. In addition, in multiple myeloma phase I study, heparanases inhibitors (e.g. Roneparstat) combined with dexamethasone or bortezomib therapy is effective in blocking multiple myeloma growth through immune-mediated killing, inhibition tumour neo-angiogenesis and bone metastasis [27] [28].

In this work, I demonstrated that CLL induces a profound change in the stromal compartment that is characterized by chemokine secretion and stroma/ECM remodelling. I further showed that retinoic acid signalling is involved in such changes and that blocking this pathway is an effective strategy to control disease progression.

Hence, given the high expression of RA nuclear receptors found in both murine and human CLL cells, and the possible activation of the RA-signalling pathway in CLL patients, the development of a combined therapy that could include retinoid-antagonists together with classical chemotherapeutic drugs that target B-CLL cells may result in an overall increase in therapeutic efficacy. Indeed, my work showed that targeting RA-signalling effects multiple pathways, which include adhesion, chemokine secretion and ECM remodelling that are likely involved in CLL pathogenesis. Of note, Ibrutinib a recently approved and effective drug for the treatment of CLL has been also shown effective in a model of pancreatic cancer by limiting stromal cell activation and ECM

remodelling including fibrosis. This finding suggests that great efficacy of Ibrutinib in CLL may also result from targeting the non-hematopoietic stromal microenvironment. Retinoid-antagonist therapy indeed may also function in a similar manner - that is to target downstream pathways implicated in CLL pathogenesis that affect adhesion, migration, stromal cell activation and ECM remodelling. Emerging data from the literature clearly indicate that stromal cell activation and ECM deposition contribute to chemoresistance by limiting drug diffusion. In light of this, it will be intriguing to assess whether anti-fibrotic treatment can also have an effect by counteracting stromal cell activation and ECM remodelling thus favouring mobilization of leukaemia cells from their supportive niches. However, in relation to retinoid-antagonist therapy further work is needed to better understand i) which stromal cells produce retinoids in vivo, and at which stage of disease progression, ii) how retinoid-antagonist therapy during CLL progression affect the distribution of stromal cells and the ECM, and finally iii) what is the role of retinoids in CLL cells survival and expansion.

6.4 FINAL CONCLUSIONS BIBLIOGRAPHY

1. Ghia, P. and F. Caligaris-Cappio, *The indispensable role of microenvironment in the natural history of low-grade B-cell neoplasms.* Adv Cancer Res, 2000. **79**: p. 157-73.
2. ten Hacken, E. and J.A. Burger, *Microenvironment dependency in Chronic Lymphocytic Leukemia: The basis for new targeted therapies.* Pharmacol Ther, 2014. **144**(3): p. 338-48.

3. Caligaris-Cappio, F., M.T. Bertilaccio, and C. Scielzo, *How the microenvironment wires the natural history of chronic lymphocytic leukemia.* Semin Cancer Biol, 2014. **24**: p. 43-8.
4. Heinig, K., et al., *Access to follicular dendritic cells is a pivotal step in murine chronic lymphocytic leukemia B-cell activation and proliferation.* Cancer Discov, 2014. **4**(12): p. 1448-65.
5. Bagdi, E., et al., *Follicular dendritic cells in reactive and neoplastic lymphoid tissues: a reevaluation of staining patterns of CD21, CD23, and CD35 antibodies in paraffin sections after wet heat-induced epitope retrieval.* Appl Immunohistochem Mol Morphol, 2001. **9**(2): p. 117-24.
6. Tandon, B., et al., *Chronic lymphocytic leukemia/small lymphocytic lymphoma: another neoplasm related to the B-cell follicle?* Leuk Lymphoma, 2015. **56**(12): p. 3378-86.
7. Wang, X., et al., *Follicular dendritic cells help establish follicle identity and promote B cell retention in germinal centers.* J Exp Med, 2011. **208**(12): p. 2497-510.
8. Lu, T.T. and J.L. Browning, *Role of the Lymphotoxin/LIGHT System in the Development and Maintenance of Reticular Networks and Vasculature in Lymphoid Tissues.* Front Immunol, 2014. **5**: p. 47.
9. Mionnet, C., et al., *Identification of a new stromal cell type involved in the regulation of inflamed B cell follicles.* PLoS Biol, 2013. **11**(10): p. e1001672.
10. Rehm, A., et al., *Cooperative function of CCR7 and lymphotoxin in the formation of a lymphoma-permissive niche within murine secondary lymphoid organs.* Blood, 2011. **118**(4): p. 1020-33.
11. Sangaletti, S., et al., *Defective stromal remodeling and neutrophil extracellular traps in lymphoid tissues favor the transition from autoimmunity to lymphoma.* Cancer Discov, 2014. **4**(1): p. 110-29.
12. Cader, F.Z., et al., *The EBV oncogene LMP1 protects lymphoma cells from cell death through the collagen-mediated activation of DDR1.* Blood, 2013. **122**(26): p. 4237-45.
13. Tadmor, T., et al., *Significance of bone marrow reticulin fibrosis in chronic lymphocytic leukemia at diagnosis: a study of 176 patients with prognostic implications.* Cancer, 2013. **119**(10): p. 1853-9.

14. Kuter, D.J., et al., *Bone marrow fibrosis: pathophysiology and clinical significance of increased bone marrow stromal fibres.* Br J Haematol, 2007. **139**(3): p. 351-62.
15. McClanahan, F., et al., *Mechanisms of PD-L1/PD-1-mediated CD8 T-cell dysfunction in the context of aging-related immune defects in the Emicro-TCL1 CLL mouse model.* Blood, 2015. **126**(2): p. 212-21.
16. Riedel, A., et al., *Tumor-induced stromal reprogramming drives lymph node transformation.* Nat Immunol, 2016. **17**(9): p. 1118-27.
17. Brekken, R.A., *Faulty ECM signaling facilitates autoimmune lymphomagenesis.* Cancer Discov, 2014. **4**(1): p. 25-6.
18. Mikaelsson, E., et al., *Fibromodulin, an extracellular matrix protein: characterization of its unique gene and protein expression in B-cell chronic lymphocytic leukemia and mantle cell lymphoma.* Blood, 2005. **105**(12): p. 4828-35.
19. Mikaelsson, E., et al., *A proline/arginine-rich end leucine-rich repeat protein (PRELP) variant is uniquely expressed in chronic lymphocytic leukemia cells.* PLoS One, 2013. **8**(6): p. e67601.
20. Suzuki, K., et al., *The sensing of environmental stimuli by follicular dendritic cells promotes immunoglobulin A generation in the gut.* Immunity, 2010. **33**(1): p. 71-83.
21. Gorgun, G. and F. Foss, *Immunomodulatory effects of RXR rexinoids: modulation of high-affinity IL-2R expression enhances susceptibility to denileukin diftitox.* Blood, 2002. **100**(4): p. 1399-403.
22. Sukhai, M.A., et al., *Evidence of functional interaction between NuMA-RARalpha and RXRalpha in an in vivo model of acute promyelocytic leukemia.* Oncogene, 2008. **27**(34): p. 4666-77.
23. Karaosmanoglu, A.D., M.A. Blake, and J.K. Lennerz, *Abundant macroscopic fat in intra-abdominal lymph nodes involved in the course of a patient with chronic lymphocytic leukaemia: presentation of imaging findings with biopsy correlation.* Br J Radiol, 2012. **85**(1012): p. e91-3.
24. Malvicini, M., J.B. Aquino, and G. Mazzolini, *Combined therapy for gastrointestinal carcinomas: exploiting synergies between gene therapy and classical chemo-radiotherapy.* Curr Gene Ther, 2015. **15**(2): p. 151-60.

25. Malvicini, M., et al., *Tumor Microenvironment Remodeling by 4-Methylumbelliferone Boosts the Antitumor Effect of Combined Immunotherapy in Murine Colorectal Carcinoma.* Mol Ther, 2015. **23**(9): p. 1444-55.
26. Lu, Y., et al., *Curcumin Micelles Remodel Tumor Microenvironment and Enhance Vaccine Activity in an Advanced Melanoma Model.* Mol Ther, 2016. **24**(2): p. 364-74.
27. Ritchie, J.P., et al., *SST0001, a chemically modified heparin, inhibits myeloma growth and angiogenesis via disruption of the heparanase/syndecan-1 axis.* Clin Cancer Res, 2011. **17**(6): p. 1382-93.
28. Ramani, V.C., et al., *Targeting heparanase overcomes chemoresistance and diminishes relapse in myeloma.* Oncotarget, 2016. **7**(2): p. 1598-607.

CHAPTER 7. OTHER PUBLICATIONS

1. Transcription factor TLX1 controls retinoic acid signalling to ensure spleen development. Lenti E, Farinello D, Yokoyama KK, Penkov D, Castagnaro L, Lavorgna G, Wuputra K, Sandell LL, Tjaden NE, Bernassola F, Caridi N, De Antoni A, Wagner M, Kozinc K, Niederreither K, Blasi F, Pasini D, Majdic G, Tonon G, Trainor PA, Brendolan A. J Clin Invest. 2016 Jul 1;126(7):2452-64.

2. A Retinoic Acid-dependent Stroma-Leukaemia Crosstalk Promotes Tissue Remodelling And Chronic Lymphocytic Leukaemia Progression. D. Farinello*, M. Wozinska*, Elisa Lenti, L. Genovese[1,2], S. Bianchessi[1,2], EPM. Migliori[1,2], N. Sacchetti[1,2], A. di Lillo[1,2], R. Valsecchi, Andreas Aghatangelidis, Cristina Scielzo, Claudia de Lalla, Laura Mauri, Sandro Sonnino, Lydia Scarfò, Dejan Lazarevic, Sabrina Bascones Gleave, Rosa bernardi, Maurilio Ponzoni, Andrea Cerutti, Linda Pattini, MTS. Bertilaccio[1], F. Caligaris-Cappio[1,4], P. Ghia[1,3] and A. Brendolan[1,2]. (Manuscript under submission).

Acknowledgements

La parte più importante di un discorso sono sempre i ringraziamenti. Come si può degnamente ricordare momenti belli e brutti passati assieme alle persone che ci circondano? Com'è possibile non sminuire nessuno? Ogni persona conosciuta ed ogni azione intrapresa causano un effetto sulla propria vita e determinano scelte uniche, nel bene e nel male. Tutti sono quindi importanti, senza alcuna eccezione.

Questa è la fine di un ciclo, non solo di dottorato, ma di un'esperienza di vita che non si ripeterà e rimarrà dunque unica… Neil Gaiman scrisse nel suo romanzo Anansi boys "Stories are like spiders, with all they long legs, and stories are like spiderwebs, which man gets himself all tangled-up in but which look pretty when you see them under a leaf in the morning dew, and in the elegant way that they connect to one another, each to each". La storia del mio dottorato è quindi connessa con infinite altre storie, e la mia vita durante questo periodo si è quindi legata alla vita di altri; nonostante tutto questo groviglio di esperienze possa risultare confuso e quasi spaventoso, se non compreso e vissuto, sotto una determinata luce emerge la sua bellezza e la sua unicità.

Come ogni storia che si chiude, anche la fine di questa esperienza porta con sé un leggero sapore amaro, quasi come se non si volesse realmente terminare; ma non dura a lungo, perché si arriva a realizzare che tutta la fatica, le infinite ore perse, le nottate passate in bianco, tutto lo stress accumulato, ma anche le molteplici piccole e grandi gioie che,

convergendo, mi hanno guidato verso questo importantissimo traguardo.

I miei ringraziamenti non possono che partire da lei, la persona con la quale sto condividendo tutto e con la quale continuerò a condividere tutto: Sabrina. Non starò qui ad elencare tutti i momenti nei quali fino ad ora mi ha dato una mano, ma posso assicurare che senza di lei non ce l'avrei fatta. È per questo che non smetterò mai di esserle grato e sono infinitamente contento che il destino abbia fatto incrociare le nostre strade. Ringrazio anche moltissimo la mia famiglia intera (parenti diretti, acquisiti e nipoti!), verso la quale ho riscoperto un affetto veramente sincero e profondo; mi sono stati vicini durante la mia laurea, ma ancora di più in questi tre anni e mezzo, abbiamo condiviso le mie gioie ed i miei dolori, dandomi sempre consigli ed aiutandomi quando possibile. Naturalmente, parlando di famiglia, non posso che ringraziare anche la famiglia di Sabrina, nella quale sono stato accolto benissimo, quasi fossi un ospite d'onore.

Quello che sono ora lo devo anche alle persone con le quali ho condiviso i momenti cruciali della mia crescita e maturazione (quantomeno parziale!). Alcune persone le conobbi decine d'anni fa, altre solo negli ultimi anni, ma tutte sono state fondamentali nel mio percorso, risultando anche cruciali per alcune mie scelte intraprese.

Non sarei sicuramente il ricercatore che sono ora se non avessi incontrato Andrea ed Elisa; se posso ritenermi contento di quello che so fare e di come so ragionare lo devo anche a loro. Non posso che ringraziarli anche per tutto ciò che hanno fatto per me, che va ben al di là di dell'ambito lavorativo. Un ringraziamento va anche a Luca, che mi ha fatto scoprire il significato della frase "piccolo grande uomo", ed

a Silvia, con la quale ho condiviso dei meravigliosi momenti alla Sandra e Raimondo! Come non ricordare poi in questo momento Alessia, con la sua dolcezza mista ad ansia, Nicolò, con la sua ironia e la sua piacevole compagnia, Maria Teresa, con la sua disponibilità e simpatia, ed Edoardo Pericle Maria (mi farò odiare per questo) per i bei momenti (e cioccolatini!) condivisi. Ringrazio anche il chiarissimo, magnifico, illustrissimo Dr. Ph.D. Mario Tirone, per tutto il supporto e per le magnifiche chiacchierate scientifiche condivise.

Naturalmente non mi sono scordato degli amici!

L'amico è quella persona che nel momento del bisogno è presente e che anche se non ti comporti bene, ti perdona e non cambia atteggiamento nei tuoi confronti. Ad essere onesto… Da questo punto di vista mi ritengo davvero molto fortunato… Sono molti i miei amici e non voglio perderne nemmeno uno! La mia compagnia biraghese, sempre immancabilmente unita e presente, mi ha aiutato a superare momenti difficili ed a fare baldoria nei momenti felici. Non posso dunque scordarmi di Beppe, Lucy, il Biondo, il Dona, Gra, Kojak 1 (Luca), la Patty, Kojak 2 (Marco), il Poli, il Benzo, Guido, il Bria e lo Ste. La mia compagnia dell'università, fuori di testa nelle feste e molto propositiva nelle discussioni, è stato un supporto per lasciarsi andare e smaltire lo stress quotidiano, come anche un orecchio al quale confidare i propri segreti e pensieri. Quindi Ale, Gaia, Leons, Elia, Francy (Norris!), Silvia, Rufy, Andrea, Ari, grazie di essere stati presenti!

Sicuramente mi sto scordando persone molto importanti, alle quali farò di persona i miei ringraziamenti, ma non vorrei mai che i miei ringraziamenti divenissero più lunghi della discussione della mia tesi!

Grazie di cuore a tutti voi, vi ricorderò sempre!